PICARD, a mission dedicated to study the Sun

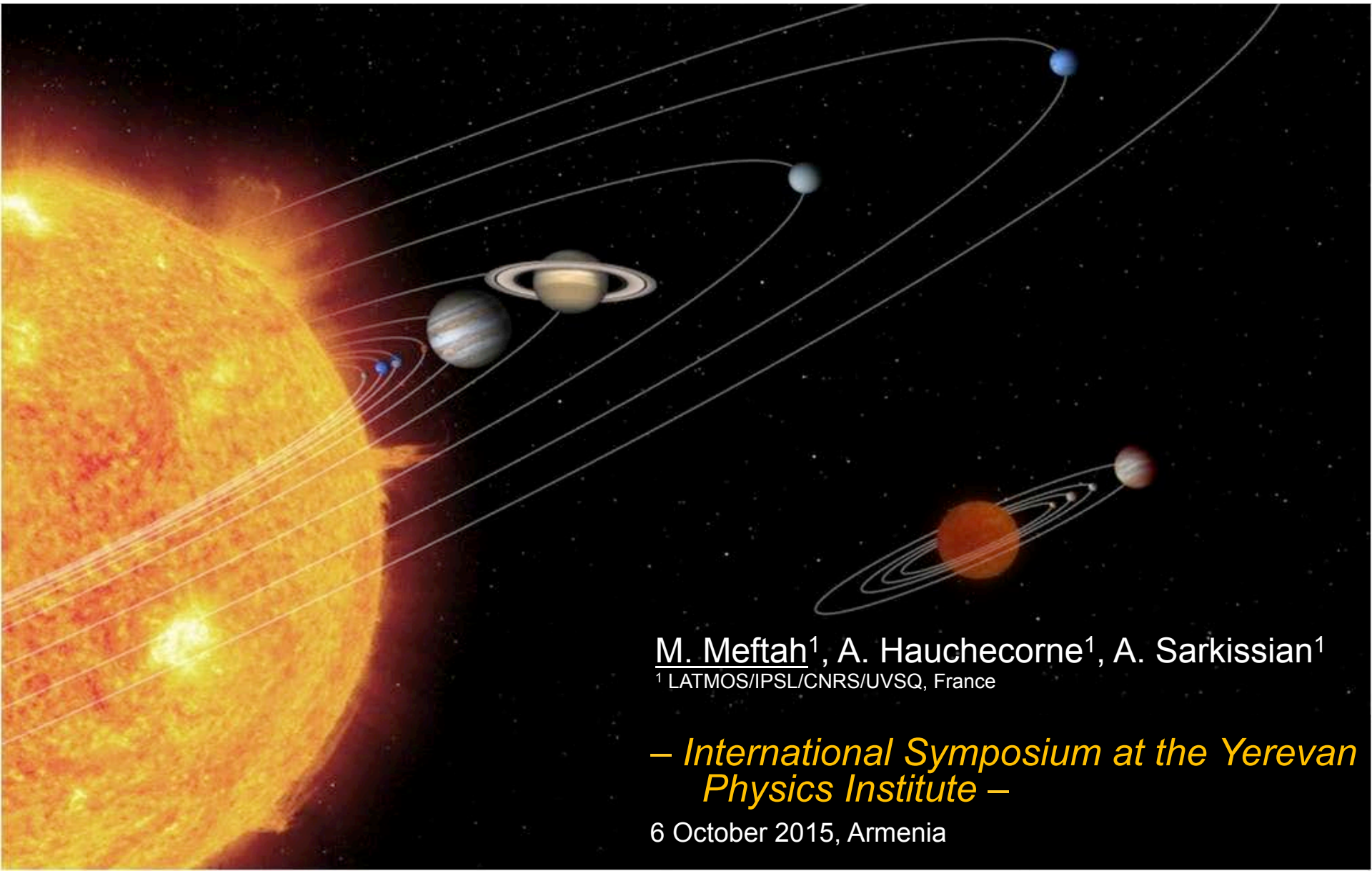

M. Meftah[1], A. Hauchecorne[1], A. Sarkissian[1]
[1] LATMOS/IPSL/CNRS/UVSQ, France

– International Symposium at the Yerevan Physics Institute –

6 October 2015, Armenia

On solar radius measurements during the rising phase of solar cycle 24

Presentation outline

- The PICARD mission and the scientific objectives
- The payload of the PICARD mission
- PICARD SOL, our ground-based facility
- Scientific results
- Conclusion

1 – The PICARD mission and the scientific objectives (1/9)

PICARD is a scientific mission dedicated to the study of the Sun.

The name of the mission comes from Jean Picard (1620-1682), a pioneer of precise modern astrometry, who observed the sunspots, and measured their rotation velocity and the solar diameter.

The Picard mission expands observations of the global parameters of the Sun in the hope of linking the variability of its total and spectral irradiance to its geometric shape.

PICARD observations are made during the ascending phase and the plateau of solar cycle 24.

Jean Picard
(1620-1682)

Five Years of Solar Observation

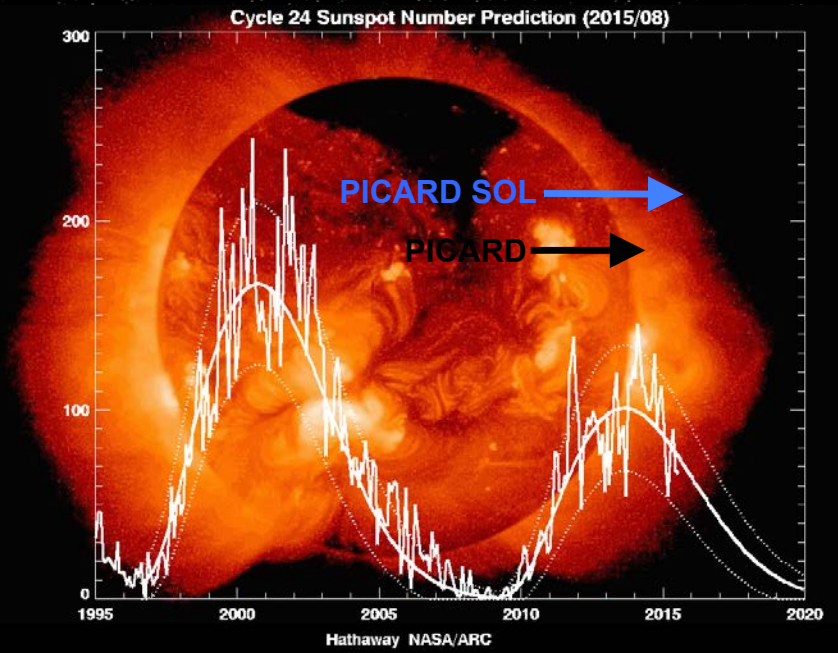

1 – The PICARD mission and the scientific objectives (2/9)

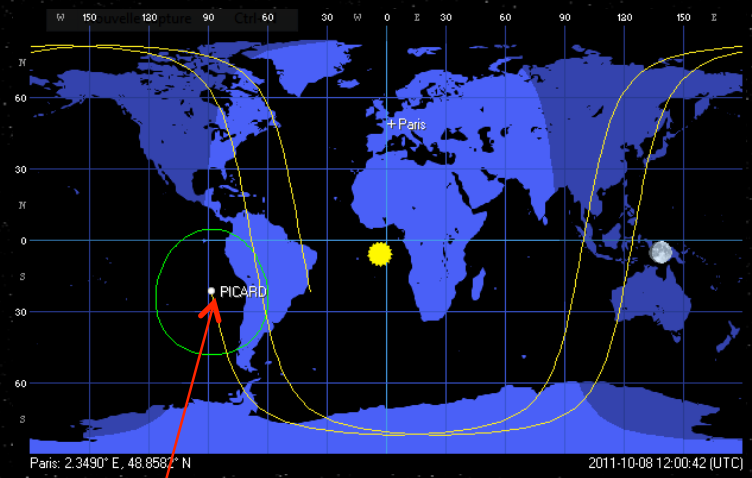

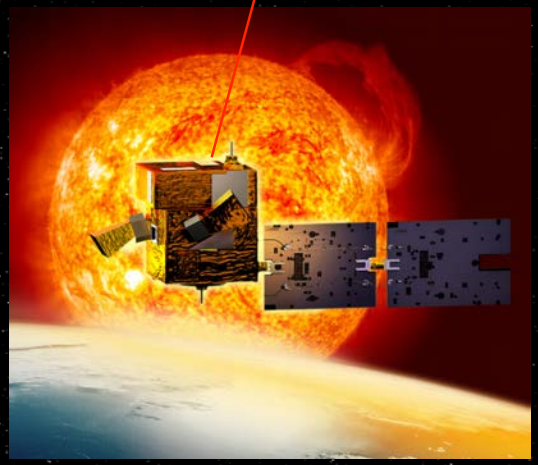

PICARD is a space mission, which was successfully launched on 15 June 2010 into a Sun synchronous dawn-dusk orbit (735 km, Inclination: 98.29°).

PICARD SOL is the ground component of the PICARD mission and is operational since March 2011 (Calern, France) – OCA and LATMOS (CNRS).

1 – The PICARD mission and the scientific objectives (3/9)

PICARD

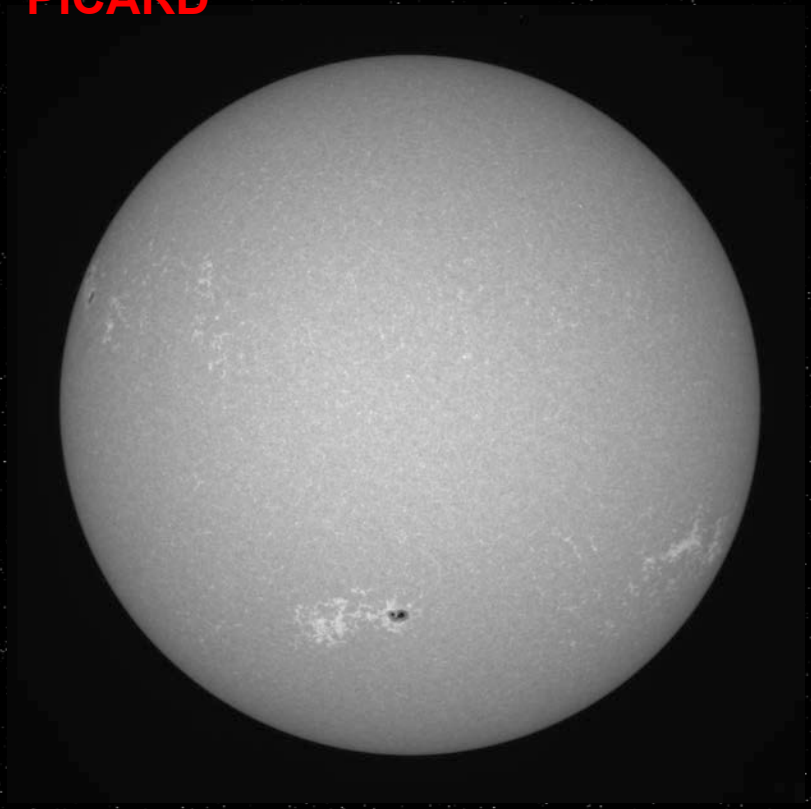

~ 1,300,000 images acquired

PICARD has recorded more than one million solar images from June 2010 to April 2014.

PICARD SOL

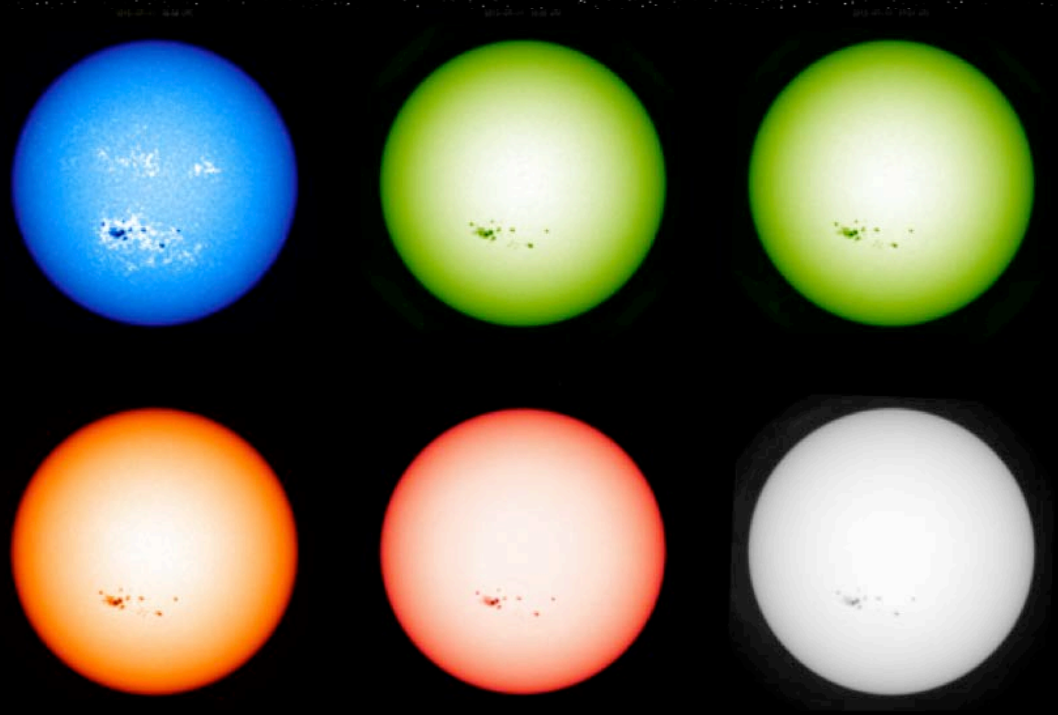

~ 100,000 images acquired

PICARD SOL operates nominally since 2011.

1 – The PICARD mission and the scientific objectives (4/9)

- Solar Astrometry

Measure the diameter and the solar oblateness of the Sun (absolute values) and their changes over time.

- Radiometry and photometry

Measure the total solar irradiance (TSI) in absolute and over time.
Impact on the climate.

Establish the relationship: variation of the solar diameter / change of the TSI (solar parameter W).

Measure the variations of the solar spectral irradiance in the UV (influence on ozone and climate).

- Helioseismology

Observations of low-frequency acoustic oscillations and detection of the p-modes (detailed study of the nuclear core and his dynamics).

1 – The PICARD mission and the scientific objectives (5/9)

Variability of the solar radius, solar oblateness, and magnetic field

Why it varies ? What is the impact on the variability of the spectral irradiance ?

Time variation of the solar radius

– Influence of inner magnetic field ?
– Other influences ?
– Order of magnitudes: measurable or not ?

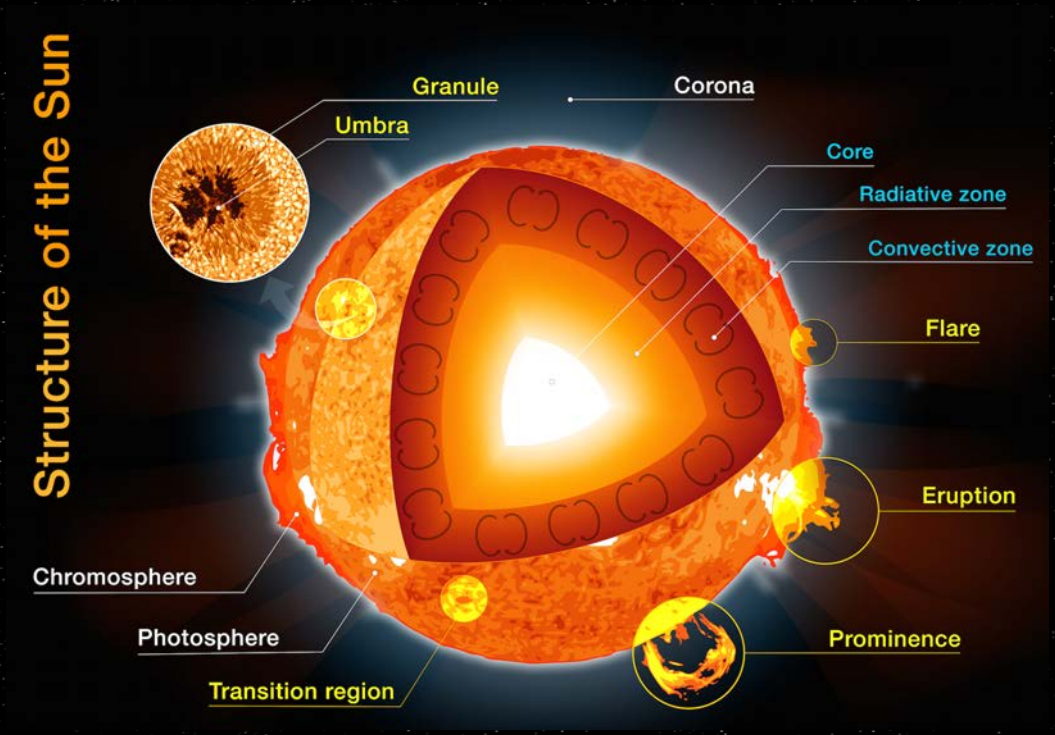

1) The first step is to determine the evolution of the solar radius during the solar cycle 24.

2) Next, we will determine the evolution of the spectral solar irradiance over time.

1 – The PICARD mission and the scientific objectives (6/9)

The Sun is not a solid body.

That's a huge glowing ball. The Sun is made up entirely of gas (sensitive to magnetism).

- Sun's radius:

695 990 km (Allen, 1973)
Near 959.62 arc seconds at 1 A.U.

- Luminosity:

3.846×10^{26} W

- Temperature (photosphere):

5 778 Kelvin

- Mean distance from Earth:

149 597 870 km at 1 A.U.

- Mass:

1.989 billion of billion of billion tons

etc.

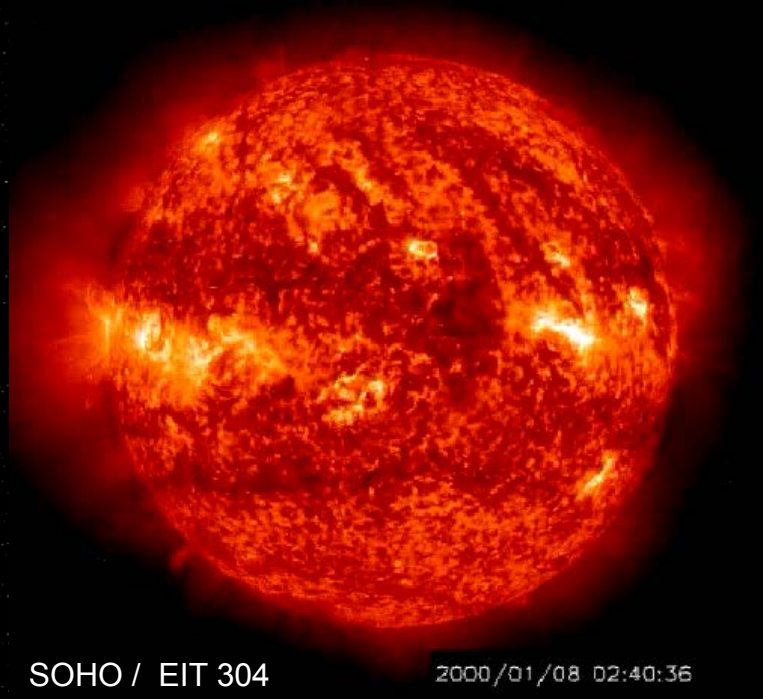

1 – The PICARD mission and the scientific objectives (7/9)

Study of the structure of the sun:

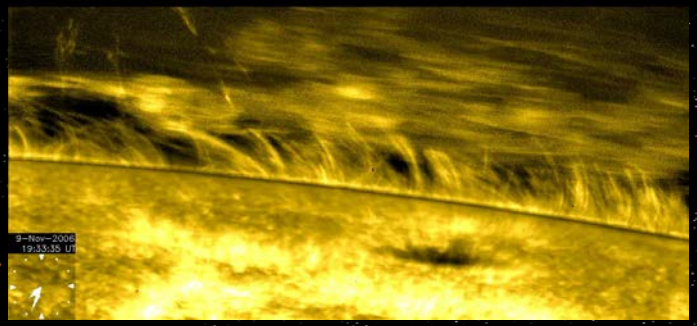

HINODE JAXA, NAOJ, PPARC and NASA.

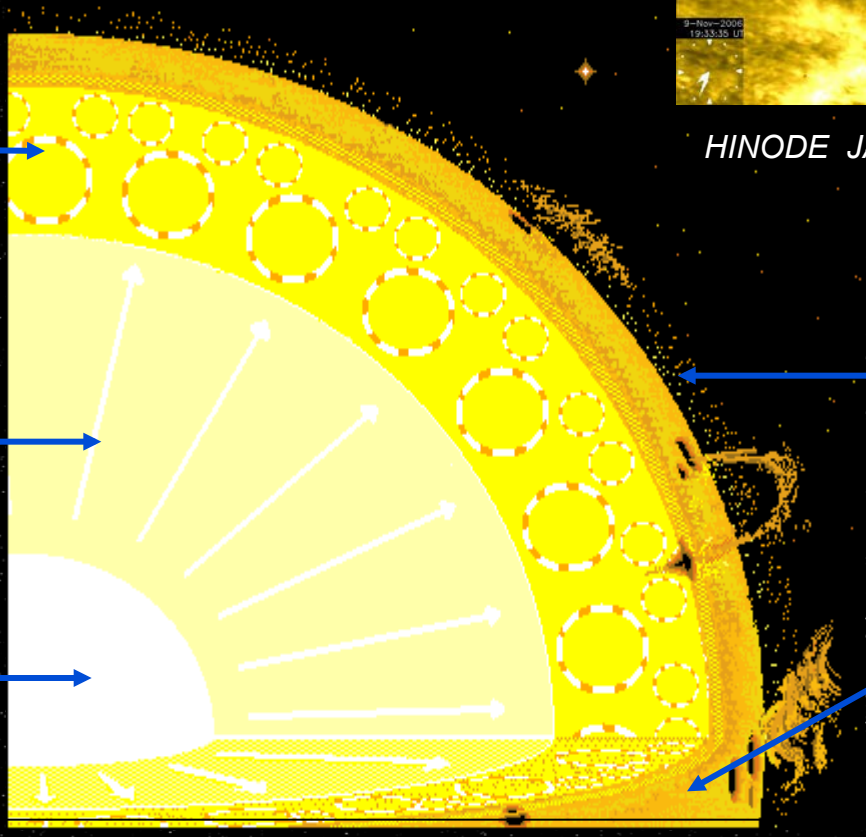

From H. Haubold and A. M.Mathai, http://www.seas.columbia.edu/~ah297/un-esa/sun/sun-chapter1.html

1 – The PICARD mission and the scientific objectives (8/9)

Measuring the Sun's radius remains complex. It is usually measured by determining the inflection point of solar limbs. CLV (Center to Limb Variation – Pecker and Schatzman, 1959) contains information about solar photosphere that can not be derived from observations of the disk center:

- At the limb, the optical depth of the solar atmosphere steeply decreases and becomes optically tin resulting in a drop of emerged intensity over the entire solar spectrum,
- The CLV is an important characteristic to constrain/test models.

- Solar limb shape:

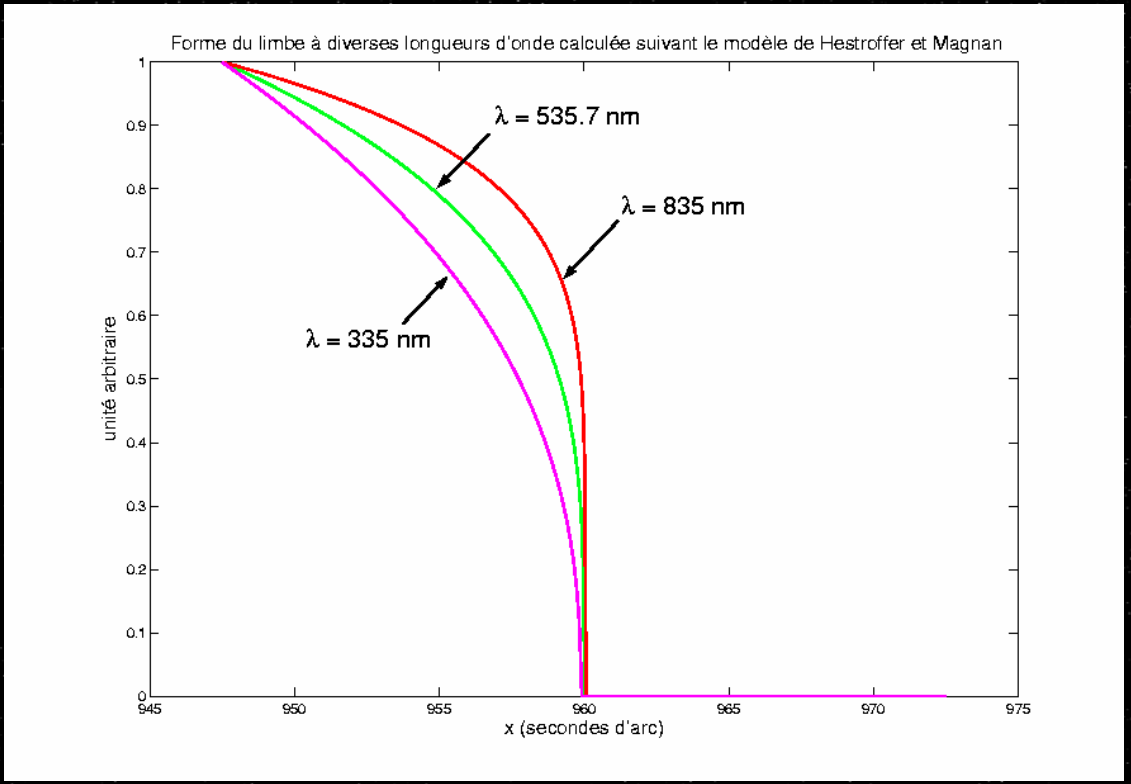

1 – The PICARD mission and the scientific objectives (9/9)

The Sun's activity is not constant but varies over an 11-year cycle. The 11-year sunspot cycle is related to a 22-year cycle for the reversal of the Sun's magnetic field.
Solar Cycle 24 (started January 2009) is the 24th solar cycle since 1749, when recording of solar sunspot activity began.

- Sun's activity (example with the solar cycle 23):

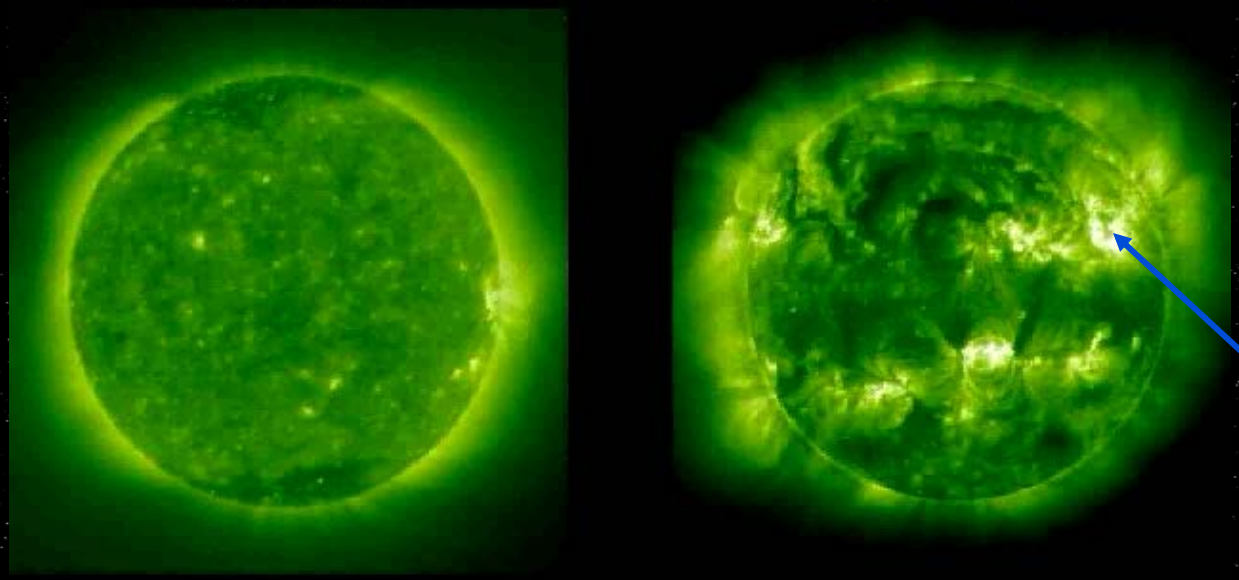

SOHO / EIT 195A

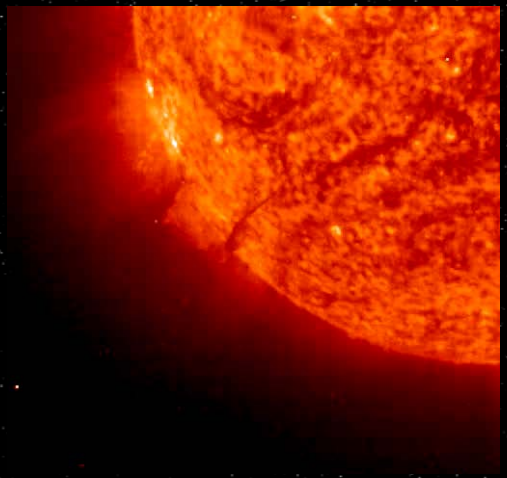

SOHO / EIT 304

The eruptions lead to solar activity, which includes such phenomena as sunspots, flares, and coronal mass ejections.

Presentation outline

- The PICARD mission and the scientific objectives
- The payload of the PICARD mission
- PICARD SOL, our ground-based facility
- Scientific results
- Conclusion

2 – The payload of the PICARD mission (1/6)

PICARD is a microsatellite of 130 kg mass (CNES), dedicated to the study of the Sun.

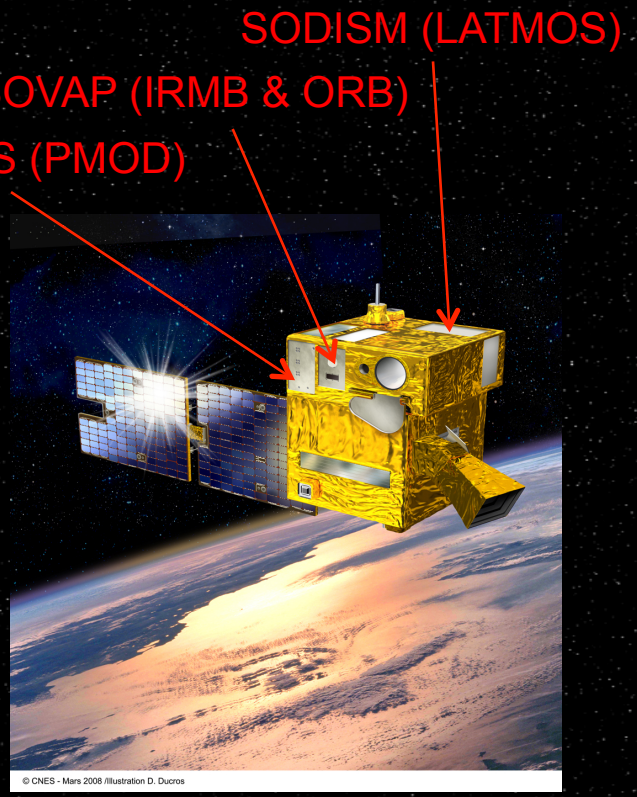

Main instruments:

- **SODISM** (SOlar Diameter Imager and Surface Mapper) is an imaging telescope
- **SOVAP** (SOlar VAriability PICARD) is a radiometer
- **PREMOS** (PREcision MOnitoring Sensor) is a photometer and radiometer
- **PGCU** is an onboard electronics

Responsibility of the payload (LATMOS)

2 – The payload of the PICARD mission (2/6)

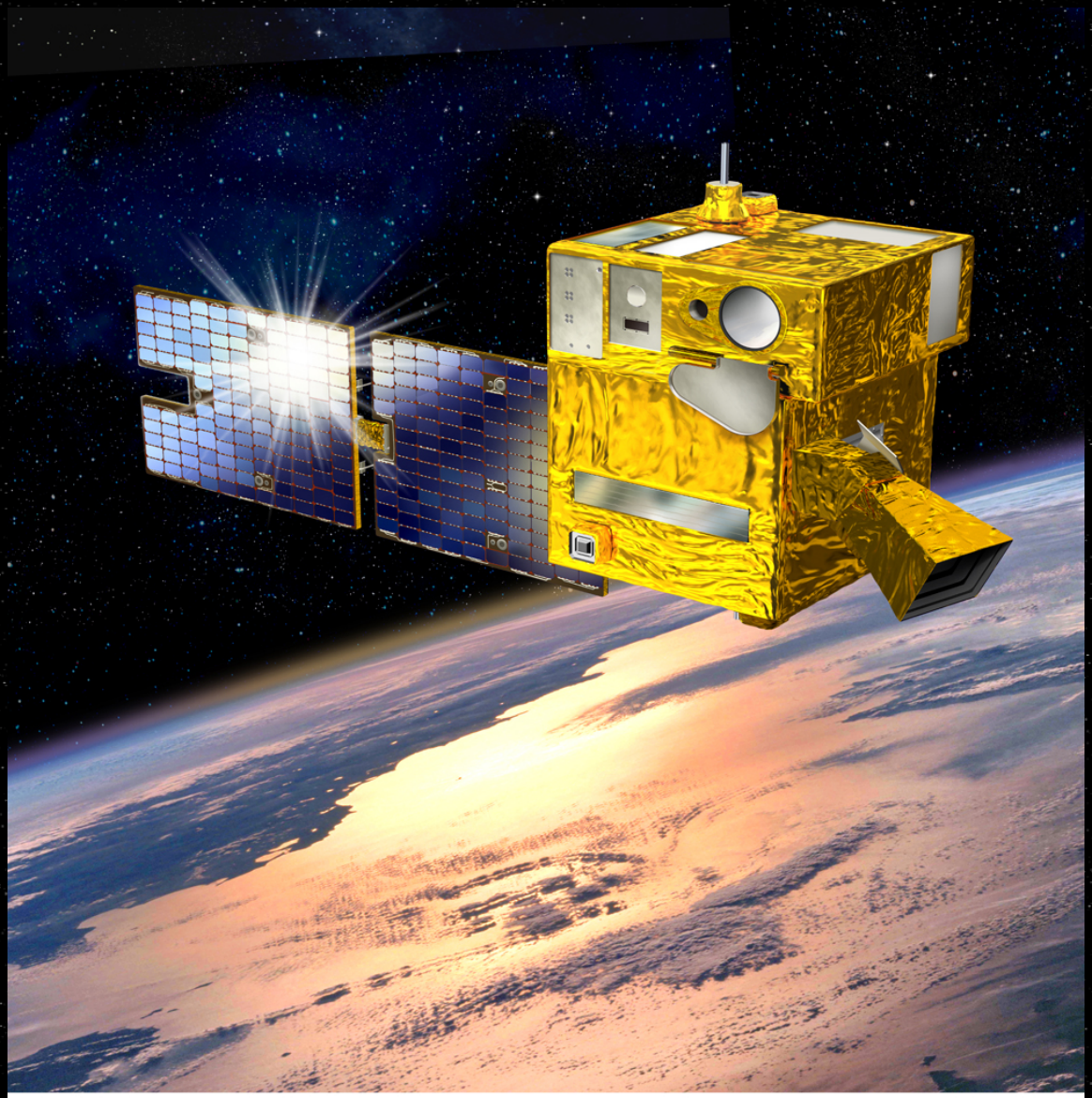

2 – The payload of the PICARD mission (3/6)

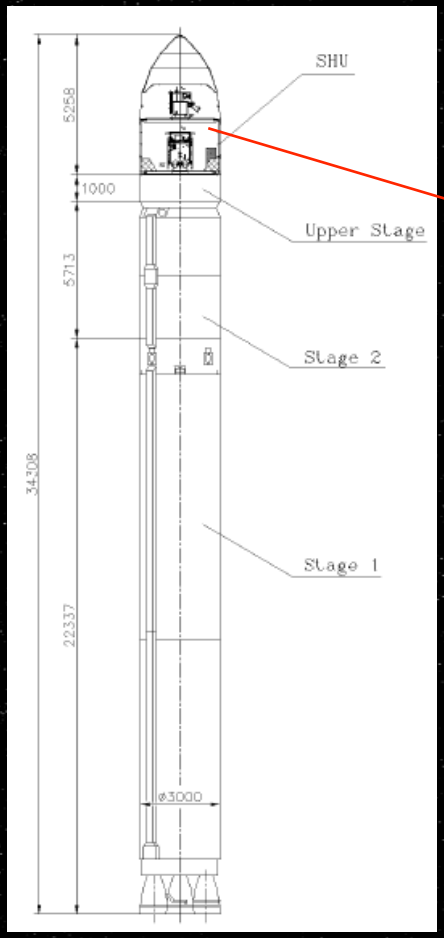

Launch vehicle

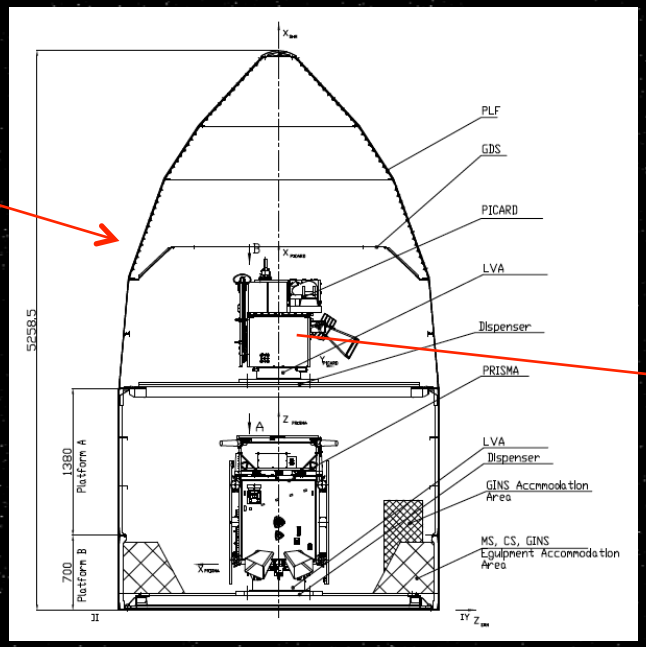

Rocket payload unit general view

Stowed view (launch)

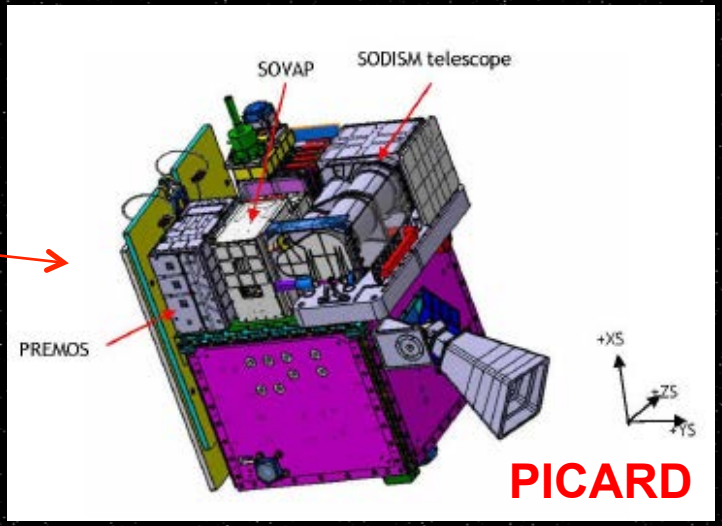

Deployed on orbit

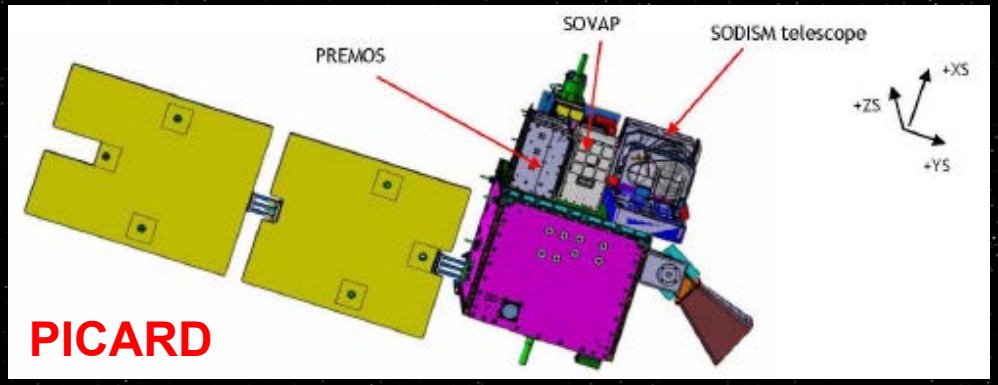

2 – The PICARD/SODISM space instrument (4/6)

SODISM is an 11-cm Ritchey-Chretien imaging telescope developed at CNRS by LATMOS (ex. Service d'Aéronomie, France) associated with a 2Kx2K Charge-Coupled Device (CCD), taking solar images at five wavelengths.

SODISM main characteristics:

- Telescope type: Ritchey Chretien
- Focal length: 2626 mm
- Field of view: 35 arc-minutes
- Angular resolution: 1.06 arc-second
- Dimensions: 300x308x370 mm^3
- Mass: 26.4 kg
- Power: 30.6 W
- Data flow: 2.2 Gbits per day
- One image per minute

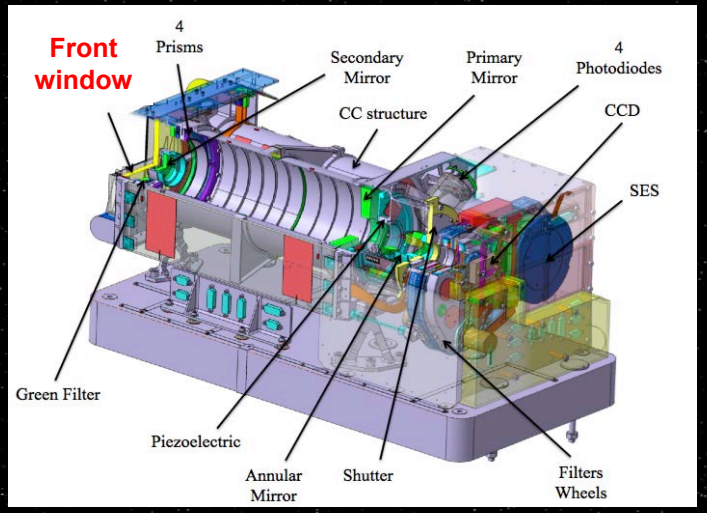

2 – The PICARD/SODISM space instrument (5/6)

SODISM optical path and interferential filters characteristics

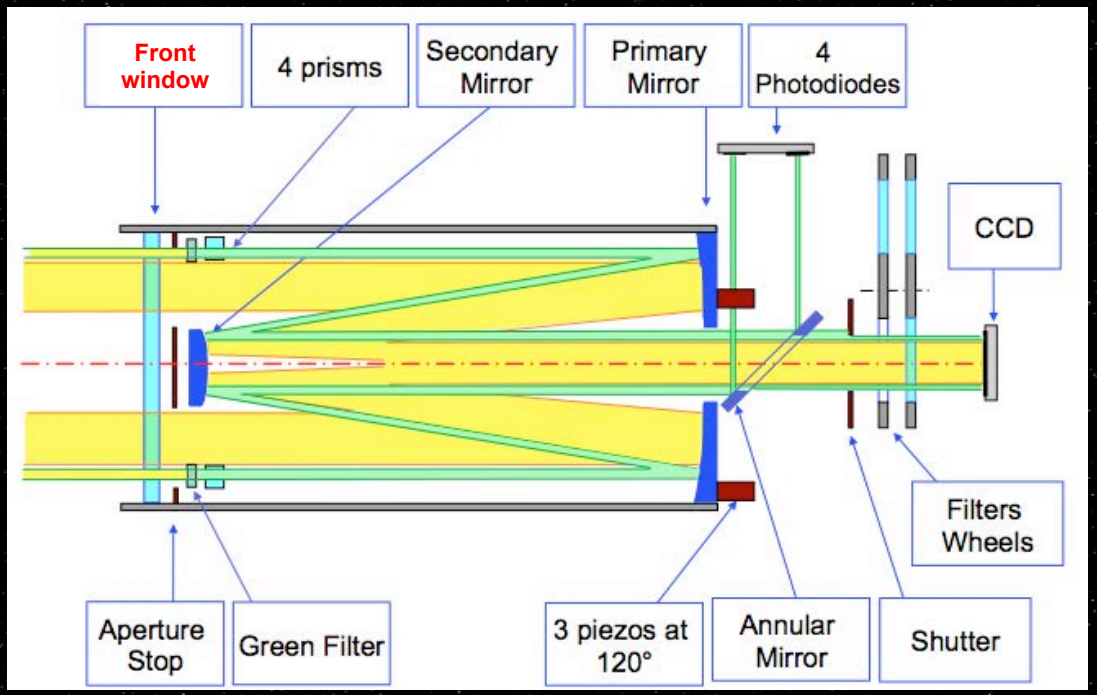

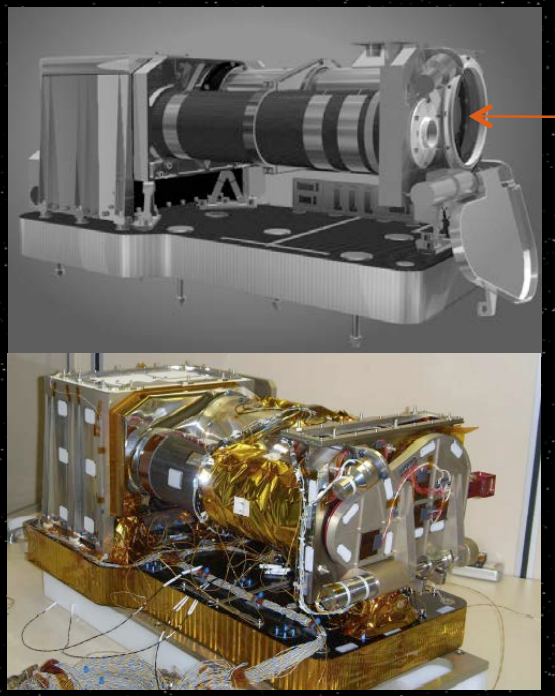

Wavelength λ in nm	Bandwidth Δλ in nm	Function
215.0	7	Sun activity, O3, measurement, diameter
393.37	0.7	Active regions observation
535.7	0.5	Oscillations (helioseismology)
535.7	0.5	Diameter, oscillations (helioseismology)
607.1	0.7	Diameter
782.2	1.6	Diameter

2 – The PICARD/SODISM space instrument (6/6)

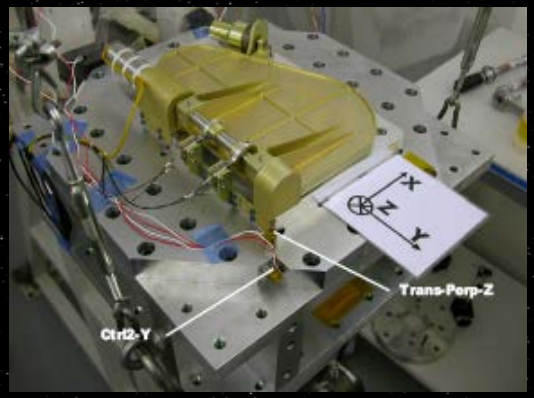

SODISM, an imaging telescope with a lot of mechanisms and many technology

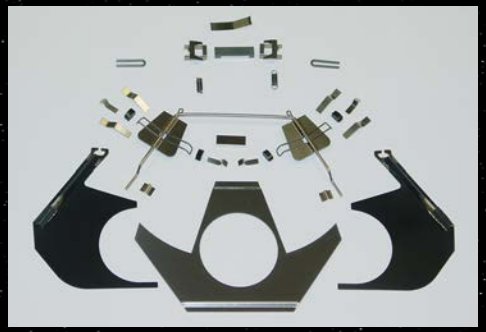

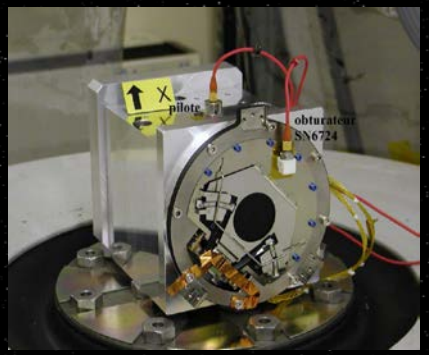

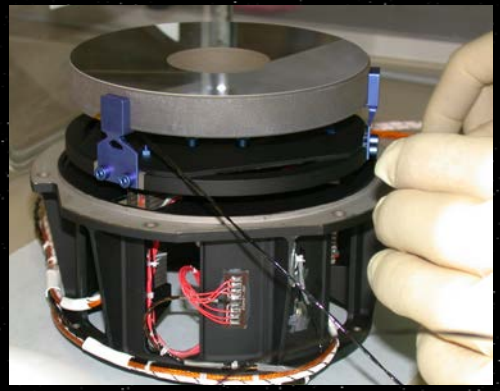

Presentation outline

- The PICARD mission and the scientific objectives
- The PICARD/SODISM space instrument
- PICARD SOL, our ground-based facility
- Scientific results
- Conclusion

3 – PICARD SOL, our ground-based facility (1/2)

Solar diameter telescope (SODISM-2)

Turbulence monitor

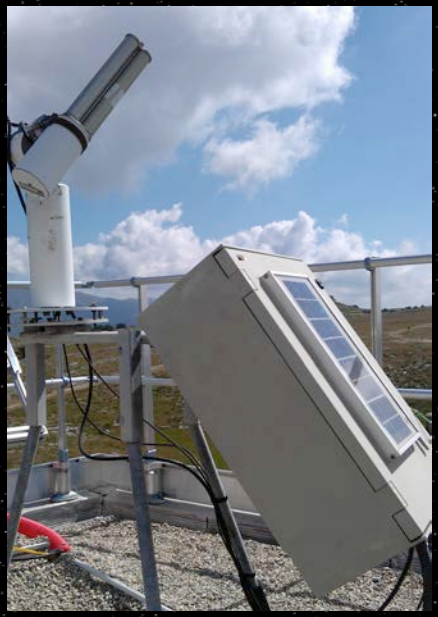

Photometer

Pyranometer

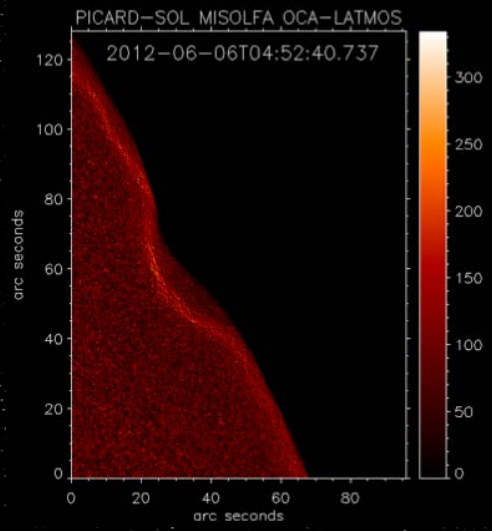

During the 2012 transit of Venus

3 – PICARD SOL, our ground-based facility (2/2)


SODISM-2
HEIDENHAIN
Calern, France

Presentation outline

- The PICARD mission and the scientific objectives
- The PICARD/SODISM space instrument
- PICARD SOL, our ground-based facility
- Scientific results
- Conclusion

Calibration

4 – Scientific results

The first image of the Sun was taken by the SODISM instrument on July 22, 2010.
It is a raw image, level L0, thus obtained before processing.

The PICARD/SODISM pointing mechanism is very important.

- Correct the main optical and radiometric defaults of the raw image

Several solar images at different wavelength have been recorded since the beginning of the mission for create the best Flatfield.
Flatfield corrections are important for achieving good quality images and for improved photometric measurements.
Kuhn, Lin and Loranz (1991) present methods of flatfielding using only image data and the first SODISM flat-fields were computed using the algorithm of Kuhn et al.

→ Use of the PICARD/SODISM mechanism
We move the image on the matrix using the mechanism.
The movement is limited by the stroke of the piezoelectrics (60 arcseconds or pixels).

- Stabilize the Sun image on the CCD with an accuracy of 0.2 arcseconds

→ Use of the PICARD/SODISM mechanism

4 – Scientific results

- Correct the main optical and radiometric defaults of the raw image

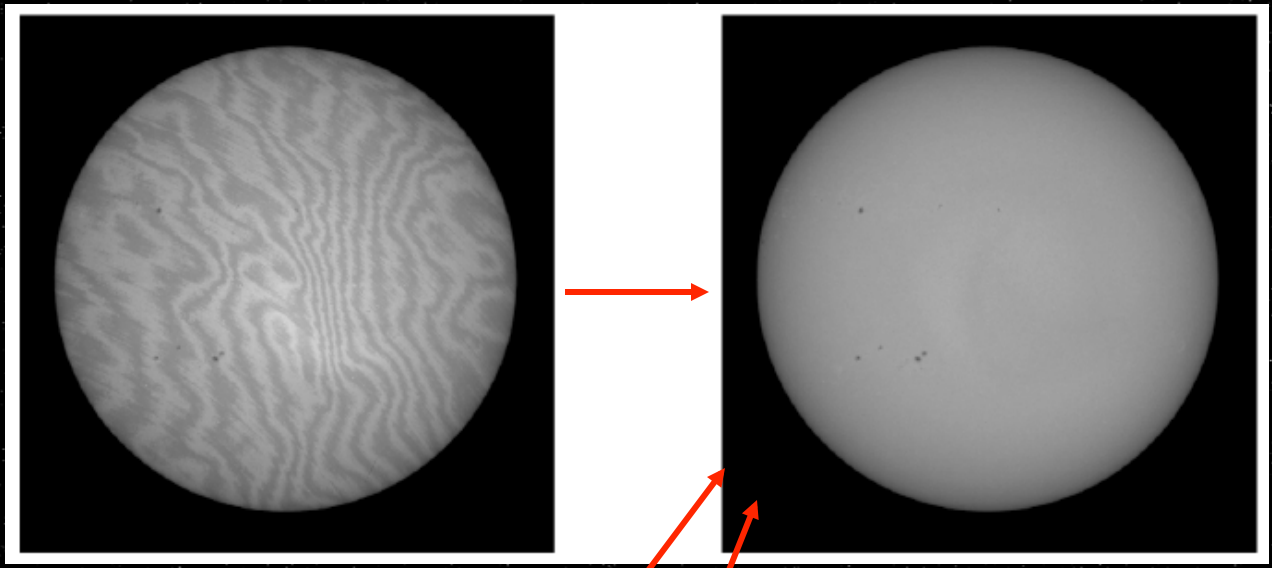

Raw image of the Sun, level L0

Image of the Sun, level L1

Coverage area of the CCD (limited by the stroke of the piezoelectrics)

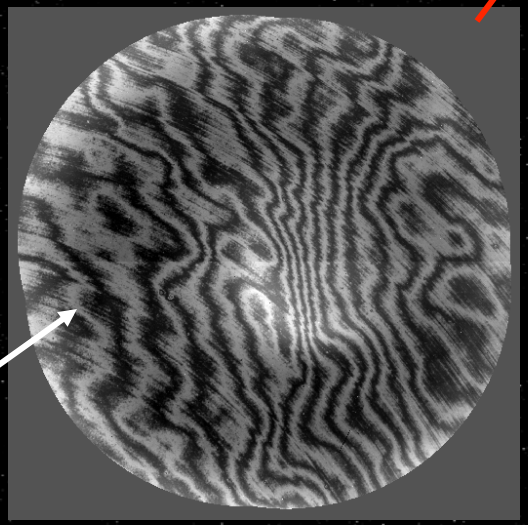

Flat Field at 782 nm

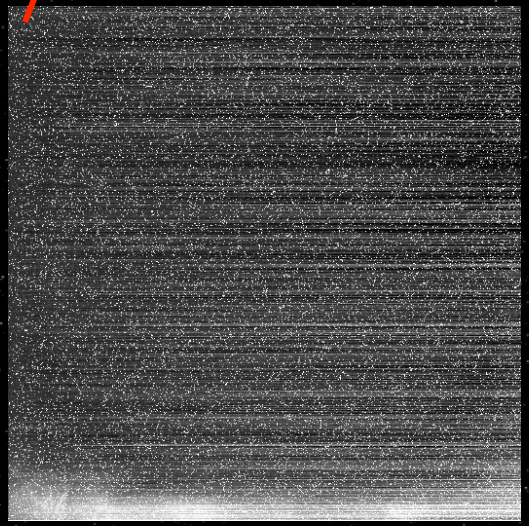

Dark current, 1 second

4 – Scientific results

- Correct ghost on images

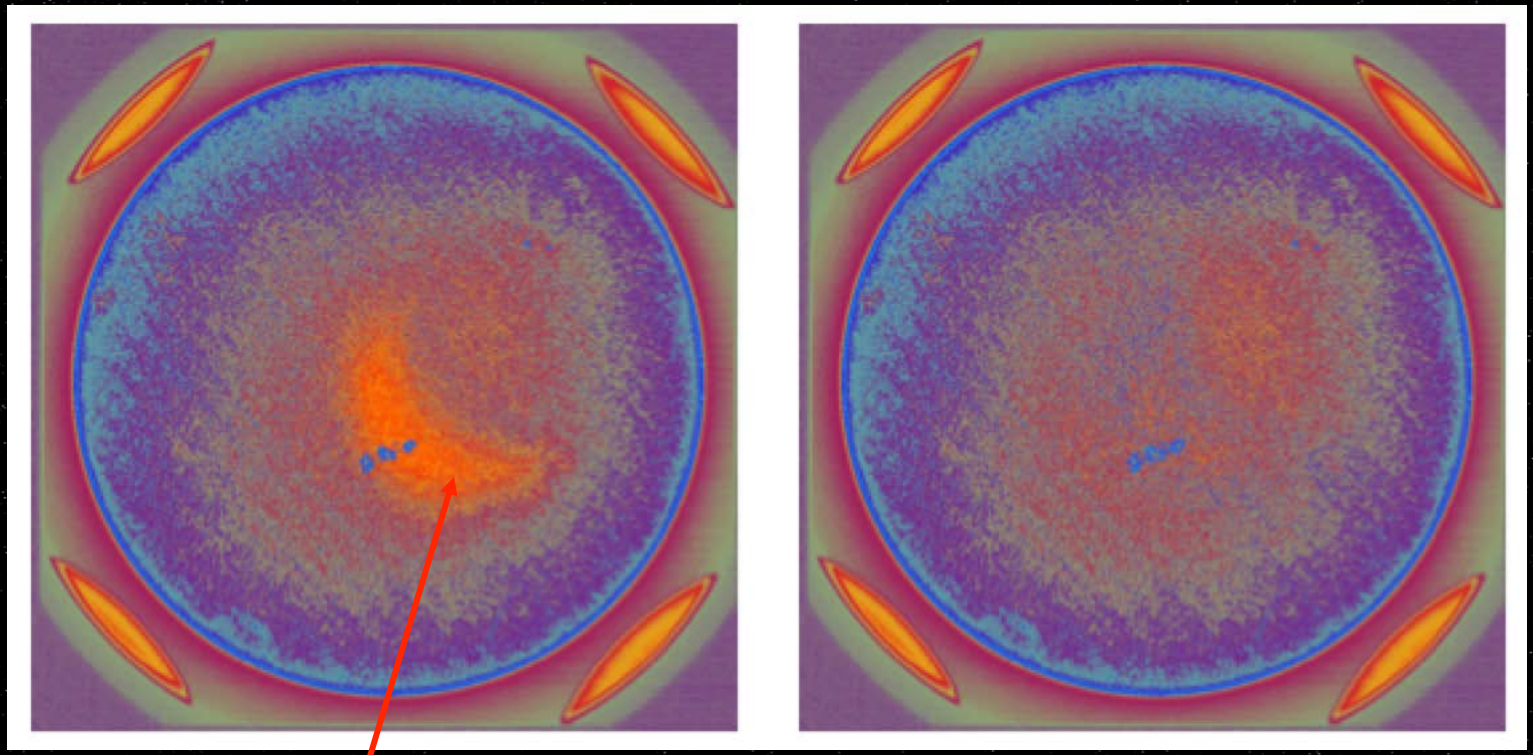

4 – Scientific results

- Stabilize the Sun image on the CCD with an accuracy of 0.2 arcseconds

An image is taken every 2 minutes, leading to 720 images per day.
The Figure 1 shows the angular deviations performed by the pointing mechanism over 3 days. The standard deviation is equal to 0.31 pixel (whose size corresponds to 1.06 arcsecond).
This means that the image stability (standard deviation) corresponds to an angular value of +/- 0.234 arcsecond. The initial specification was +/- 0.2 arcsecond.
It can be concluded that the pointing mechanism implemented and qualified in the SODISM instrument is effective.

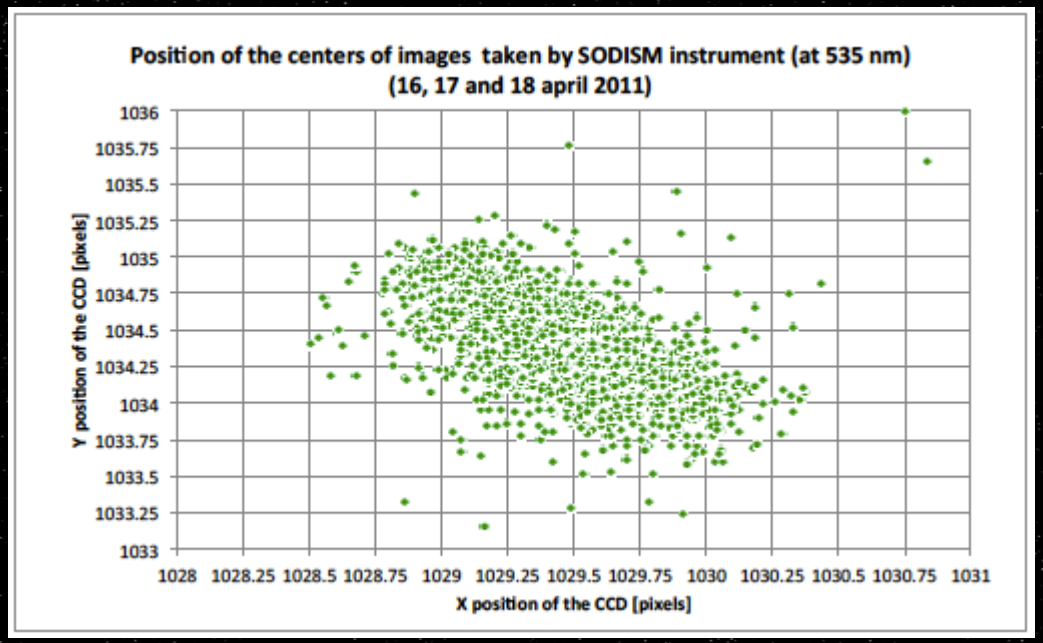

Figure 1: Angular correction performed by the mechanism

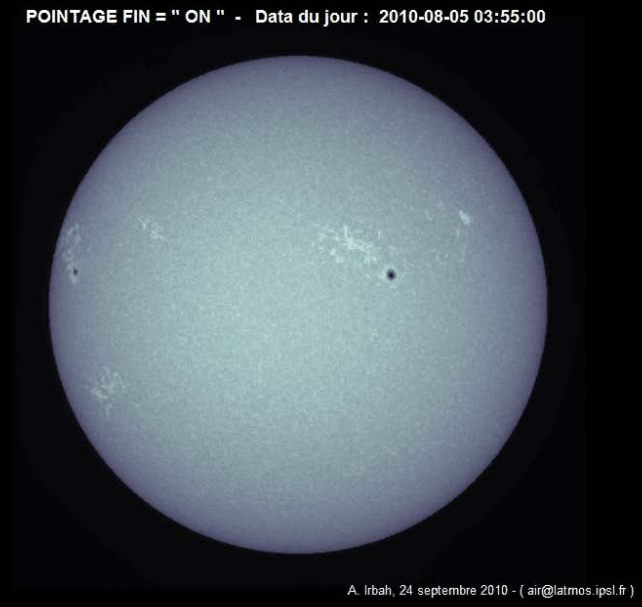

PICARD/SODISM: Sun image at 393 nm – Pointing ON

4 – Scientific results

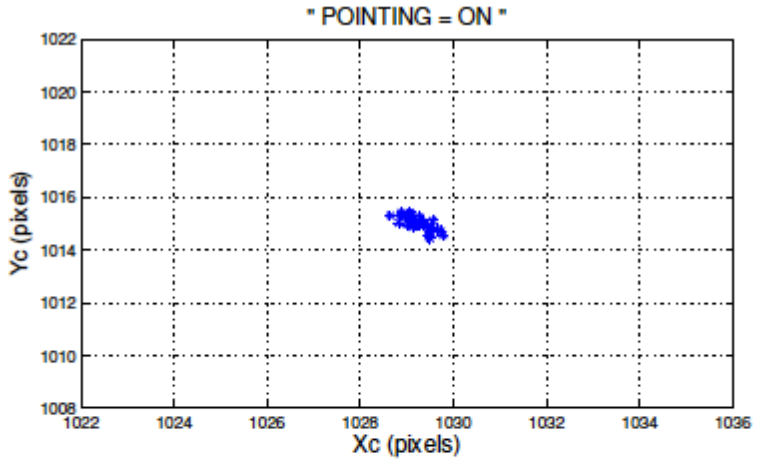

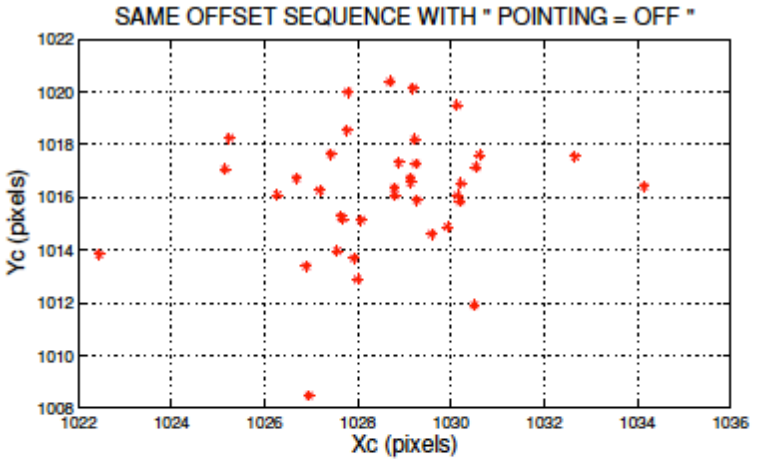

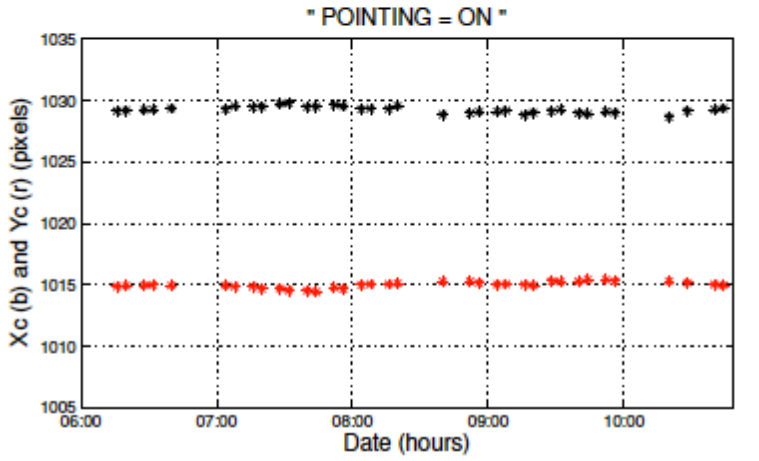

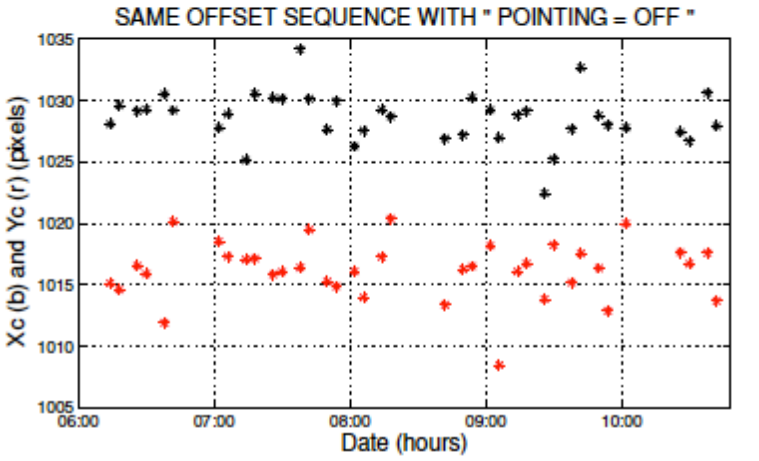

Sun image centers remain within one pixel - Pointing mechanism ON (left) and OFF (right). September 4, 2010.

4 – Scientific results

The SODISM CCD camera is in fact strongly impacted by the particles when the satellite crosses the SAA (South Atlantic Anomaly). We can also observe that it has a periodic variation on the Sun Diameter which corresponds to the satellite orbital period. This effect needs to be modeled (instrumental effect) to correct the solar radius measurements.

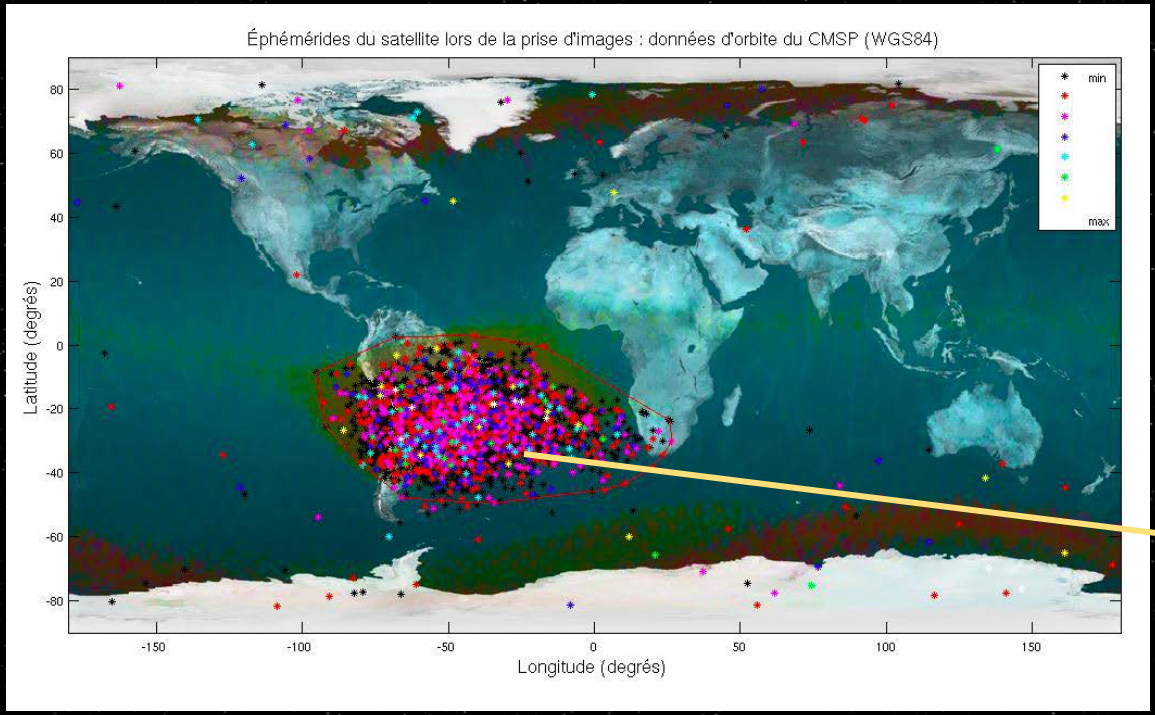

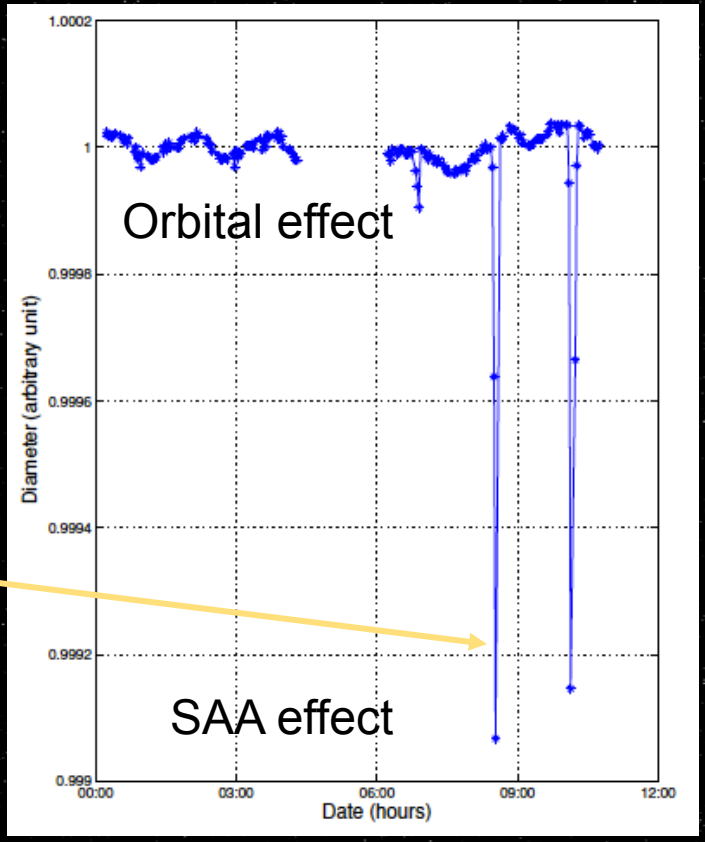

Sun diameter evolution (arbitrary units)

4 – Scientific results

SAA (South Atlantic Anomaly) → strong impact on the CCD

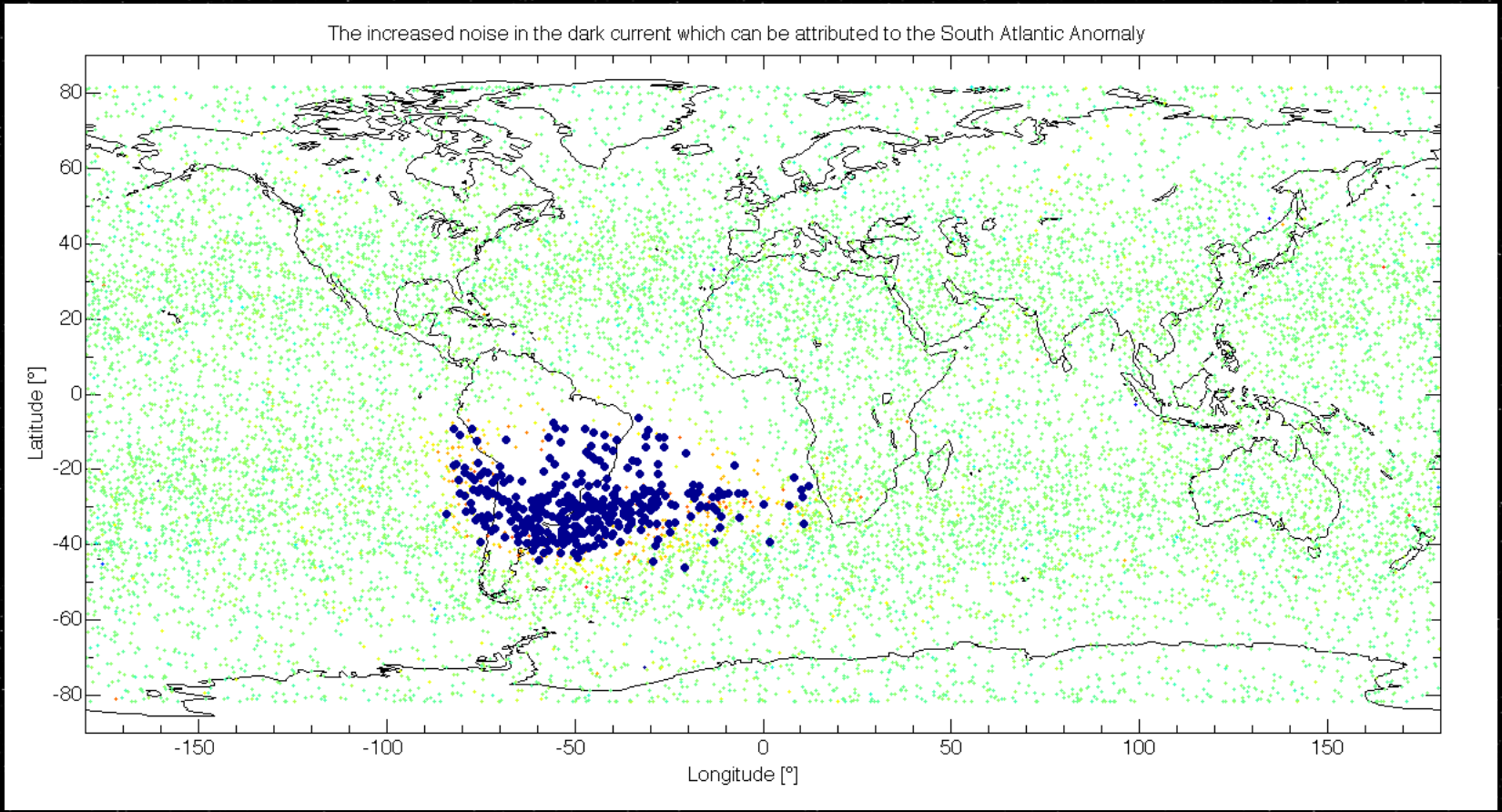

Solar Astrometry

Measure the diameter of the Sun (absolute value)

With PICARD/SODISM space instrument

4 – Scientific results

Solar radius determination is one of the oldest problems in astrophysics.
The transit of Venus on June 2012 provided a unique opportunity to determine the absolute radius of the Sun using solar imagers. The transit was observed from space by the PICARD spacecraft.

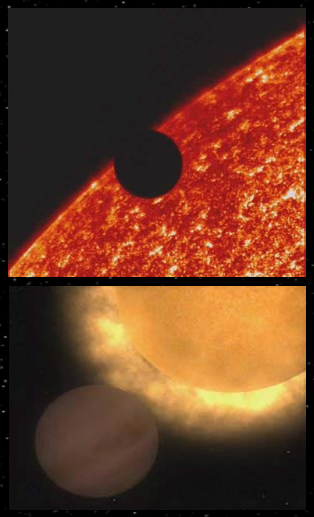

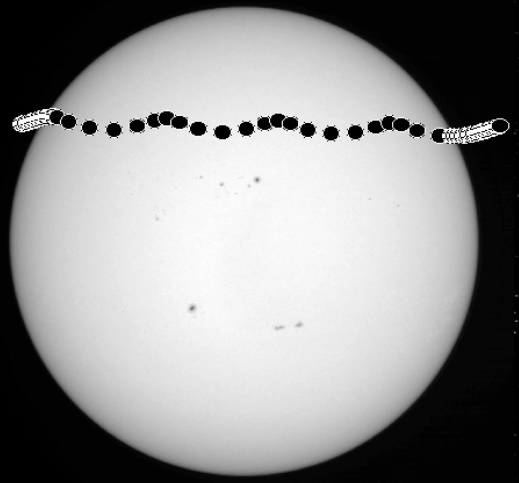

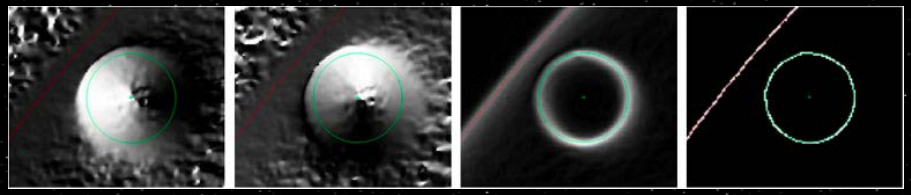

Meftah, Hauchecorne, Irbah et al., Sol. Physics, 2014

959.86 +/- 0.20 arc-seconds
Method: location of the inflection point

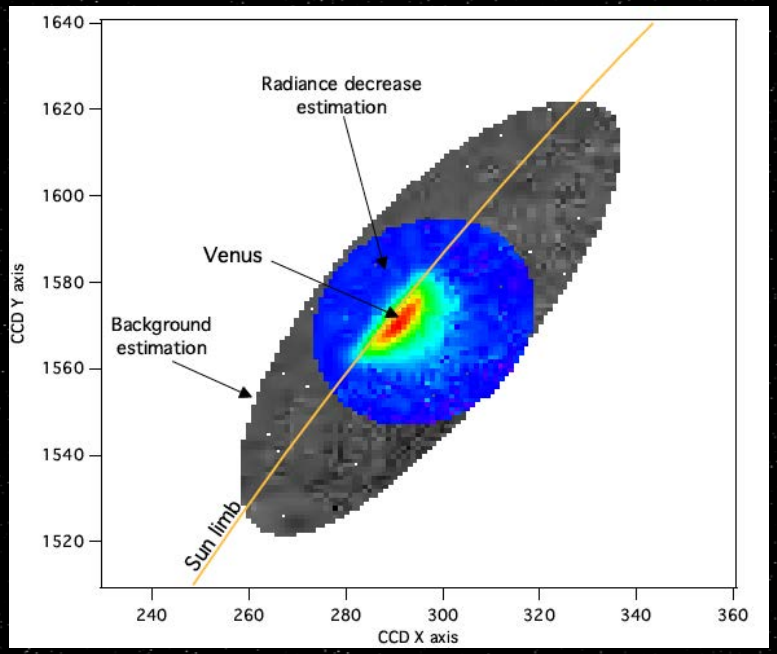

Hauchecorne, Meftah, Irbah et al., APJ, 2014

959.85 +/- 0.19 arc-seconds
Method: estimation of the decrease in the intensity (independent of the psf)

4 – Scientific results

Method for determining the radius of Venus and the Sun (IPP method)

- Noise removal (median filter to remove outlier pixels then a Gaussian blur is applied to smooth the edges in the image).
- Extracting contours (using a Sobel filter and the Canny method)

Auxiliary images obtained from prisms

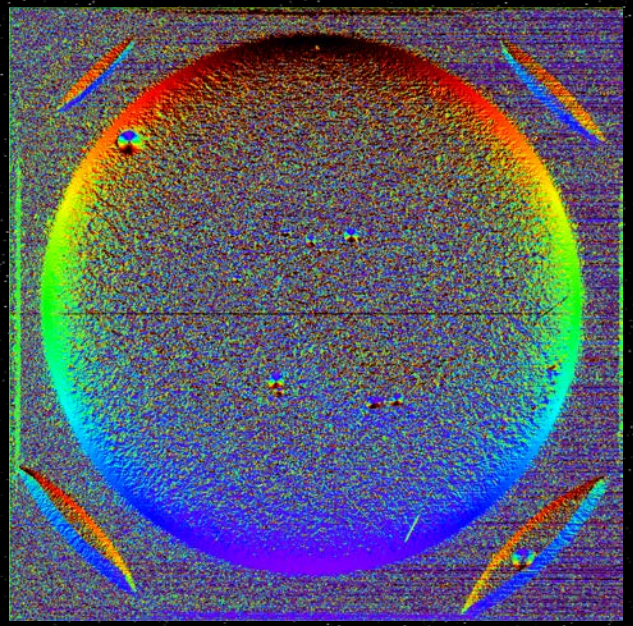

Horizontal gradient

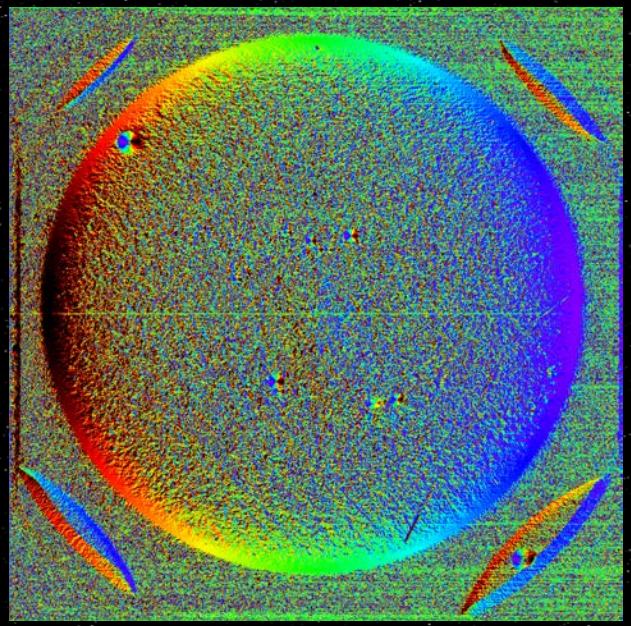

Vertical gradient

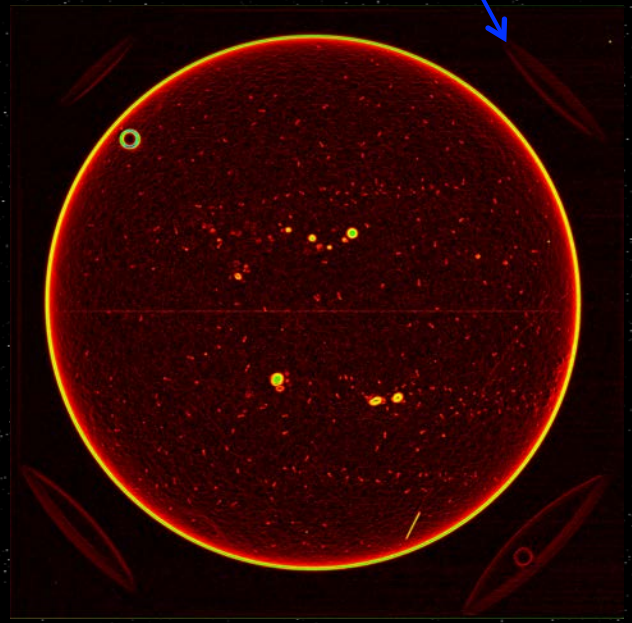

Norm of the gradient

4 – Scientific results

Method for determining the radius of Venus and the Sun (IPP method)

- Center detection using the Hough method
- Extracting the inflexion-point position (IPP)
- Characterizing the best fit (circle, ellipse, etc.)
- Determination of Venus radius and Sun radius

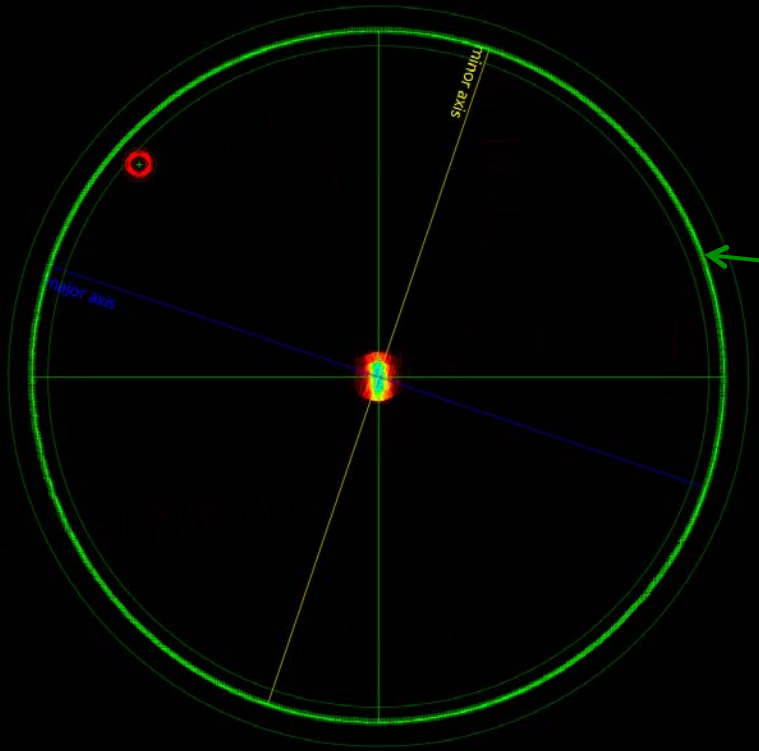

Venus and Sun “Hough” map

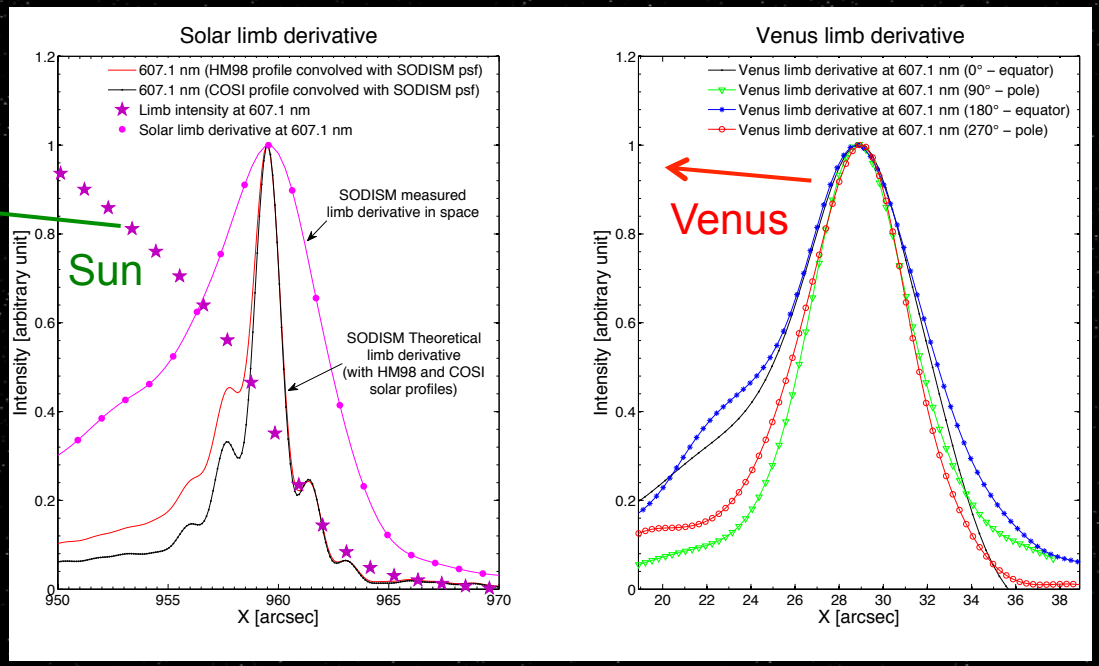

Extracting the inflexion-point position

4 – Scientific results

R = 696,156 ±145 km (PICARD)

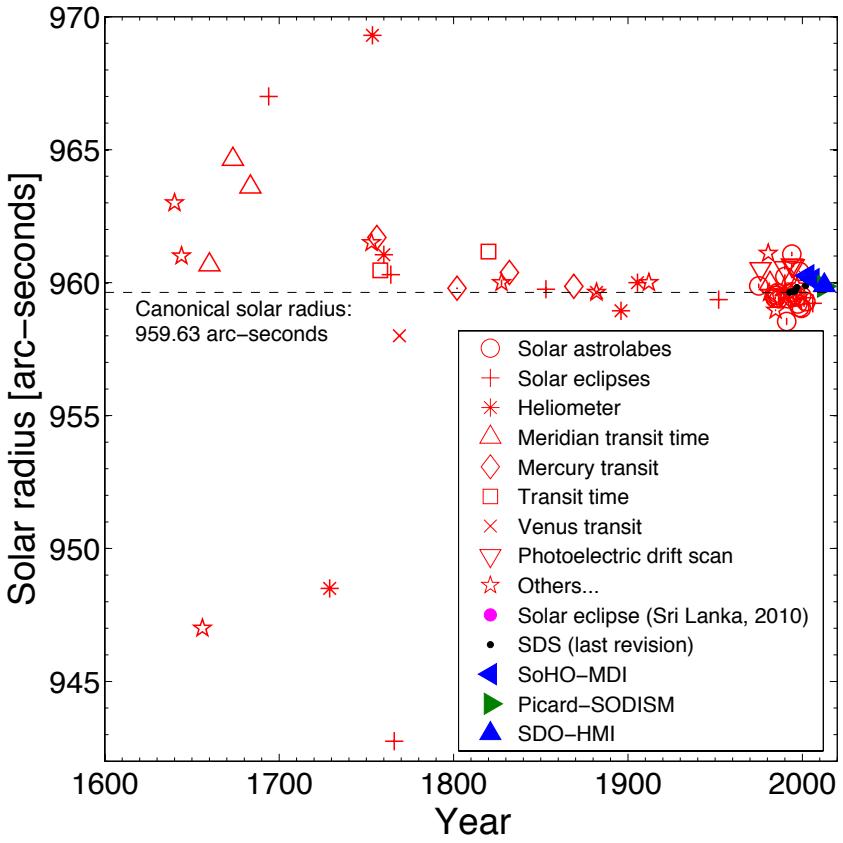

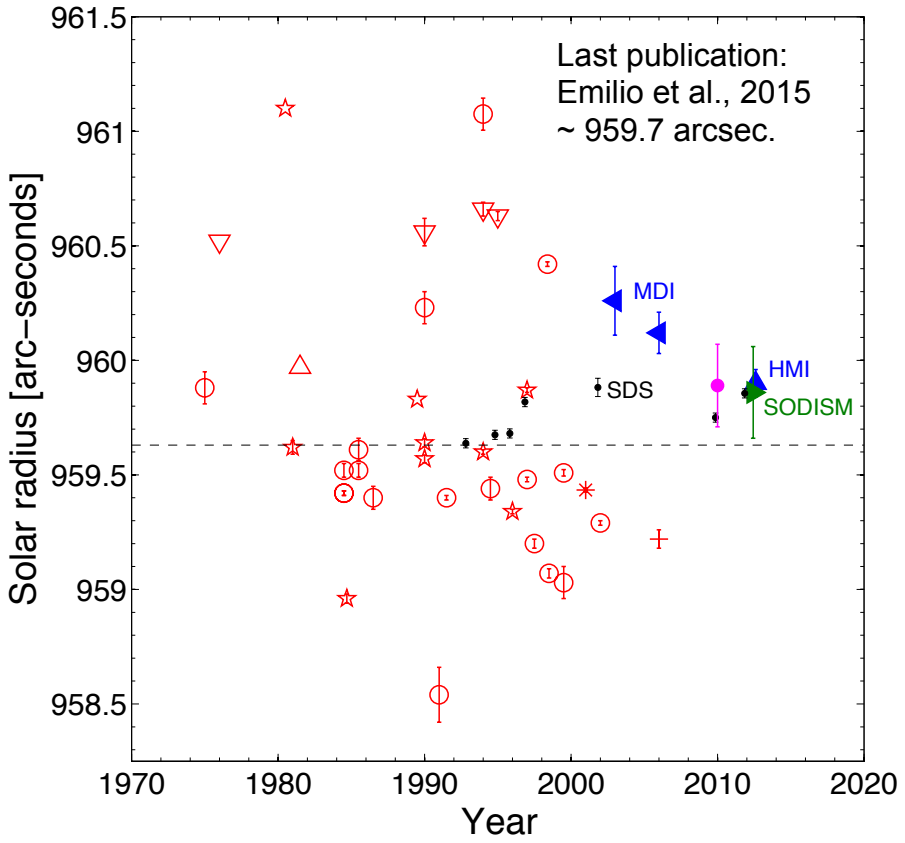

The work of the physicist is to establish a rigorous uncertainty budget.

Solar Astrometry

Measure the solar diameter variations over time

A) With PICARD ground-based facility
&
B) With PICARD/SODISM space instrument

4 – Scientific results

Measurements of the solar radius are of great interest within the scope of the debate on the role of the Sun in climate change.
Possible temporal variations of the solar radius are important as an indicator of internal energy storage and as a mechanism for changes in the TSI.

Space observations are a priori most favorable, however, space entails a harsh environment.
On ground, the instruments are affected by atmosphere.

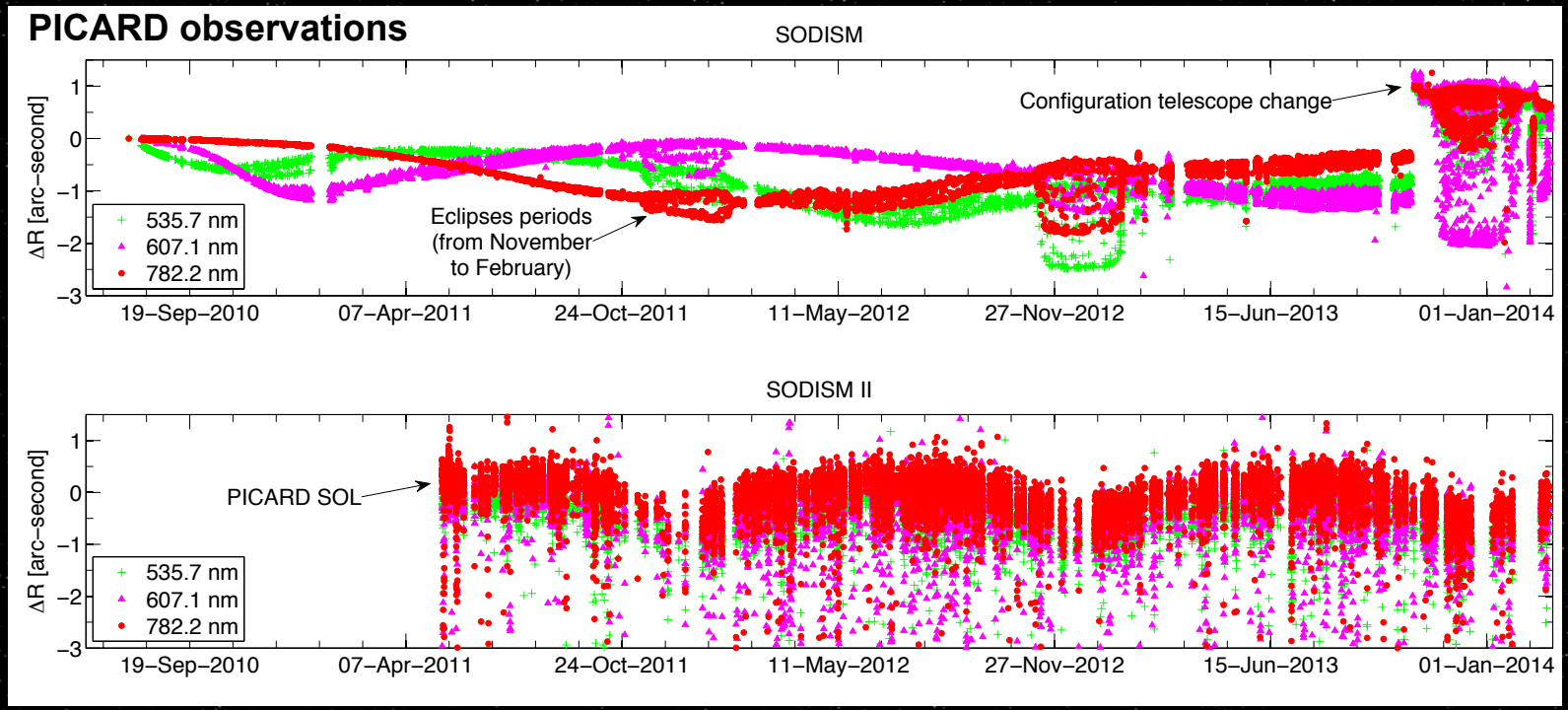

B) PICARD/ SODISM space instrument

A) PICARD ground-based facility

4 – Scientific results

After corrections

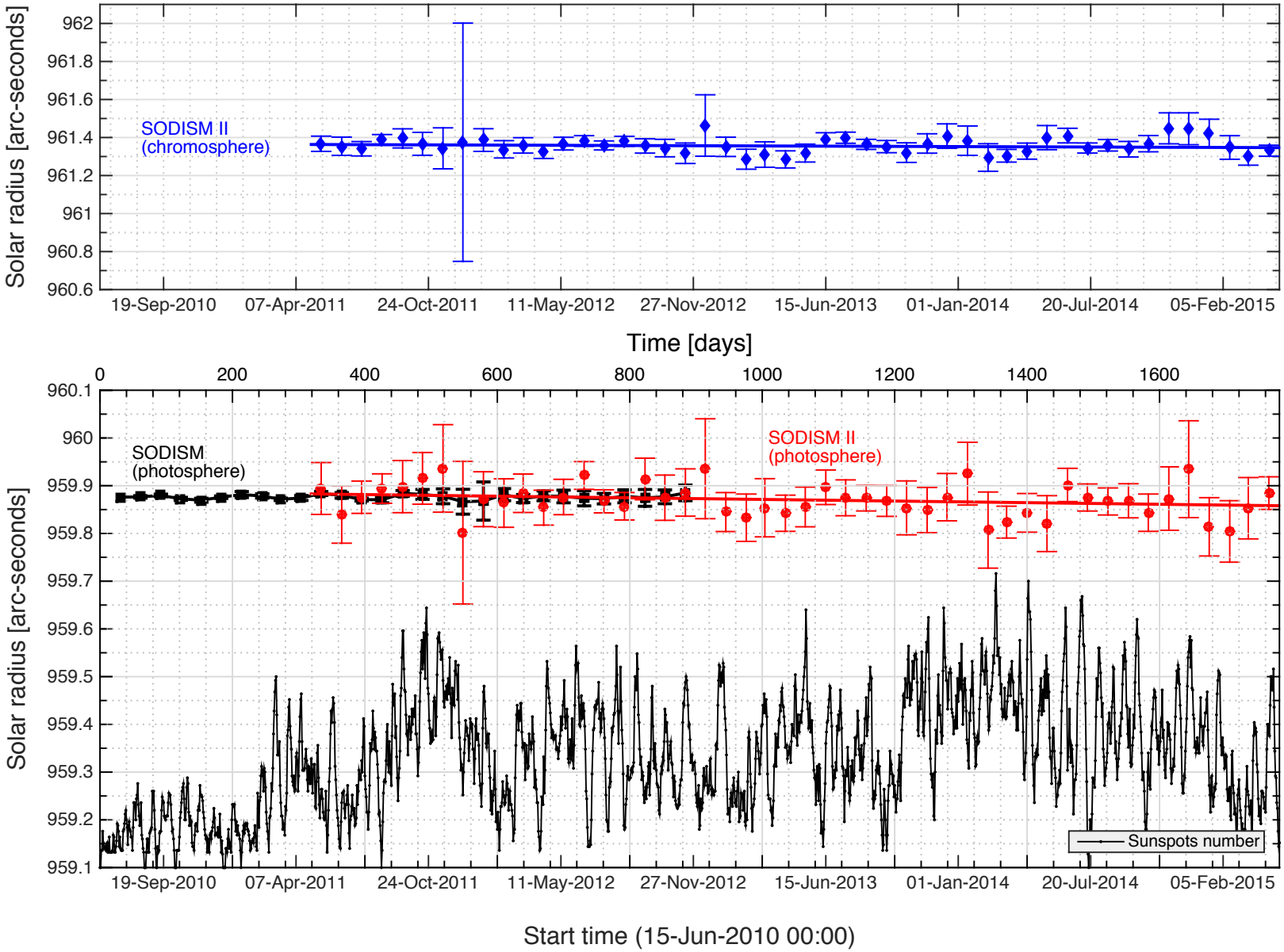

4 – Scientific results

A) PICARD ground-based facility corrections – Refraction and turbulence

Astronomical refraction (Ref) influences the solar radius measurements (more than 1 arc-seconds for observations made above 70° of zenith distance) that we obtain from images taken with SODISM II.

$$\mathrm{Ref} = \int_1^{n_{obs}} \tan\xi \frac{dn}{n} \quad (5a)$$

$$R_{cor} \simeq R_{obs} \times \left(C_{ref}\left(T_a, P_a, f_h, \lambda, z\right)\right)^{-1} \quad (5b)$$

$$C_{ref}\left(T_a, P_a, f_h, \lambda, z\right) = 1 - k\left(T_a, P_a, f_h, \lambda\right) \times \left(1 + 0.5 \times \tan^2(z)\right) \quad (5c)$$

$$k\left(T_a, P_a, f_h, \lambda\right) = \alpha_r\left(T_a, P_a, f_h, \lambda\right) \times \left(1 - \beta(T_a)\right), \quad (5d)$$

where $\alpha_r(T_a, P_a, f_h, \lambda)$ is the air refractivity for local atmospheric conditions at a given wavelength (Ciddor 1996), and $\beta(T_a)$ (see (Appendix B)) is the ratio between the height of the equivalent homogeneous atmosphere and the Earth radius of curvature at observer position assuming the ideal gas law for dry air (Ball 1908). In our calculation, we used a mean value of $k(T_a, P_a, f_h, \lambda)$.

$\alpha_r(T_a, P_a, f_h, \lambda)$ is the air refractivity for local atmospheric conditions at a given wavelength, and $n(T_a, P_a, f_h, \lambda)$ is the refractive index of air at the instrument (Ciddor 1996):

$$\alpha_r\left(T_a, P_a, f_h, \lambda\right) = n\left(T_a, P_a, f_h, \lambda\right) - 1. \quad (11)$$

$\beta(T_a)$ is the ratio between the height of the equivalent homogeneous atmosphere and the Earth radius of curvature at the observer position assuming the ideal gas law for dry air:

$$\beta(T_a) = \frac{P_a}{\rho \times g \times r_c} = \frac{C_a \times T_a}{r_c}, \quad (12)$$

where ρ is the air density, g is the gravity acceleration, C_a is a constant equal to 29.255 m K^{-1} (on the assumption that the ideal gas law is obeyed), and r_c represents the curvature of the Earth at Calern (~6,367,512 m).

Corrections are classics. Our ground results (PICARD SOL) were corrected for the effects of refraction and turbulence by numerical methods.

4 – Scientific results

The Figure shows the evolution of variations in solar radii observed at one AU by the two telescopes of the PICARD mission.

On the other hand, measurements carried out in orbit by SODISM show solar radius variations that are much greater than the expected order of magnitude (several milli-arc-seconds). The different measurements obtained from space show a temporal trend, which is wavelength dependent (this can be up to 3 arc-seconds on solar radius variations). For space data, the problem is complex.

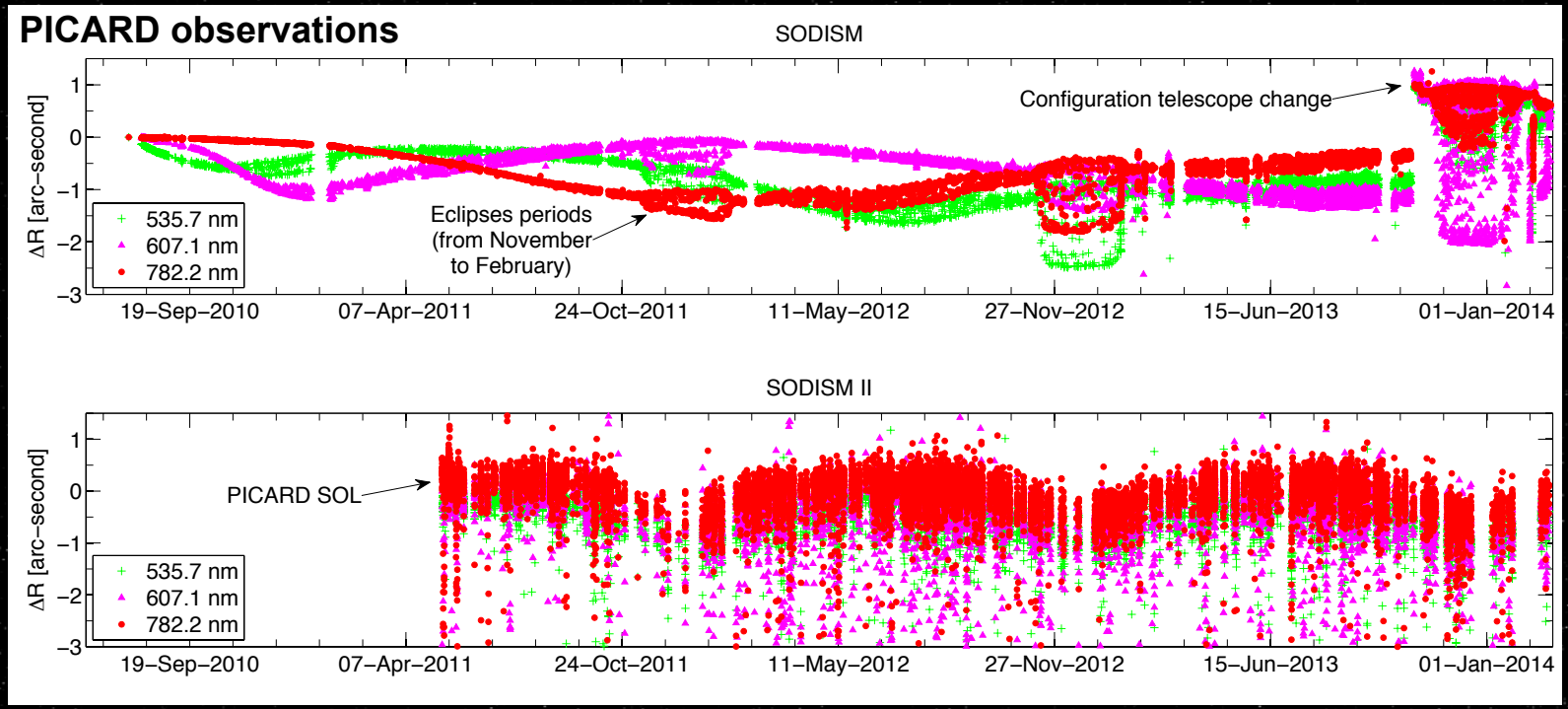

B) PICARD/ SODISM space instrument

A) PICARD ground-based facility

4 – Scientific results

B) PICARD SODISM space instrument solar radius variations and corrections

Several physical phenomena can lead to severe degradation of the optical performance of our space results (PICARD). In the case of SODISM, these effects entail solarization and polymerization of molecular contamination.

--- Normalized time series of integrated intensity during the PICARD space mission
→ High degradation in the UV

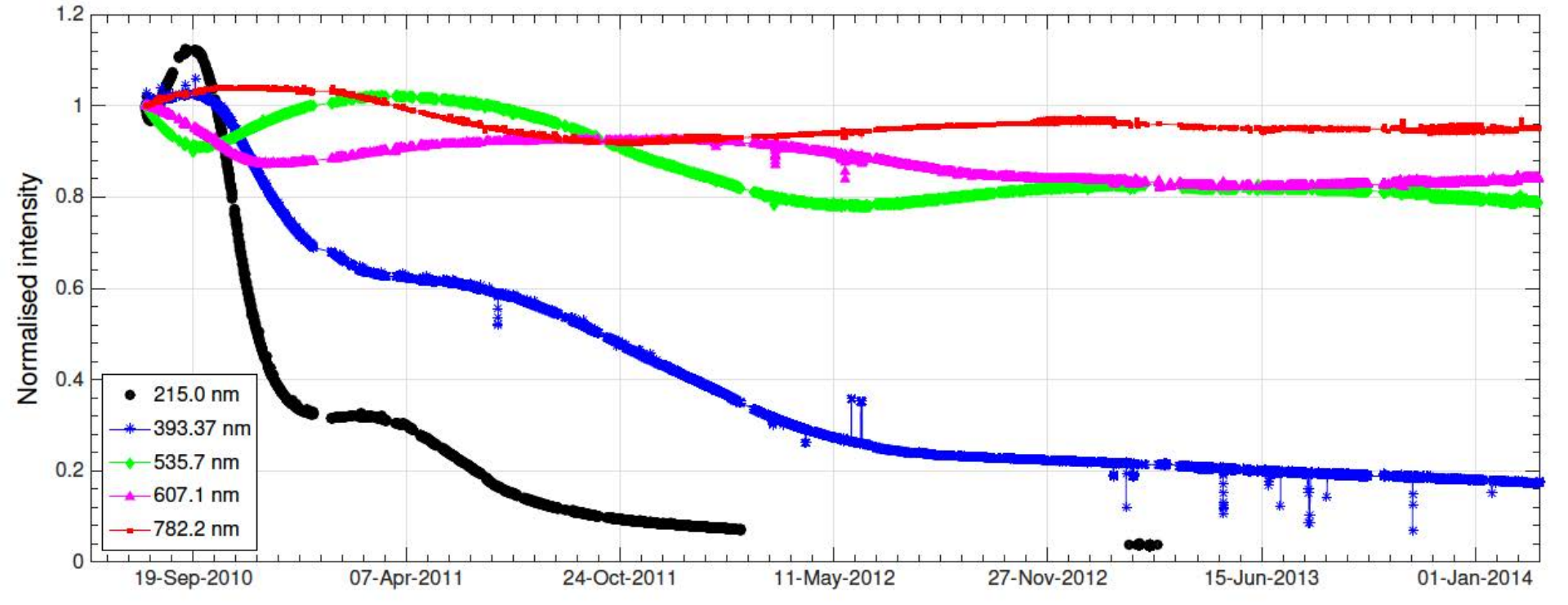

4 – Scientific results

B) PICARD SODISM space instrument solar radius variations

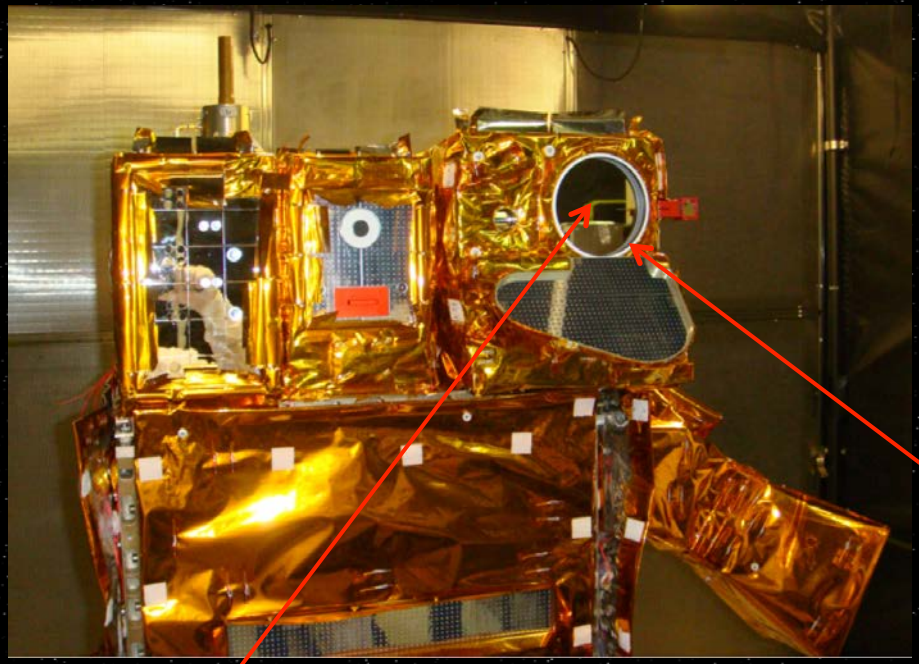

Two different solar absorption evolutions (optics, contour)

→ There is a very strong contamination of the satellite (due to solar panels, during the launch, etc.)

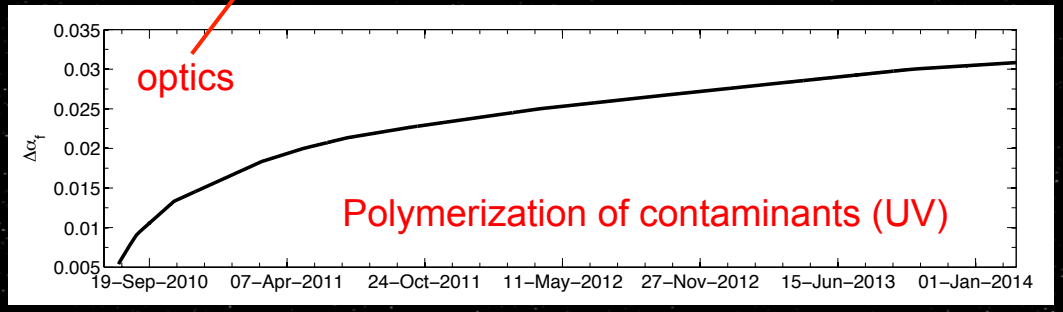

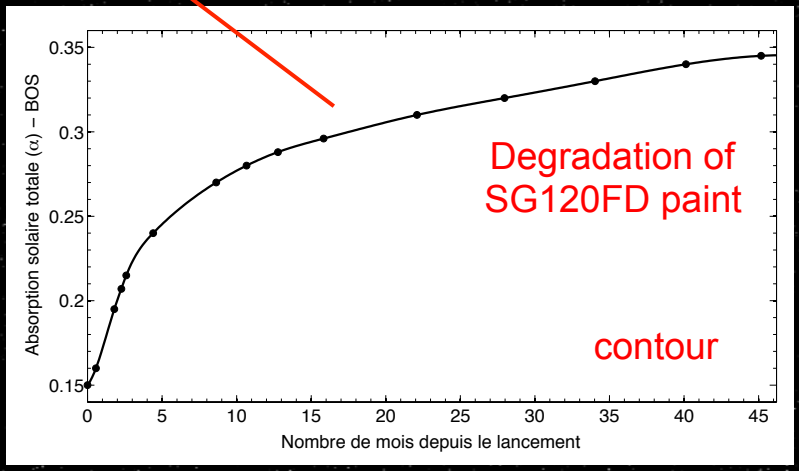

4 – Scientific results

B) PICARD SODISM space instrument measurements

--- Normalized time series evolution (contamination)

--- Important temperature change of SODISM front window and direct impact on solar radius measurements

→ How to correct the data?

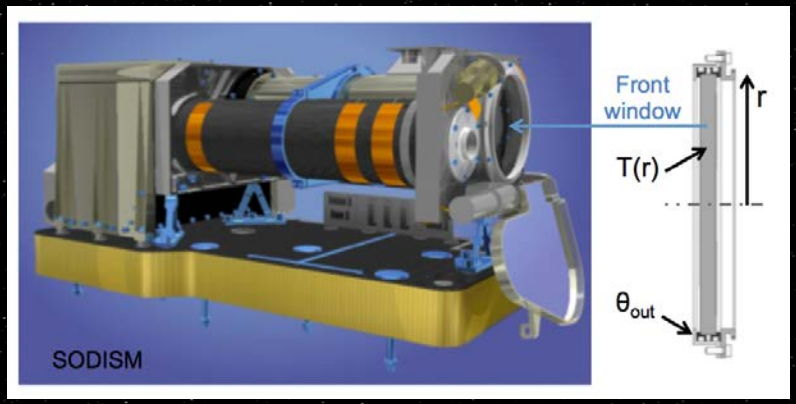

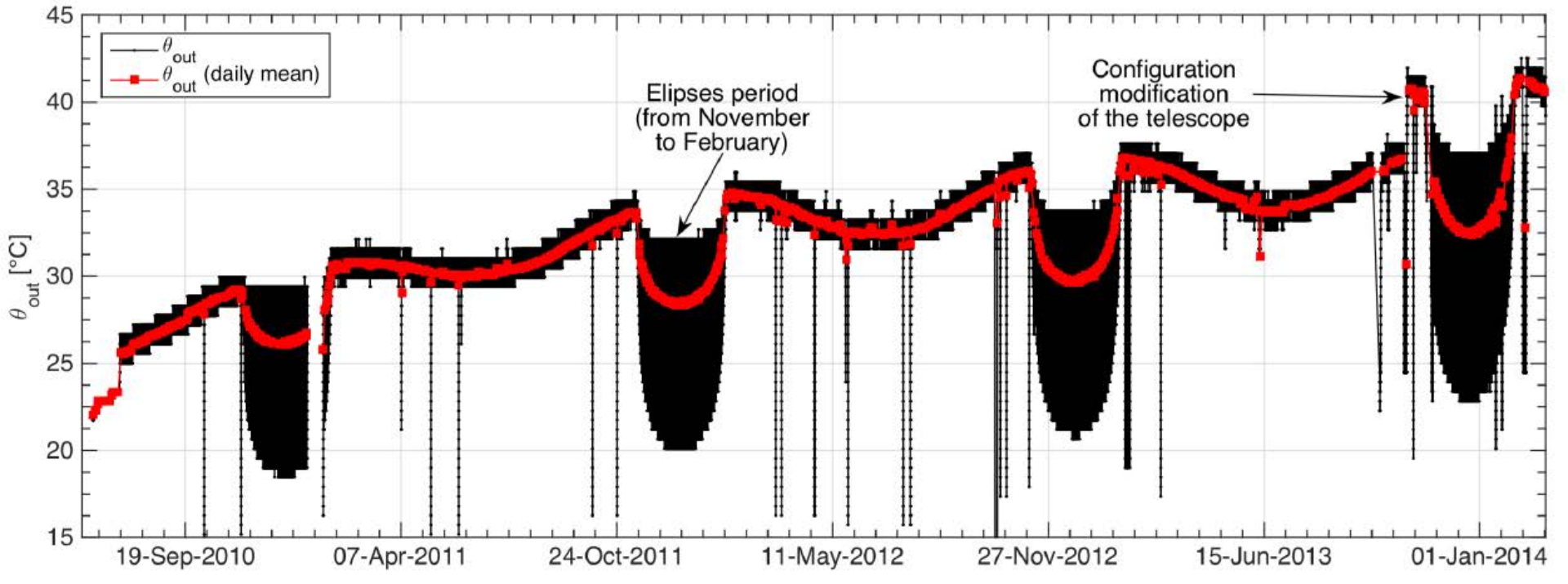

4 – Scientific results

B) PICARD SODISM space instrument measurements

We developed a simulator to try to correct the “signal” (thermo-optical effect).

Solar Spectrum (Atlas 3)
Solar flux (SOVAP, PREMOS, TIM, etc.)
IR and albedo flux (BOS)

SODISM intensities

Front window temperatures as function of housekeeping data

$$T = T_\infty + \frac{Flux}{\varepsilon_{out} \times \sigma \times \overline{T}} + C_1 \times J_0(i \times r \times C) + C_2 \times Y_0(i \times r \times C)$$

Wave-front and Zenike polynomials

$$W_0 = \sum_{k=1}^{36} Z_k = f\left(\lambda, \frac{\partial n}{\partial T}, \Delta T(\alpha_f), \ldots\right)$$

Front window index vs. temperature

$$\frac{\partial n}{\partial T} = A_0 + A_1 \times \exp\left(\frac{-\lambda}{B_1}\right) + A_2 \times \exp\left(\frac{-\lambda}{B_2}\right)$$

$$E = \exp(2i \times \pi \times W_0)$$ Complex Wave-front

$$PSF_{SODISM} = (FFT2(E))^2$$ PSF

Bi-dimensional fast Fourier transformer

$$M_{False}(t) = FI_{SODISM}(t) * M_{True}(t)$$

Many instruments have this problem.

$$LDF_{SODISM} = \left(\sum PSF_{SODISM}\right) * (LDF)$$ Limb darkening function → LDF_{SODISM}

Convolution

4 – Scientific results

B) PICARD SODISM space instrument measurements

Relation between solar radius and temperature gradient

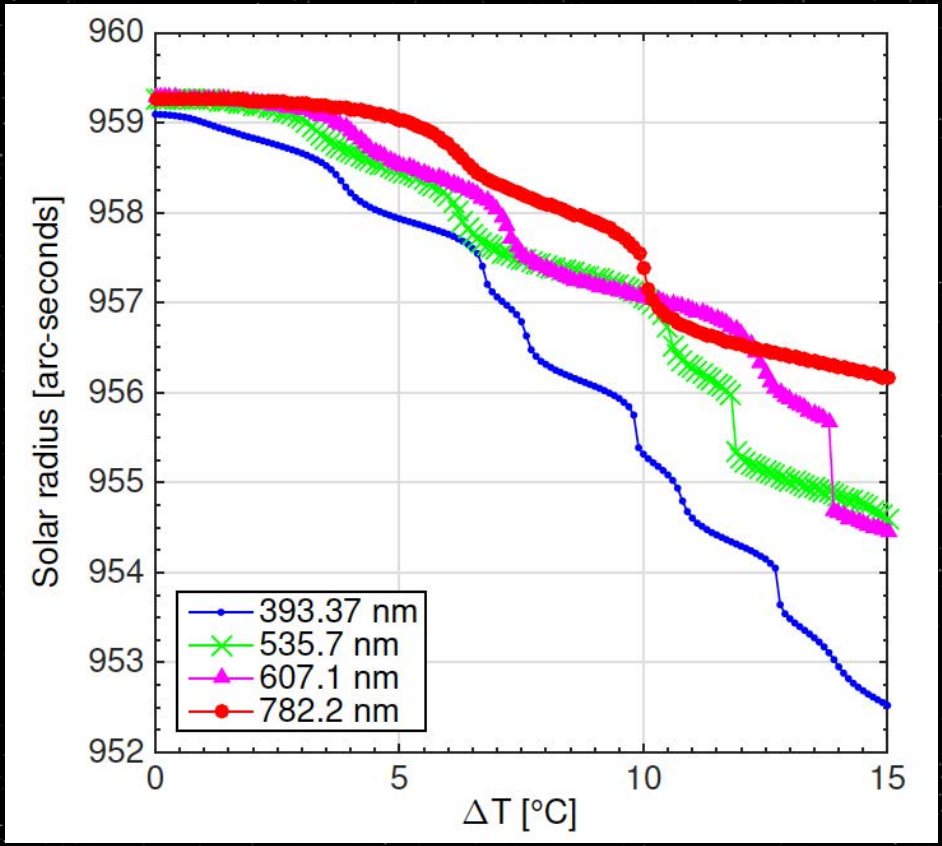

Evolution of the solar radius (determined by the inflection point method) as a function of a temperature gradient for different wavelengths.

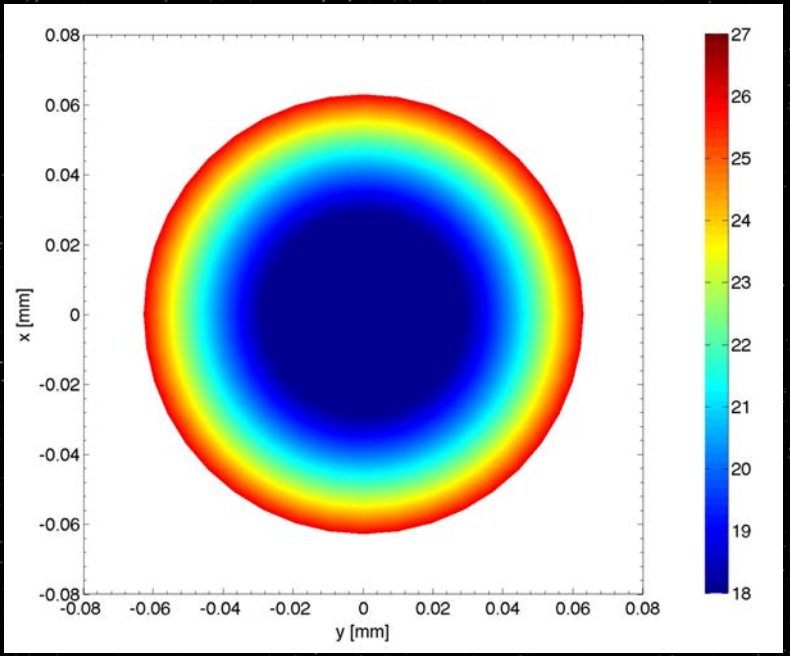

Temperature gradient on SODISM front window

4 – Scientific results

B) PICARD SODISM space instrument measurements

The space environment (UV effects, contamination, thermal cycling, etc.) combined with initial defects in telescope calibration (astigmatism, position of the focal plane, etc.) can degrade considerably the measurements taken by our instrument.

Solar models :
- COSI
- HM98
- Neckel2005

SODISM PSF is predominant

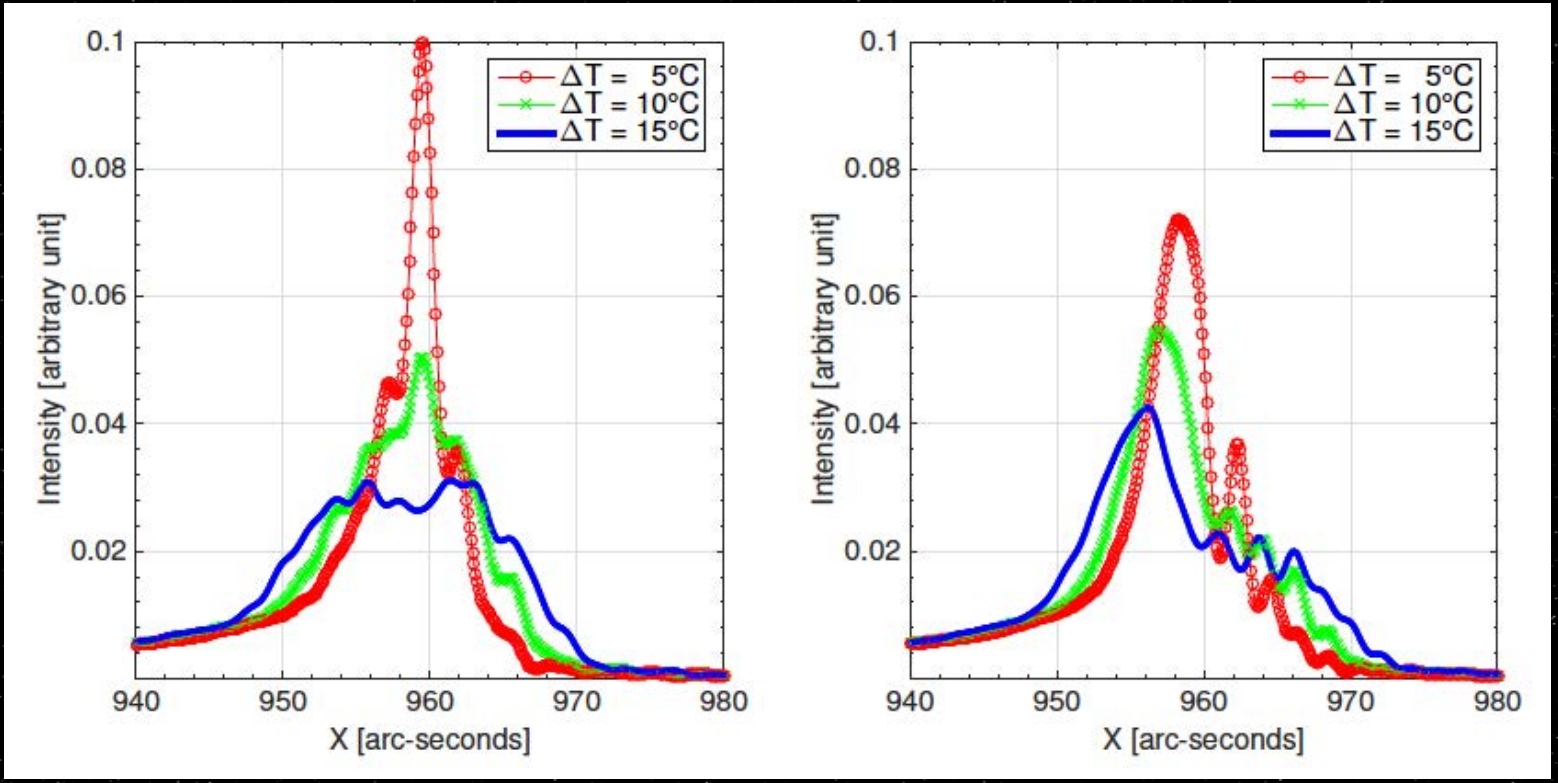

Evolution of the solar limb first derivative (simulation) for different angular sectors of the image. Consistent with what we observe.

4 – Scientific results

B) PICARD SODISM space instrument measurements

Temperature gradient evolution and uncertainty budget of the model

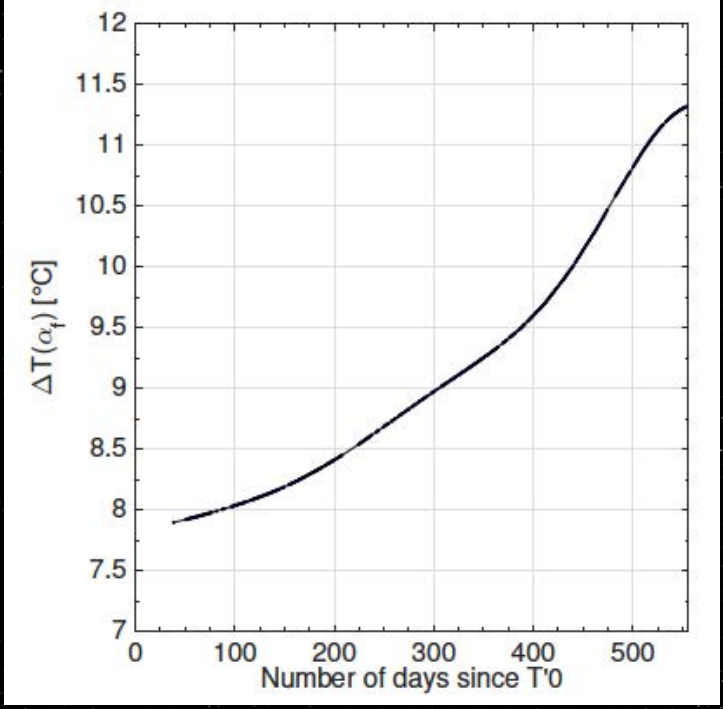

Evolution of the front window temperature gradient.

Uncertainty sources	Typical values	Uncertainty	Error on ΔT [°C]	Uncertainty type
$\alpha_f{}^{(a)}$	0.14	±0.001	±0.10	Test (S) & aging (R)
$\varepsilon_{out}{}^{(b)}$	0.81	±0.01	±0.30	Test (S)
$\Lambda^{(b)}$	1.38 $W.m^{-1}.K^{-1}$	±0.04 $W.m^{-1}.K^{-1}$	±0.31	Test (S)
$\theta_{out}{}^{(a)}$	22 °C	±0.10	±0.03	Calibration & measurement (S)
$\varphi_S{}^{(c)}$	1,362 $W.m^{-2}$	±2.4 $W.m^{-2}$	±0.02	Measurement (S)
$\varphi_{IR}{}^{(c)}$	238 $W.m^{-2}$	±6.0 $W.m^{-2}$	±0.02	Literature (S & R)
$\varphi_A{}^{(c)}$	~20 $W.m^{-2}$	±9.0 $W.m^{-2}$	±0.02	Literature (S & R)

Uncertainty budget.

- Spectral reflection and transmission measurements were performed with a spectrophotometer (Agilent Cary 5000 UV-NIS-NIR). The estimated tolerances are expected to be less than +/-1%.
- Near-normal IR reflectance measurements were performed in accordance with ASTM E408 (with an IR Reflectometer model DB100). The estimated tolerances are expected to be less than +/-1.5%.
- etc…

4 – Scientific results

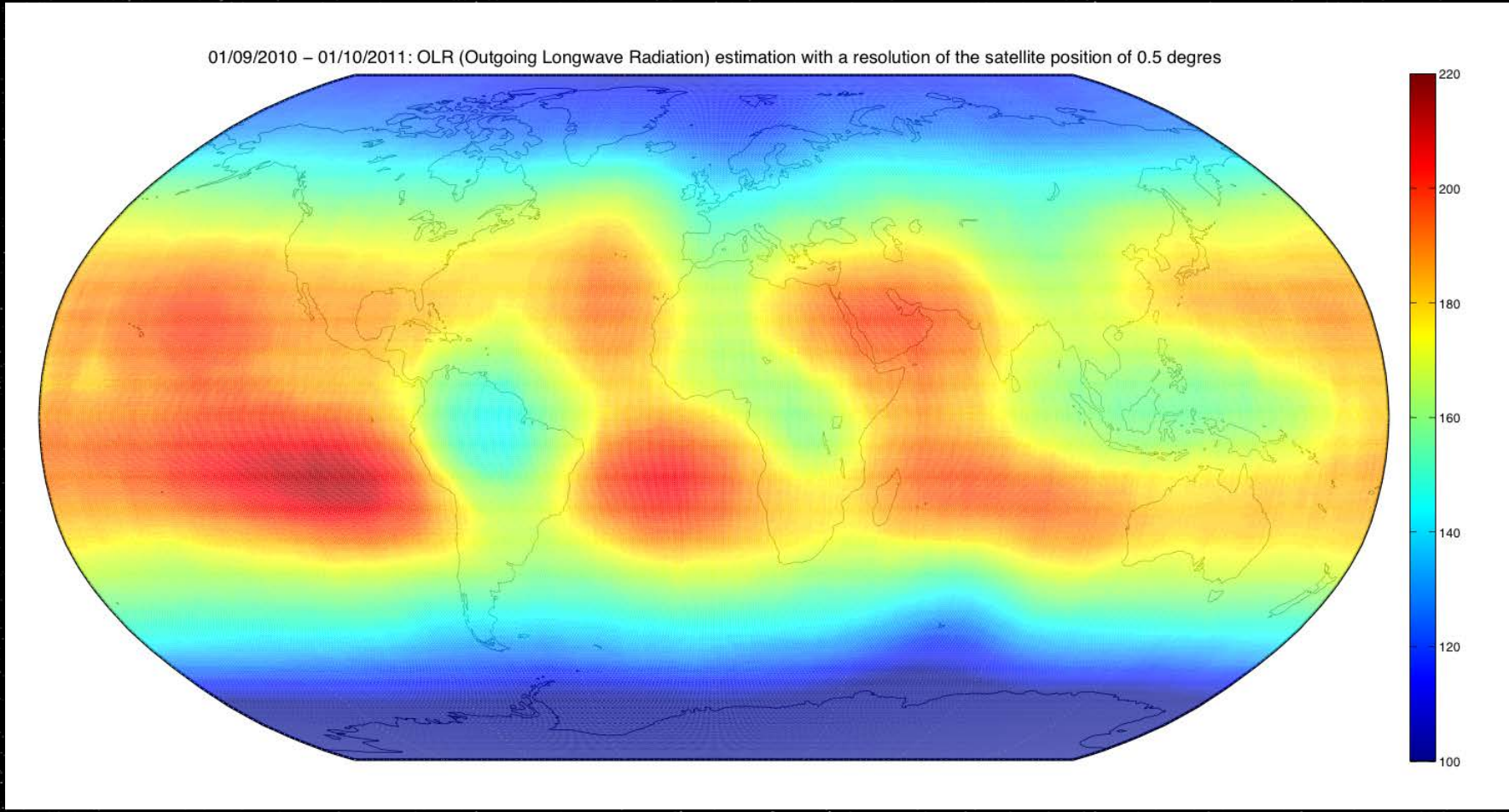

IR flux used in the model (obtained with PICARD data).

4 – Scientific results

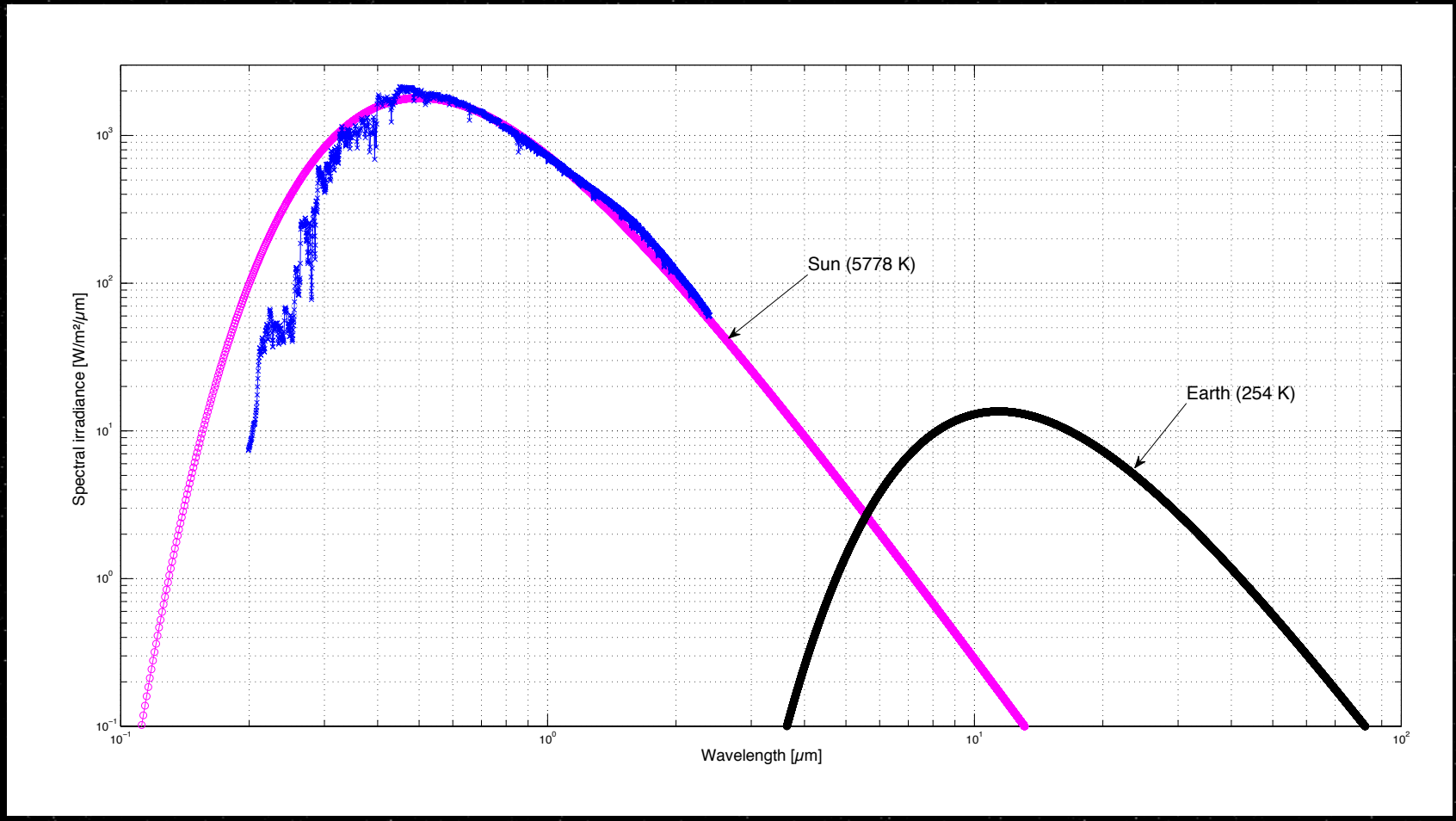

Solar spectrum used (ATLAS 3) in the model (obtained with PICARD data).

4 – Scientific results

Model equations:

$$T_{it+1}(r,t) = T_\infty + \frac{\text{Flux}(t)}{\varepsilon_{\text{out}} \times \sigma_b \times \overline{T(t)}} + C_1(t) \times J_0(i \times r \times C(t)) + C_2(t) \times Y_0(i \times r \times C(t)) \quad (3a)$$

$$\text{Flux}(t) = \alpha_f(t) \times \varphi_S(t) + \varepsilon_{\text{out}} \times fv_{ir}(t) \times \varphi_{IR}(t) + \alpha_f(t) \times fv_a(t) \times \varphi_A(t) \quad (3b)$$

$$\overline{T(t)} = \left(T_\infty + T_{it}(r,t)\right) \times \left(T_\infty^2 + T_{it}(r,t)^2\right) \quad (3c)$$

$$C(t) = \sqrt{\frac{\varepsilon_{\text{out}} \times \sigma_b \times \overline{T(t)}}{\Lambda \times h_w}} \quad (3d)$$

$$C_1(t) = \left(-\theta_{\text{out}}(t) \times Y_1\left(i \times r_c \times C(t)\right)\right) / \left(J_1\left(i \times r_c \times C(t)\right) \times Y_0\left(i \times r_{\text{out}} \times C(t)\right) - J_0\left(i \times r_{\text{out}} \times C(t)\right) \times Y_1\left(i \times r_c \times C(t)\right)\right) \quad (3e)$$

$$C_2(t) = \frac{-C_1(t) \times J_1\left(i \times r_c \times C(t)\right)}{Y_1\left(i \times r_c \times C(t)\right)}, \quad (3f)$$

Thermal model with Bessel functions

Optical model

$$w_0 = \sum_{k=1}^{36} C_k \times Z_k(\rho, \theta) \quad (1a)$$

$$C_3 = \frac{\delta \times D_{PS}^2}{16 \times \lambda \times f_S^2} + \frac{1}{2 \times \lambda} \times \frac{\partial n}{\partial T} \times h_w \times \Delta T(\alpha_f) \quad (1b)$$

$$\frac{\partial n}{\partial T} = A_0 + A_1 \times \exp\left(\frac{-\lambda}{B_1}\right) + A_2 \times \exp\left(\frac{-\lambda}{B_2}\right), \quad (1c)$$

$$W\left(P_x, P_y\right) = A_{D_{PS}} \times e^{2i \times \pi \times w_0} \quad (2a)$$

$$\text{PSF}_{\text{SODISM}}(x,y) = \int_{-\infty}^{+\infty} \int_{-\infty}^{+\infty} W\left(P_x, P_y\right) \times e^{2i \times \pi \times \left(x \times P_x + y \times P_y\right)} \, dP_x \, dP_y \quad (2b)$$

$$\text{LDF}\left(r_S, \lambda\right) = \sqrt{1 - r_S^2}^{\,\alpha_S(\lambda)} \quad (2c)$$

$$\text{LDF}_{\text{SODISM}} = \int_{y_1}^{y_2} \text{PSF}_{\text{SODISM}}(x,y) dy \otimes \text{LDF}\left(r_S, \lambda\right). \quad (2d)$$

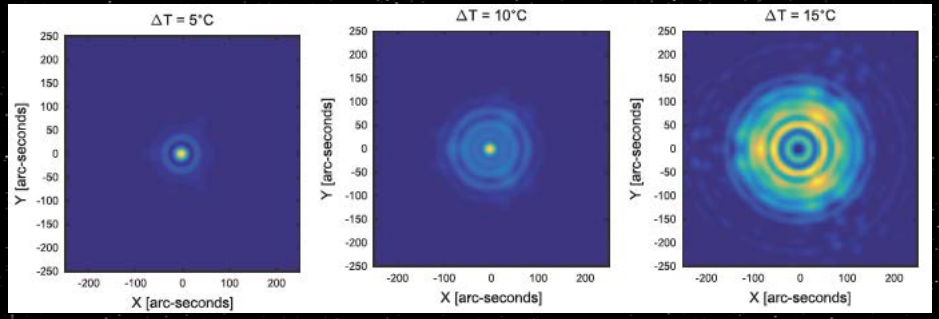

4 – Scientific results

B) PICARD SODISM space instrument measurements

Our space results (PICARD) were corrected for the temperature effects and contamination.

→ $\Delta R_{\odot} < 20$ *mas variations during the rising phase*

We find a small variation of the solar radius from space measurements with a typical periodicity (6.5 mas variation in the solar radius with a periodicity of 129.51 days → same with ground-based).

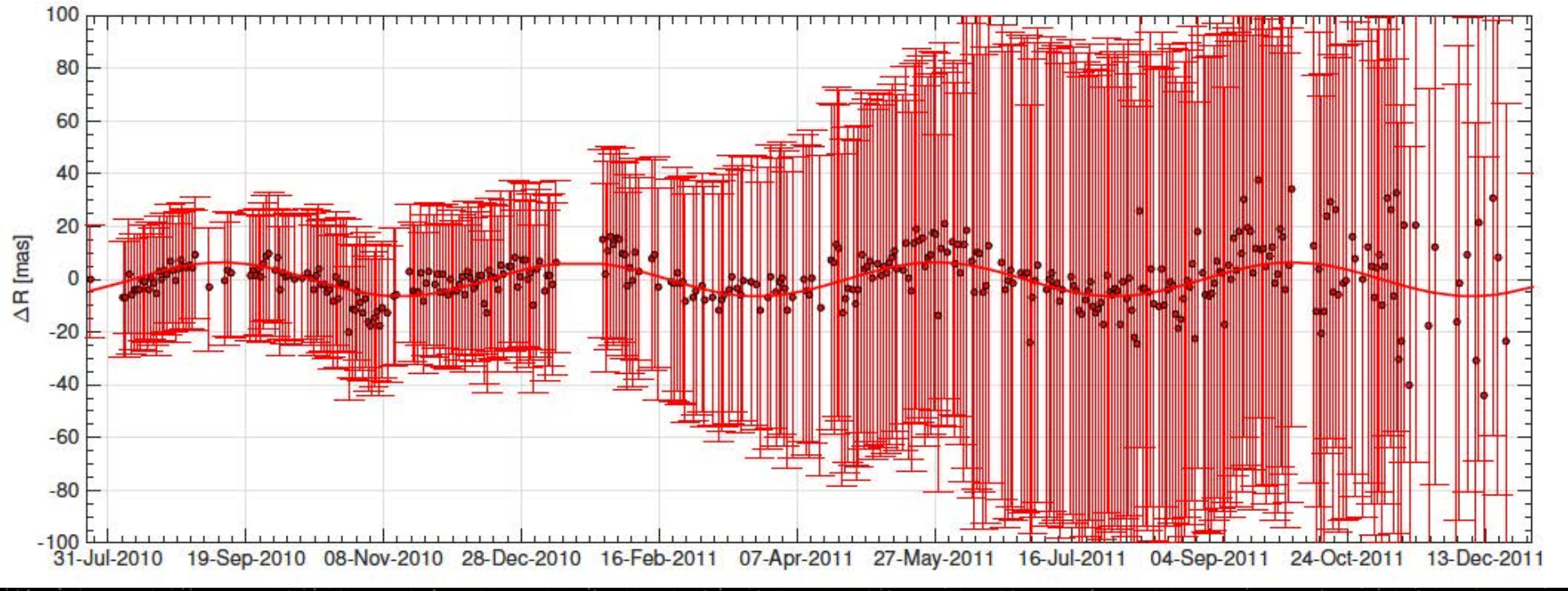

Meftah, Hauchecorne, Irbah et al., APJ (2015).

4 – Scientific results

B) PICARD SODISM space instrument measurements

For studies of our different time series data (solar radius), it is crucial to know at what time scales certain periodicities occur or recur.
In our application, we need to know the frequency and temporal information at the same time.
We use:
- Wavelet Analysis to Study Solar Radius
(in particular Morlet Wavelet)

$$W(b,a) = \frac{1}{\sqrt{a}} \int \psi^* \left(\frac{t-b}{a} \right) f(t) dt$$

It is common to have incomplete or unevenly sampled time series for a given variable. Determining cycles in such series is not directly possible with methods such as Fast Fourier Transform (FFT) and may require some degree of interpolation to fill in gaps. An alternative is the Lomb-Scargle method.

$$P_N(w) = \frac{1}{2\sigma^2} \left(\frac{\left(\sum_{k=1}^{N} (x_k - \bar{x}) \cos(w(t_k - \tau)) \right)^2}{\sum_{k=1}^{N} \cos^2(w(t_k - \tau))} + \frac{\left(\sum_{k=1}^{N} (x_k - \bar{x}) \sin(w(t_k - \tau)) \right)^2}{\sum_{k=1}^{N} \sin^2(w(t_k - \tau))} \right)$$

4 – Scientific results

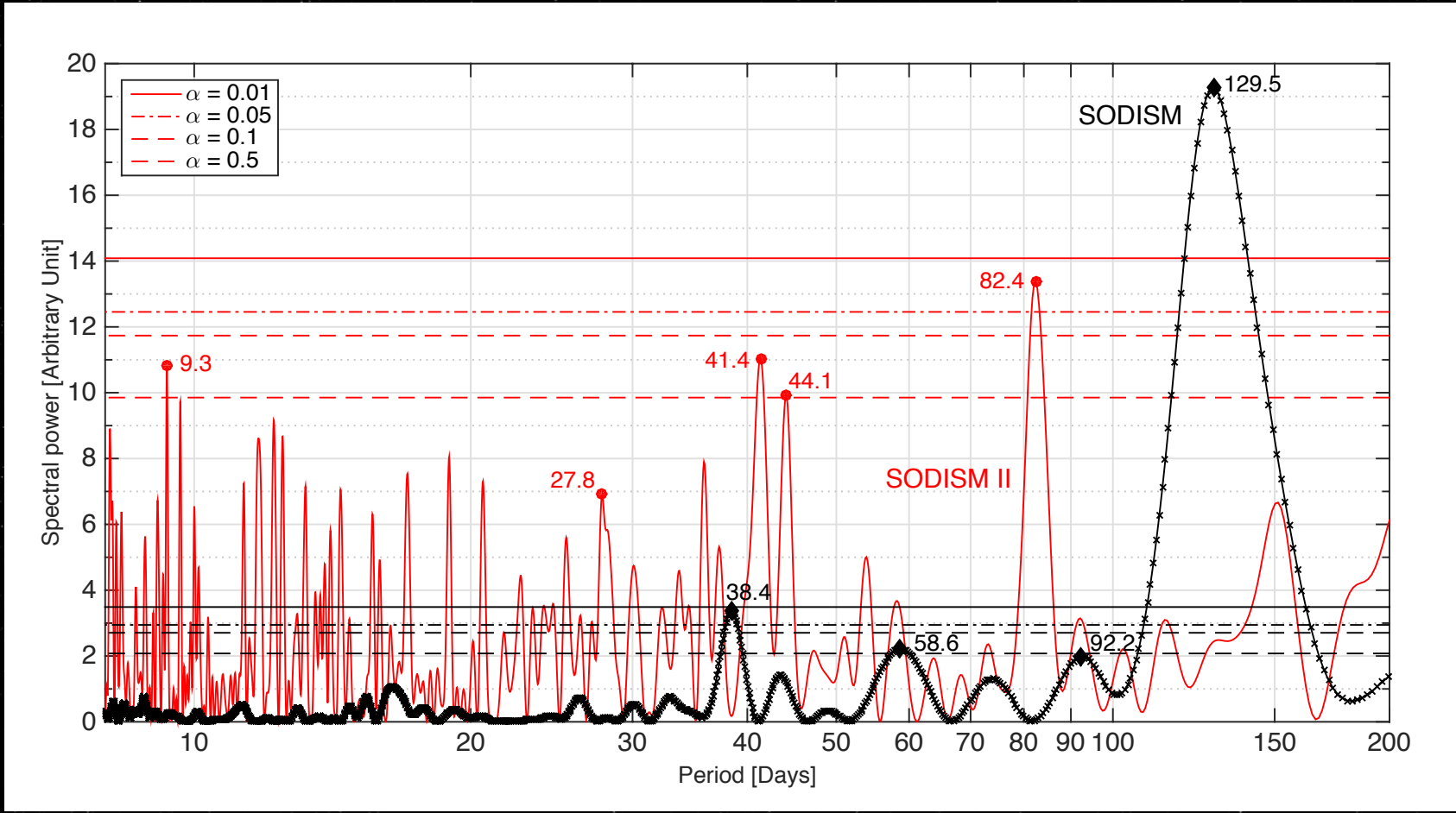

Solar radius Lomb-Scargles periodogram (all the data)

4 – Scientific results

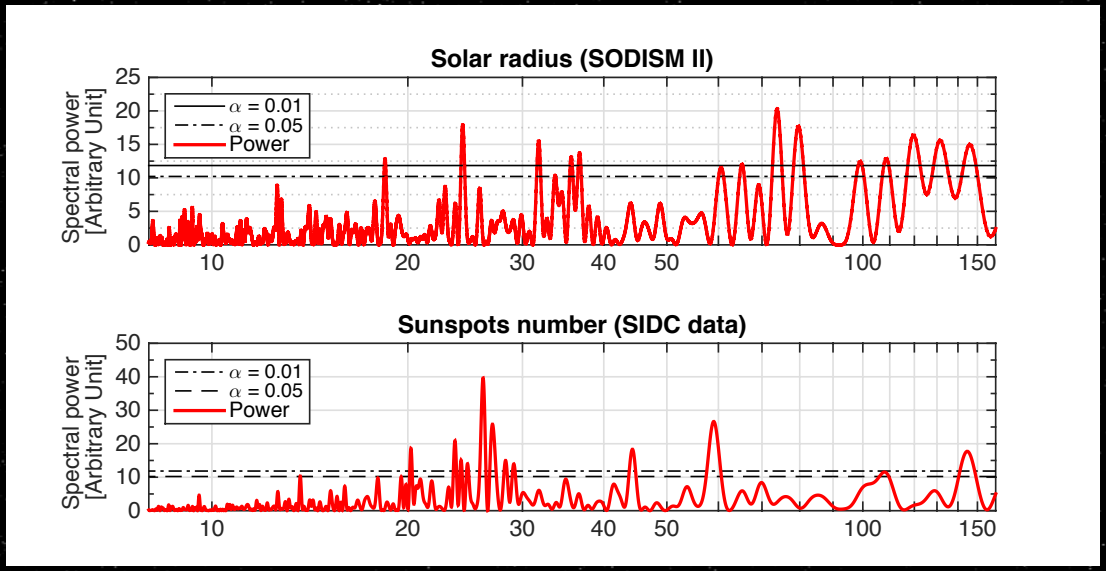

Solar radius Lomb-Scargles periodogram (daily mean) → better approach

→ $\Delta R_{\odot} < 20$ *mas variations*

Table 1. Solar radius periodicities with statistical significance level of over 99%. Long periodicities (greater than 300 days) are not resolved due to *Picard* short periods of observation.

Instrument	Period [days]	Variations [mas rms]
PICARD-SODISM	129.5	4.6
(Jul. 2010-Jan. 2012)	–	–
PICARD-SODISM II	18.4	14.5
(May 2011-May 2015)	24.3	16.2
	31.8	14.2
	35.6	12.0
	36.7	12.5
	65.1	11.5
	74.0	14.8
	79.5	14.9
	99.3	11.8
	108.4	11.1
	119.4	13.5
	131.4	13.4
	146.0	12.9

This finding sheds new light on the solar dynamo mechanism, where very small solar radius variations (0.02 arc-second root mean square) are linked with magnetic activity for typical solar periodicities (130-days (Bai, 2003) and 154-days (Rieger period)). Periodicities in Solar Flare Occurrence (130-days) link.

4 – Scientific results

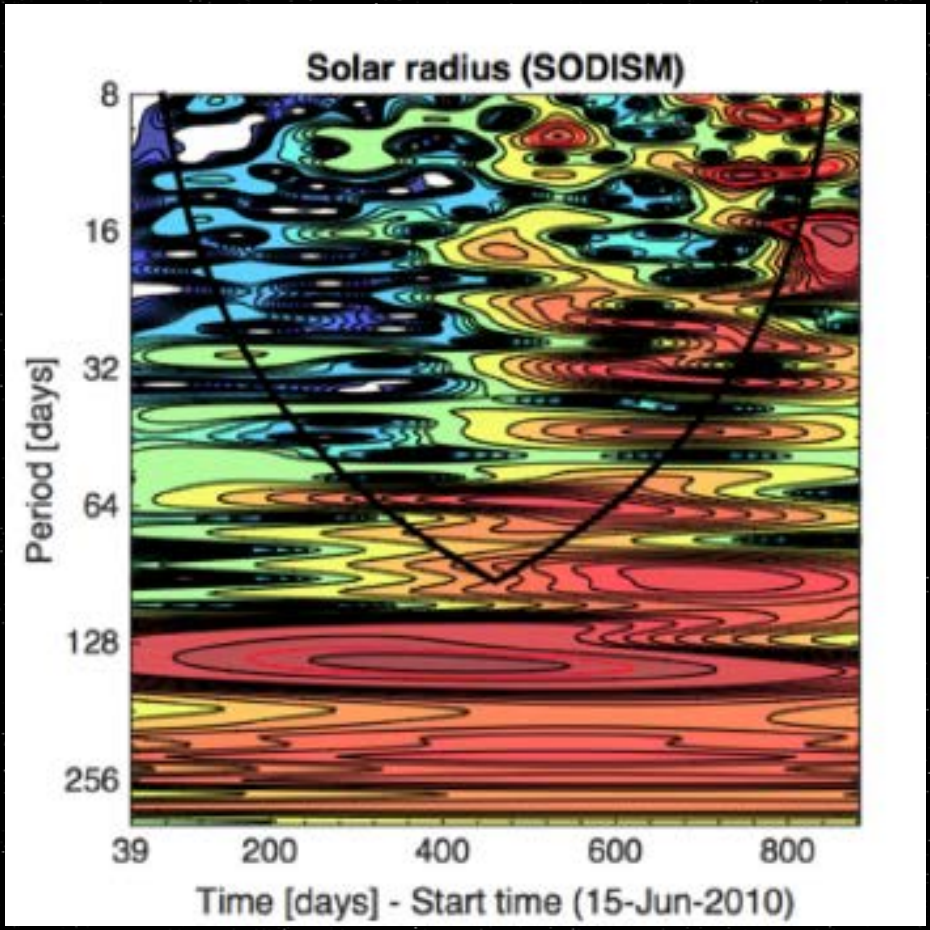

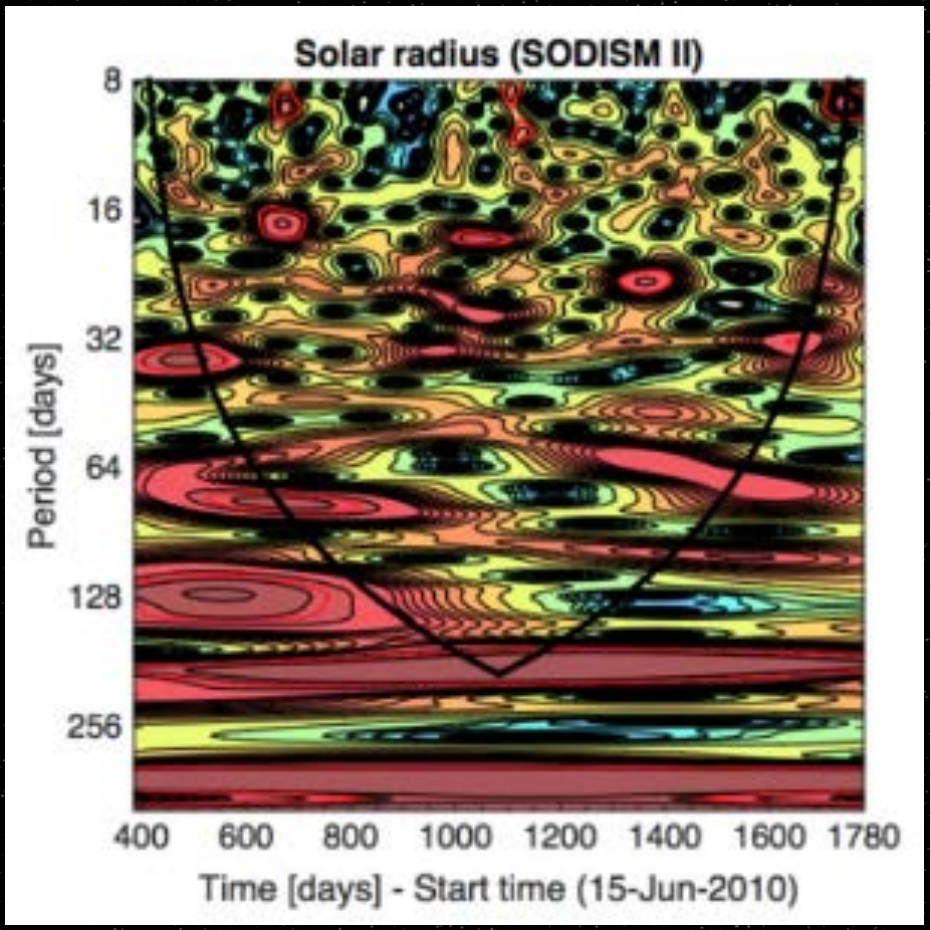

4 – Scientific results

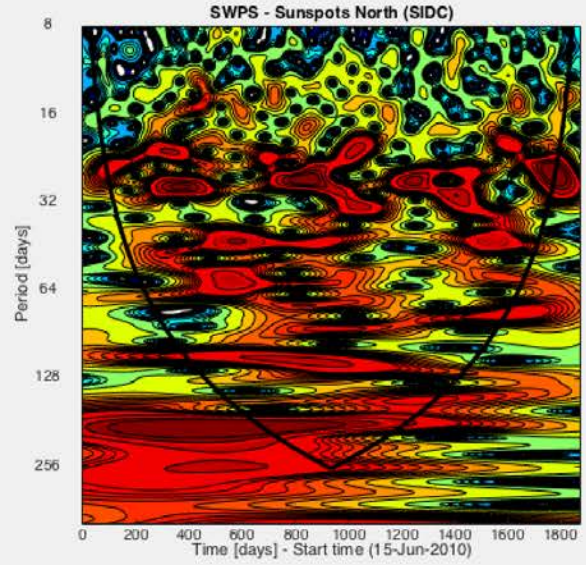

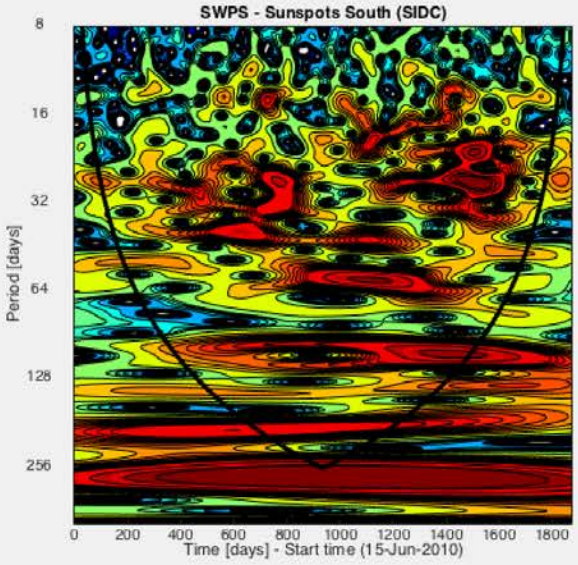

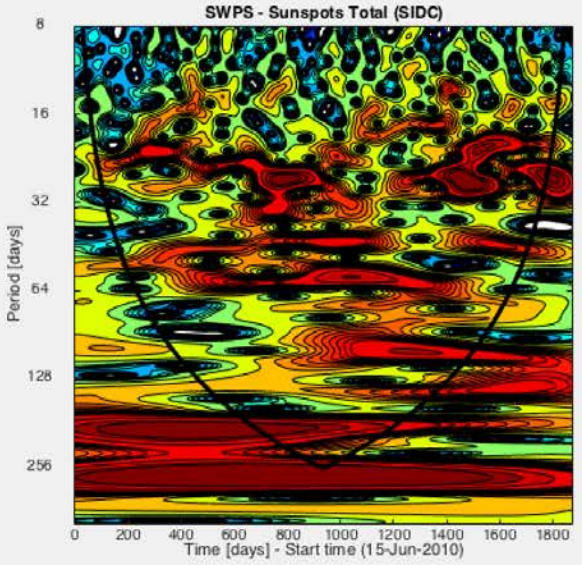

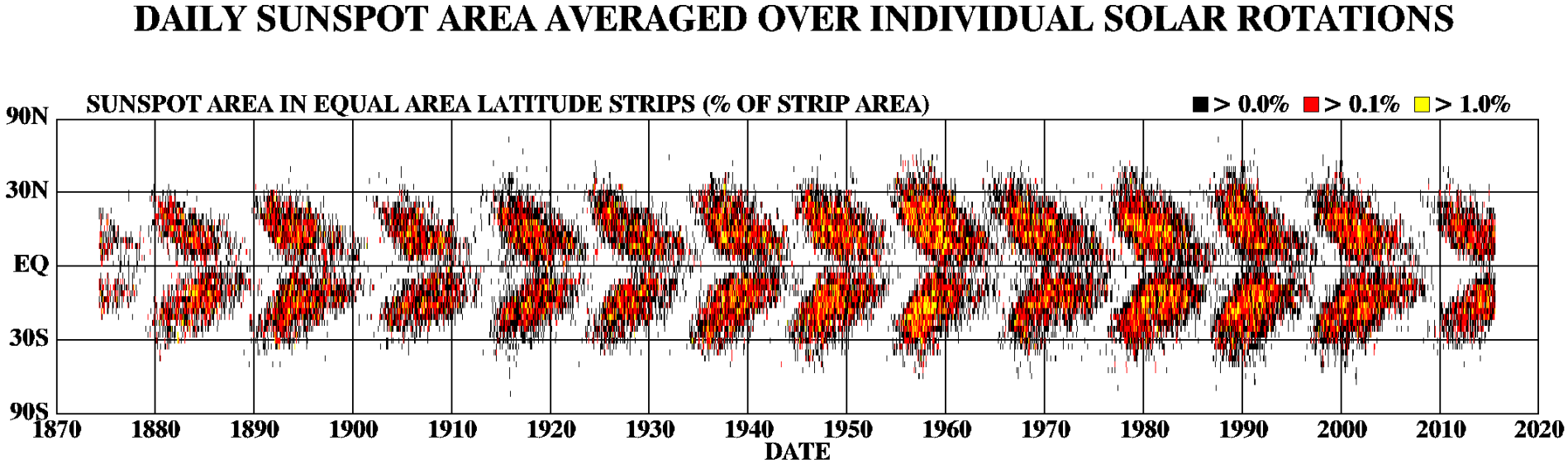

4 – Scientific results

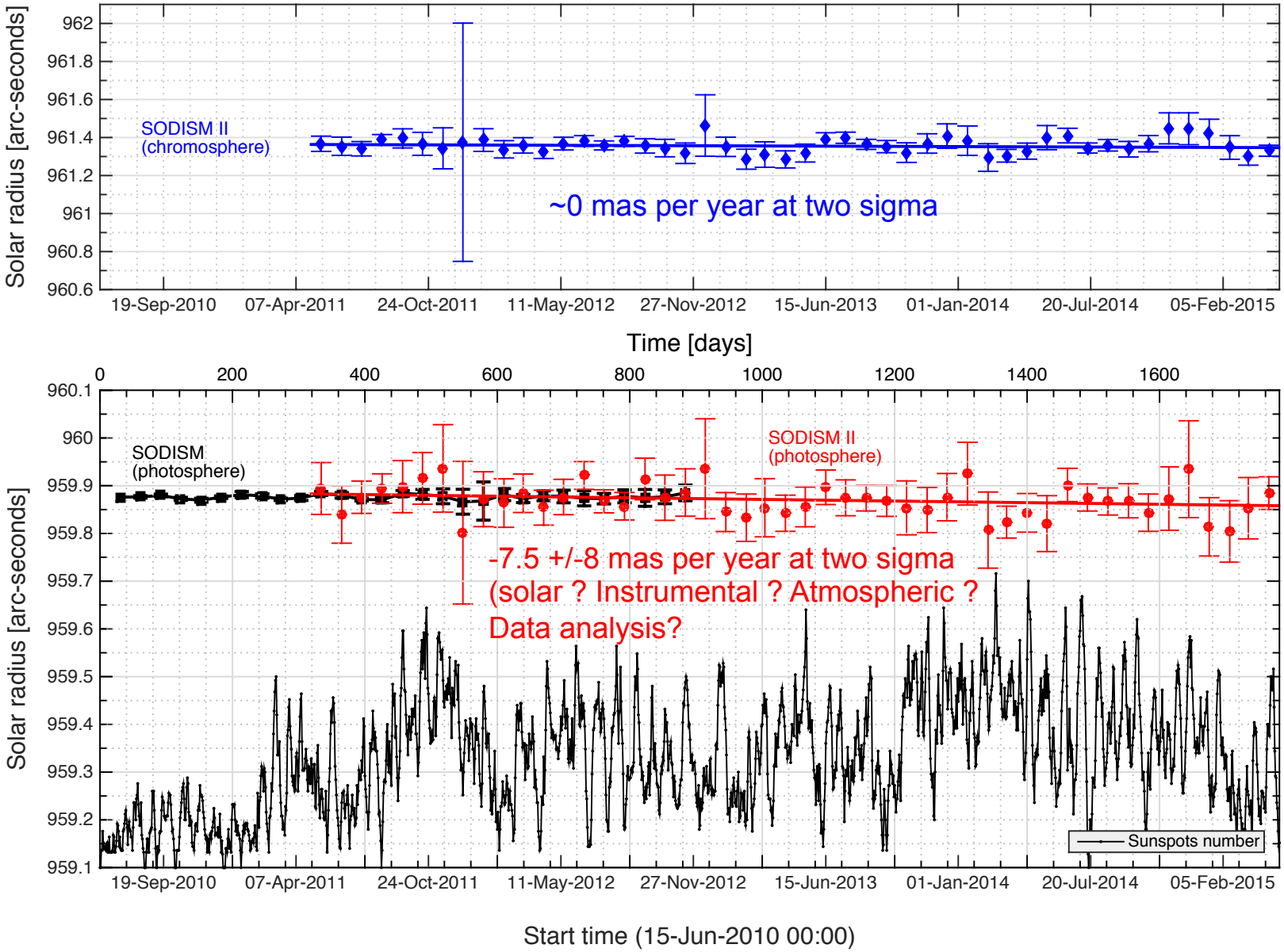

Helioseismology

4 – Scientific results

Helioseismology

4 – Scientific results

Helioseismology

- The p modes are detected in SODISM limb images.
- The steep gradient of the tachocline (transition region between the radiative interior and the differentially rotating outer convective zone) at the base of the convection zone (located at a radius of at most 0.70 times the Solar radius) is clearly seen.
- …

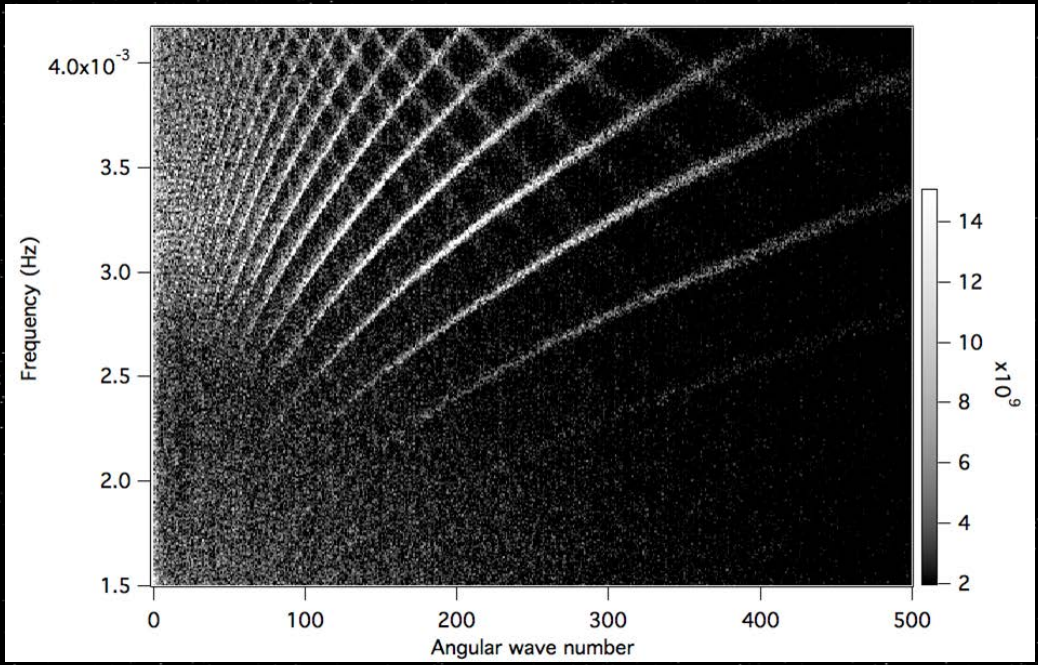

I-v diagram computed from three days of SODISM solar observations at 535 nm (limb images in April 2011).

Hauchecorne et al, 2013

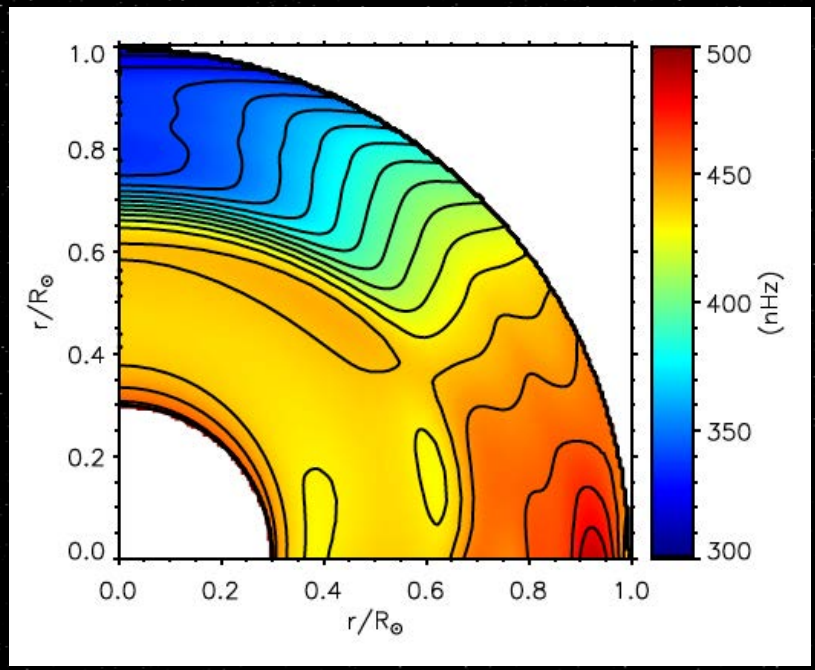

Symmetric part of the internal solar rotation rate with respect to the equator (with SODISM intensity images over the period from April to November 2011).

Corbard et al, 2013

4 – Scientific results

Solar rotation surface

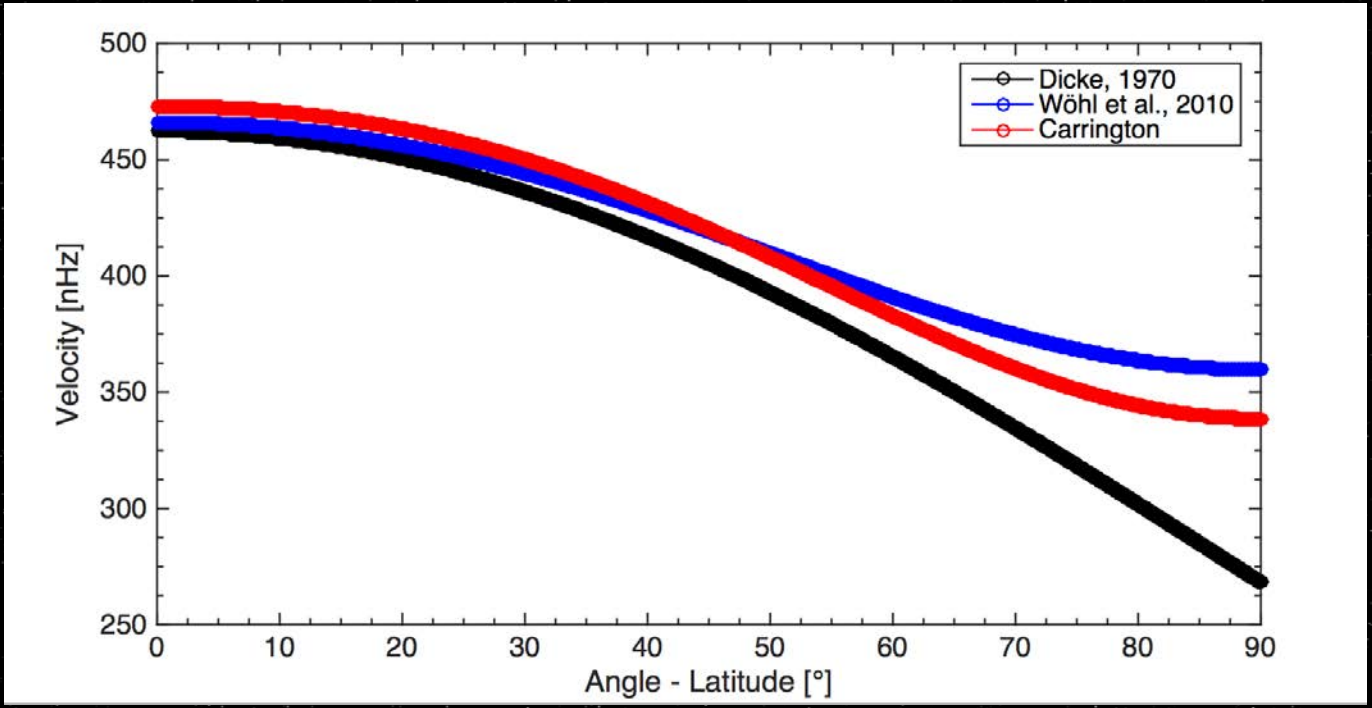

$$\Delta_\odot = \varepsilon_q + \varepsilon_s \simeq \frac{3}{2} J_2 + \frac{1}{2} \frac{\Omega^2 R_\odot^3}{G M_\odot},$$

Link between solar oblateness and solar roation surface

$$\Delta_\odot = (R_{eq} - R_{pol})/R_{pol}$$

ε_q is a measure of the distortion of the gravitational potential produced by internal rotation, and ε_s is linked to the oblateness produced by the surface rotation.
J_2 is the gravitational quadrupole moment.

Solar oblateness

4 – Scientific results

Solar oblateness

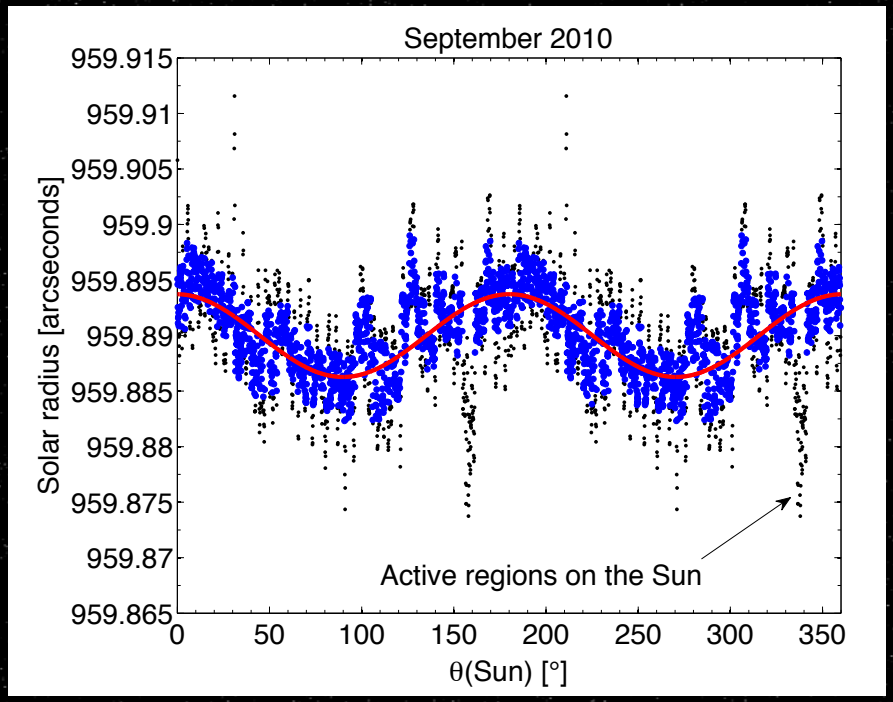

Solar oblateness determination during such campaigns.

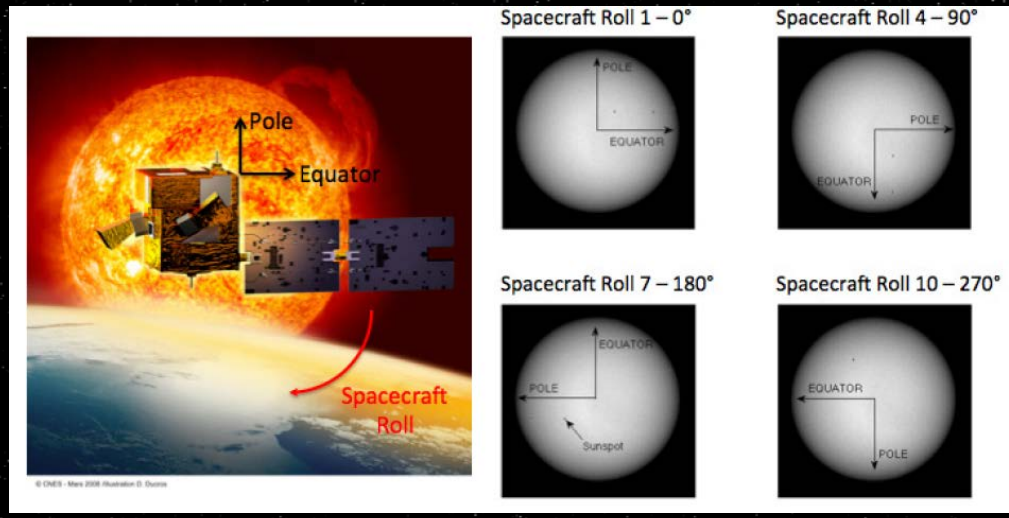

The spacecraft revolve around the PICARD-Sun axis by steps of 30° (distortion) and during a full orbit for each step (thermal evolution).

Method

$$\langle R \rangle = \frac{1}{N \times N_\theta} \sum_{m=1}^{N} \sum_{n=1}^{N_\theta} R_{(m,n)}$$

$$Rc_{(i,j)} = R_{(i,j)} + \left(\langle R \rangle - \frac{1}{N_\theta} \sum_{n=1}^{N_\theta} R_{(i,n)} \right) + G \times \left(T_{(i)} - \frac{1}{N} \sum_{m=1}^{N} T_{(m)} \right) + k_{(j)} \times \left(\langle R \rangle - \frac{1}{N} \sum_{m=1}^{N} R_{(m,j)} \right)$$

→ ΔR = **8.1± 0.6 mas** (from the mean value of the two PICARD wavelengths)

4 – Scientific results

Re - Rp = 5.9 ±0.5 km (PICARD)

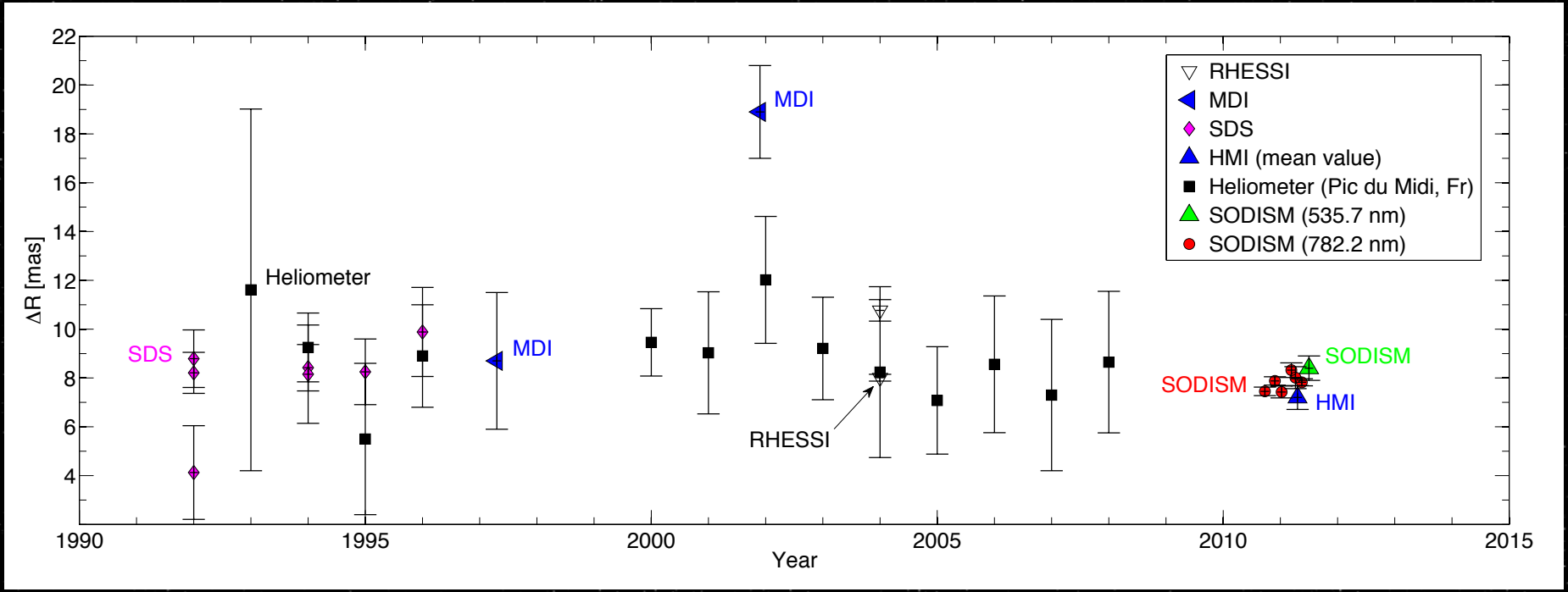

Meftah, Irbah, Hauchecorne et al., SPIE, 2014

Using differential methods (spacecraft rotation) allows to obtain good results (low uncertainty).

Indeed, the source (the Sun) does not change during the measurement, only the instrument evolves (thermal, etc.).

4 – Scientific results

Solar shape and Legendre polynomial

$$r(\Theta) = < r > \times \left(1 + \sum_{l=2,4} C_l \times \bar{P}_l(\cos(\Theta))\right) =$$
$$< r > \times \left(1 + C_2 \times \frac{1}{4} \times (3 \times \cos(2\Theta))\right) +$$
$$< r > \times \left(C_4 \times \frac{1}{64} \times (35 \times \cos(4\Theta) + 20 \times \cos(2\Theta))\right)$$

$$\Delta r_a = r\left(\frac{\pi}{2}\right) - r(0) = < r > \times \left(-\frac{3}{2}C_2 - \frac{5}{8}C_4\right),$$

PICARD - 535 nm (Irbah et al., 2014)
July 2011
C_2 = (−5.71 +/- 0.36) 10^{-6}
C_4 = (−0.36 +/- 0.43) 10^{-6}

PICARD – 782 nm (Meftah et al., 2014)
May 2011
C_2 = (−5.98 +/- 0.33) 10^{-6}
C_4 = (−1.38 +/- 0.40) 10^{-6}

C_2 (quadrupole coefficient)
C_4 (hexadecapole coefficient) determination is very difficult.

Mercury's perihelion precession:	574 arcseconds/century
Newtonian perturbations from other planets:	531 arcseconds/century
GR correction:	43 arcseconds/century
Newtonian correction from Dicke bulge:	3 arcseconds/century

PICARD
ΔR = **8.1± 0.6 mas**

Here's the data, again from Will's book:

- Amount predicted by conventional solar models	0.2 km, 0.1 ppm
- Dicke-Goldenberg (1966)	52 km, 40 ppm
- Hill (1973)	2 km, 1 ppm
- Hill (1982)	10 km, 7 ppm
- Dicke (1985)	24 km, 12 ppm

Estimates of the gravitational quadrupole moment **J**2 were found by Pijpers (1998) and Antia et al. (2008) with helioseismic data. J2 is close to 2.2 10^{-7}. Thus, ΔR is close to 8 mas.

4 – Scientific results

$$\Delta\omega = \frac{6GM_\odot}{a\left(1-e^2\right)} + J_2\frac{R_\odot^2\left(3\sin^2 i - 1\right)}{a^2\left(1-e^2\right)^2}$$

The result is a value that agrees with general relativity.
The results again give a quadrupole moment on the order of 10^{-7}, too small to affect the agreement between general relativity and the observed advance of Mercury's perihelion.

42.98 arcseconds per century

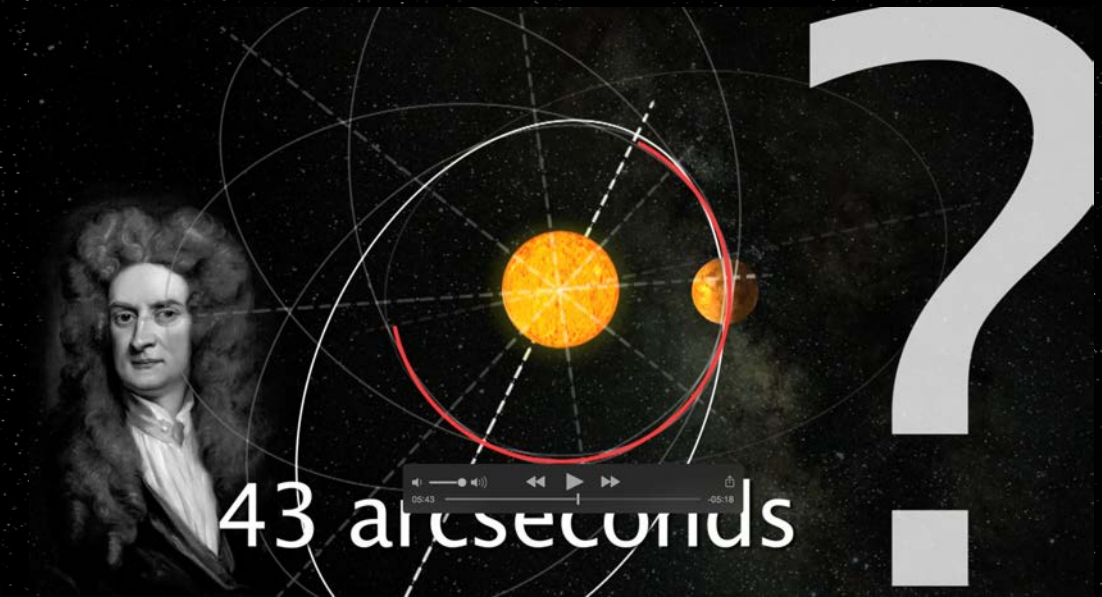

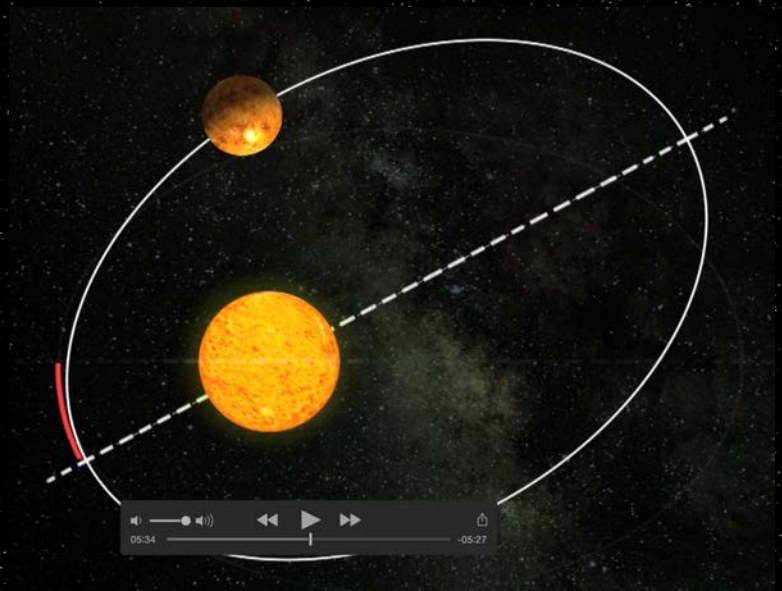

4 – Scientific results

Date	Authors	ΔR [mas]	Instrument
1961-2003	Pitjeva (2005)	8.05 ± 0.04	Radar Observations
1992	Egidi et al. (2006)	4.13 ± 1.92	SDS
1993-2008	Reis Neto et al. (2003)	13 ± 4	Rio de Janeiro solar astrolabe
1994	Egidi et al. (2006)	8.16 ± 2.02	SDS
1995	Egidi et al. (2006)	8.25 ± 1.34	SDS
1996	Egidi et al. (2006)	9.88 ± 1.82	SDS
1997	Emilio et al. (2007)	8.7 ± 2.8	SoHO/MDI
1998-2000	Damiani et al. (2011)	8.8 ± 1.7	Pic du Midi heliometer
2001	Emilio et al. (2007)	18.9 ± 1.9	SoHO/MDI
2002-2008	Fivian et al. (2008)	8.01 ± 0.14	RHESSI/SAS
2010-2011	Meftah et al. (2015b)	7.9 ± 0.3	PICARD/SODISM
2010-2012	Kuhn et al. (2012)	7.2 ± 0.49	SDO/HMI
2011	Irbah et al. (2014)	8.4 ± 0.3	PICARD/SODISM

4 – Scientific results

Application of our method on SDO-HMI

New method (work in progress)

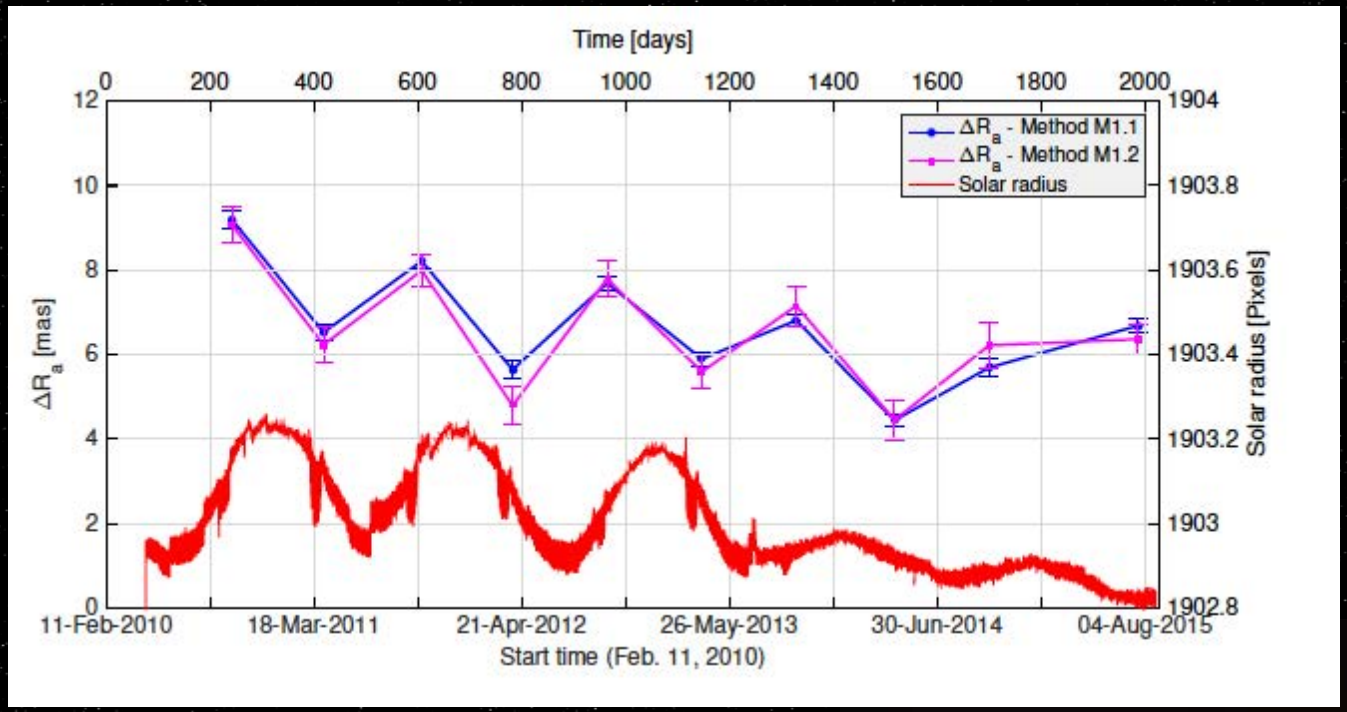

$$< B >= \frac{1}{N \times N_\theta} \sum_{m=1}^{N} \sum_{n=1}^{N_\theta} B_{(m,n)}$$

$$Rb_{(i,j)} = Rc_{(i,j)} + \alpha \left(\frac{B_{(i,j)} - < B >}{\frac{dB}{dR}_{(i,j)}} \right)$$

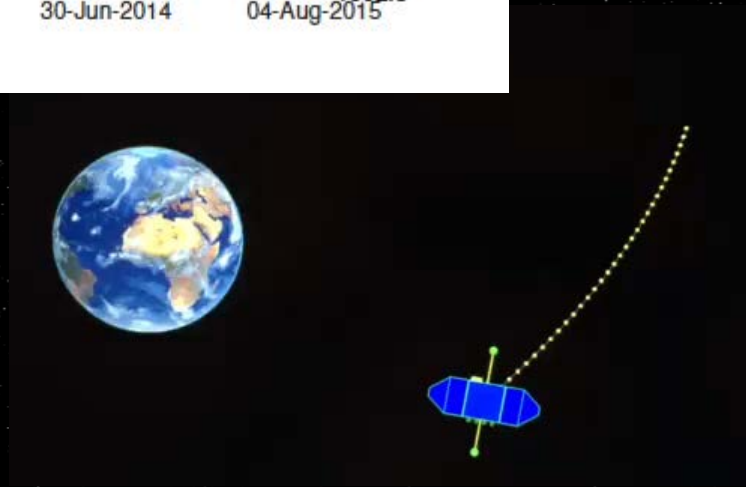

A solar oblateness measurement campaign is made in less than 7hours (10 minutes without acquisition followed by 7.5 minutes of observing time for each position during the roll).
The HMI instrument needs more than five hours to have a state of equilibrium (transient steady state before the roll maneuver). Cooperation between SDO-HMI team and PICARD team.

4 – Scientific results

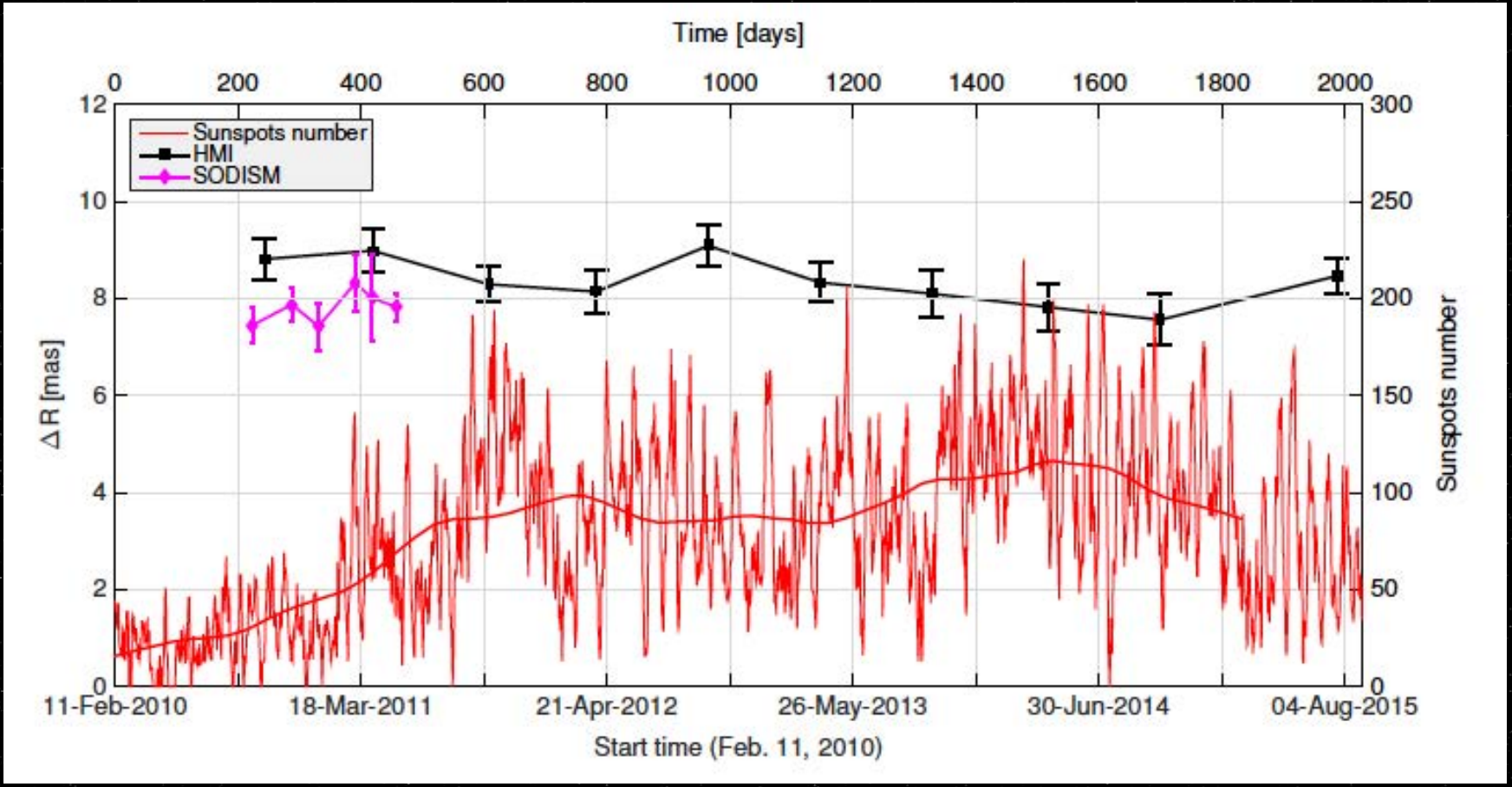

Photometry

Measure the spectral solar irradiance variations over time.

Work in progress…

4 – Scientific results

From Lean and Fröhlich (1998)

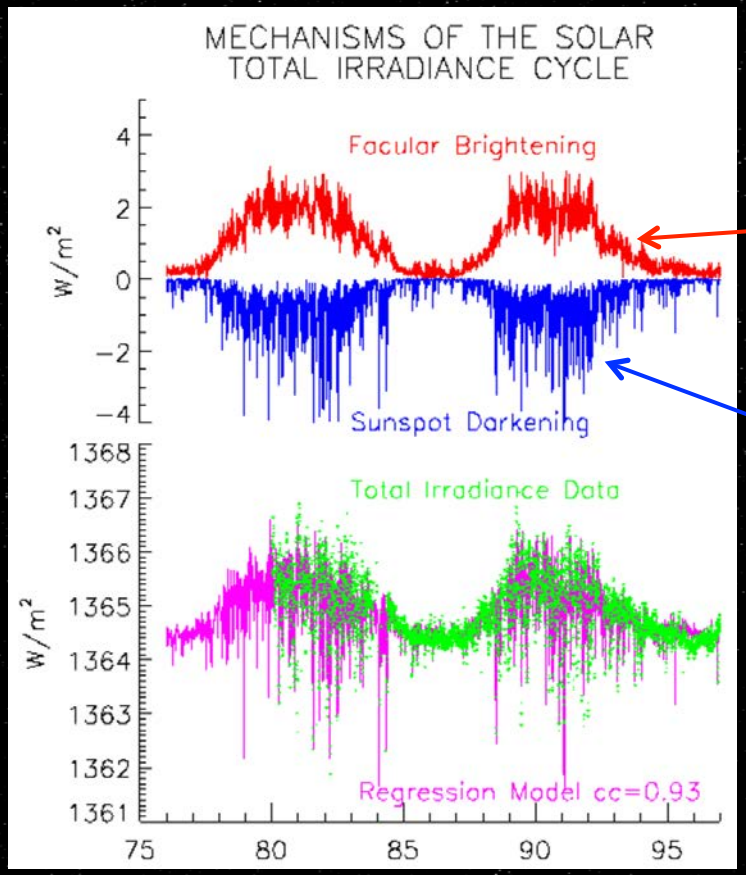

Faculae

Sunspot

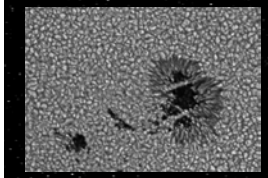

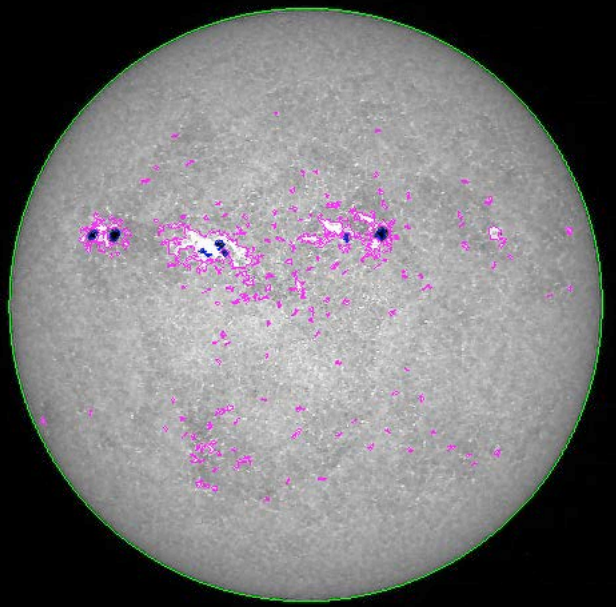

Development of technics for faculae area with SODISM 393.37 nm images (blind deconvolution)

→ SSI reconstructions during PICARD mission
→ Contributions on TSI variations during PICARD mission
→ …

More than 90% of TSI variance are due to dark sunspots and bright faculae.

Any residual TSI variations from slower changes in e.g. solar diameter or convective patterns ?

4 – Scientific results

Threshold technique Curto et al. (Solar Physics, 2008) for example	MRF (Markov Random Field) approach Turmon et al. (Solar Physics, 2010)
+ Combination of different mathematical tools (morphological operators, filters, threshold) seems to be easier + Most of the tools are already implemented + Only improvements to be done + Possible improvements: data fusion of results obtained with other wavelengths, region-growing or shrinking, additional filters, … - How to find or determine the threshold? - The threshold may depend on the input image (contrast, …) - Detection of sunspots is easier than detection of faculae	+ Possibility to work with multidimensional data (magnetic field, intensity, equivalent width) + Modeling of solar images in relation to solar physics + MRF prior allows to take into account spatial coherence of labels - Bayesian framework: more complex computations, possible longer time of execution - Hypothesis on likelihood model and priors: GMM (Gaussian Mixture Model) or IHM (Interpolated Histogram densities): similar results - Estimation step of unknown model parameters: Expectation-Maximisation, Gibbs sampler - Need of a training set or a threshold segmentation for a first estimation? <u>Contact with Turmon on 09/01/2015…</u>
Both techniques need a pre-processing step. Possible improvement: remove limb-darkening spatial attenuation,…	

4 – Scientific results

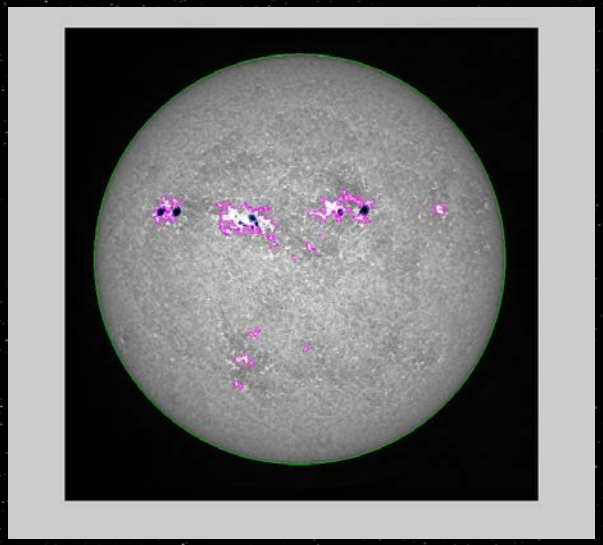

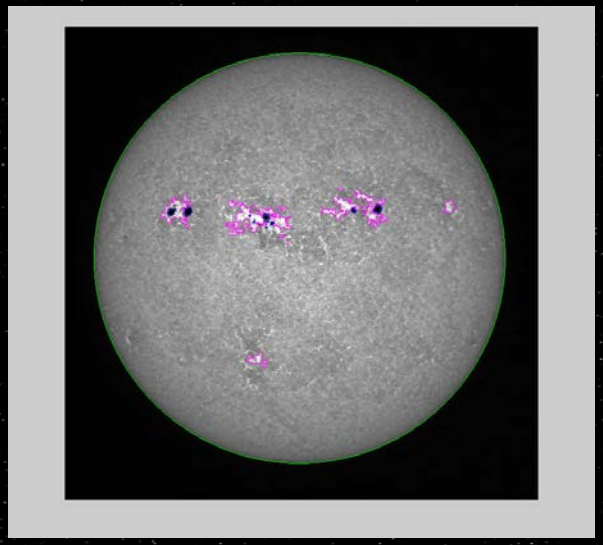

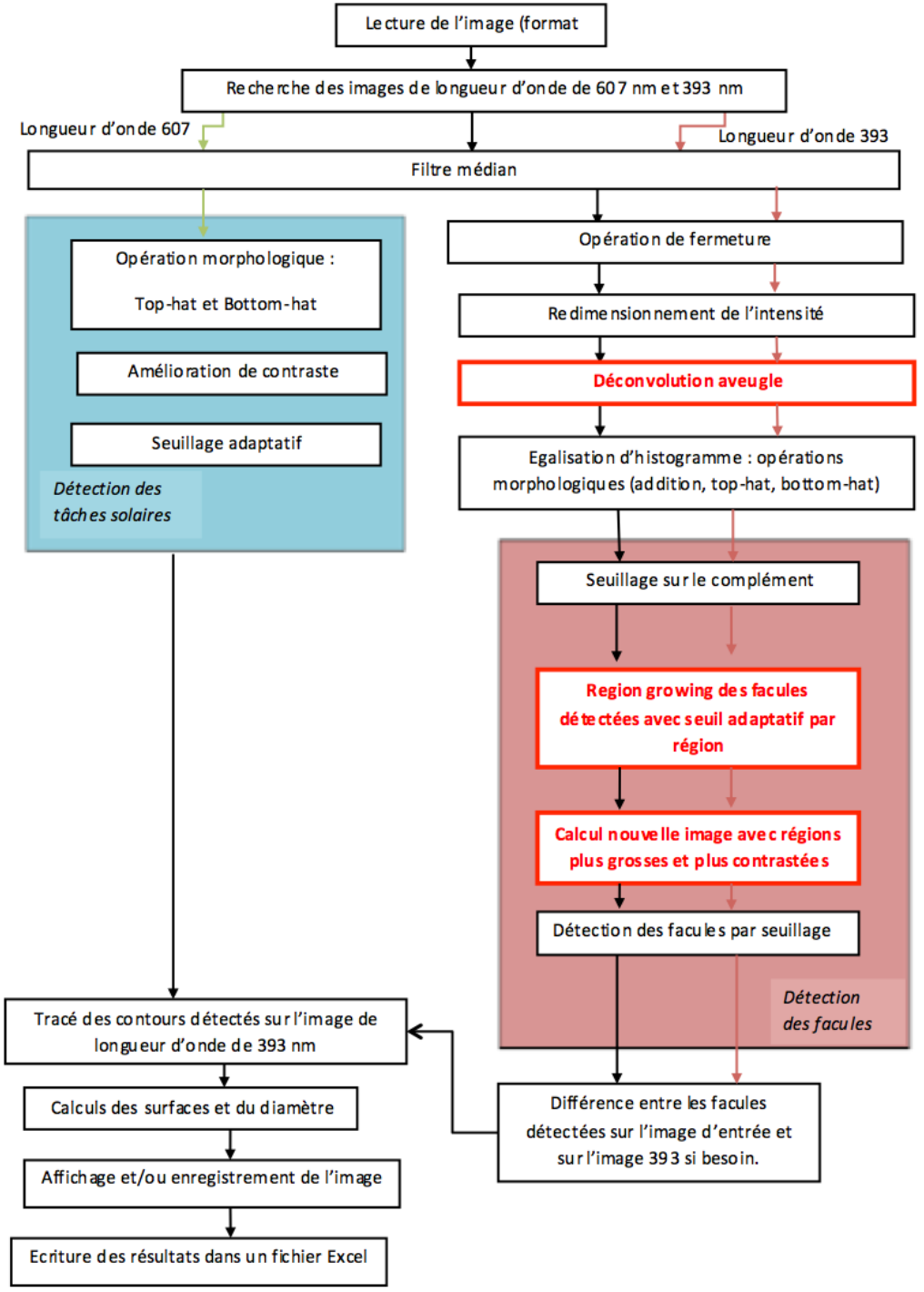

4 – Scientific results

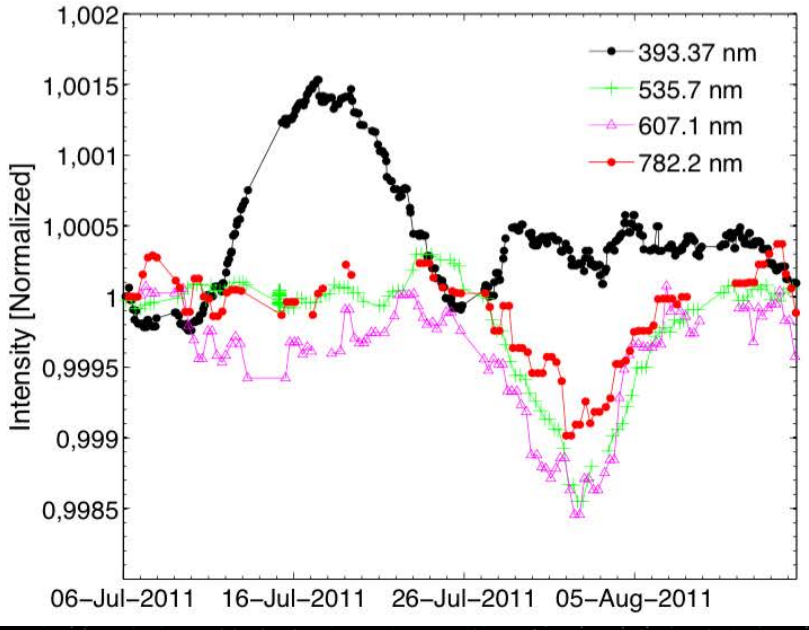

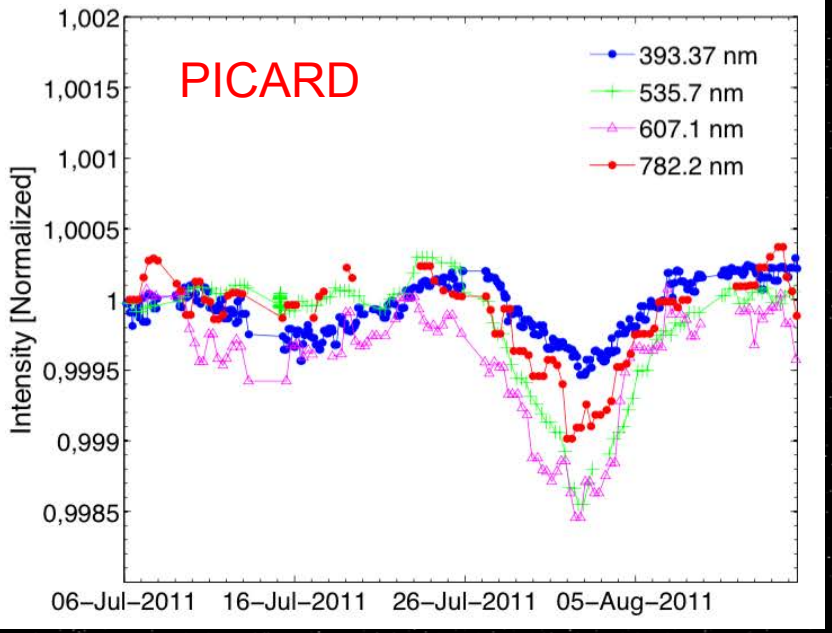

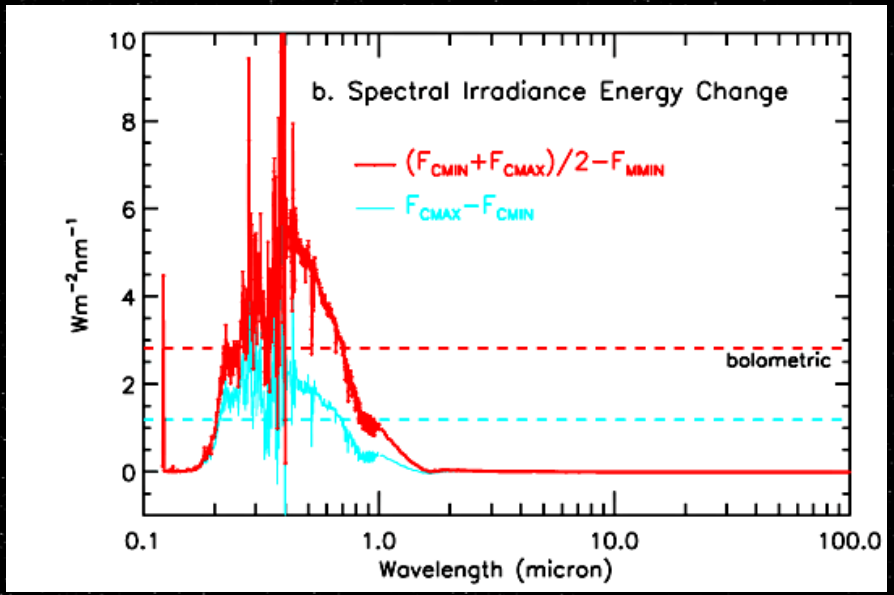

Lean, 2000

Spectral solar irradiance evolution

From minimum to maximum of the solar cycle (blue)

Form the Maunder Minimum to the present day (red)

Radiometry

Measure the total solar irradiance variations over time.
Link with the solar diameter.

Work in progress…

4 – Scientific results

Radiometry and photometry

Measure the total solar irradiance (TSI) in absolute and over time.

Total Solar Irradiance (TSI)

Instrument	Years	TSI	References
ERB/NIMBUS 7	**1978-1993**	**TSI ~ 1371 W.m^{-2}**	**Hickey et al., 1980, 1988 Kyle et al., 1994**
ACRIM 1/SMM	1980-1989	TSI ~ 1367 W.m^{-2}	Willson et al., 1981 (1368.31 W/m2)
ERBE/ERBS	1984-2003	TSI ~ 1365 W.m^{-2}	Lee et al., 1987
ERBE/NOAA 9	1985-1989	TSI ~ 1364 W.m^{-2}	Barkstrom et al., 1990
ERBE/NOAA 10	1986-1987	TSI ~ 1364 W.m^{-2}	Barkstrom et al., 1990
ACRIM2/UARS	1991-2001	TSI ~ 1365 W.m^{-2}	Willson & Mordvinov, 2001
SOVA 1/EURECA	1992-1993	TSI ~ 1365 W.m^{-2}	Crommelynck et al., 1993
DIARAD/VIRGO on SOHO	1996-present	TSI ~ 1365 W.m^{-2}	Dewitte et al., 2004
PMO6V/VIRGO on SOHO	1996-present	TSI ~ 1365 W.m^{-2}	Finsterle et al., 2006 Fröhlich et al., 1997
ACRIM3/ACRIMSAT	2000-present	TSI ~ 1365 W.m^{-2}	Willson & Helizon, 1999
TIM/SORCE	2003-2013	TSI ~ 1361 W.m^{-2}	Kopp et al., 2005
PREMOS/PICARD	**2010-present**	**TSI ~ 1361 W.m^{-2}**	**Schmutz et al., 2013**
SOVAP/PICARD	**2010-present**	**TSI ~ 1362 W.m^{-2}**	**Meftah et al., 2014 (Solar Phys.)**

Based on measurements collected from various spacecraft instruments over the last 35 years, the TSI has incrementally declined from 1371 W.m^{-2} in 1978, to 1365 in the 1990's, and to around 1362 W.m^{-2} in 2014, mainly due to calibration.

4 – Scientific results

Total Solar Irradiance (TSI)

1362 **±2.4** W.m^{-2} (PICARD)

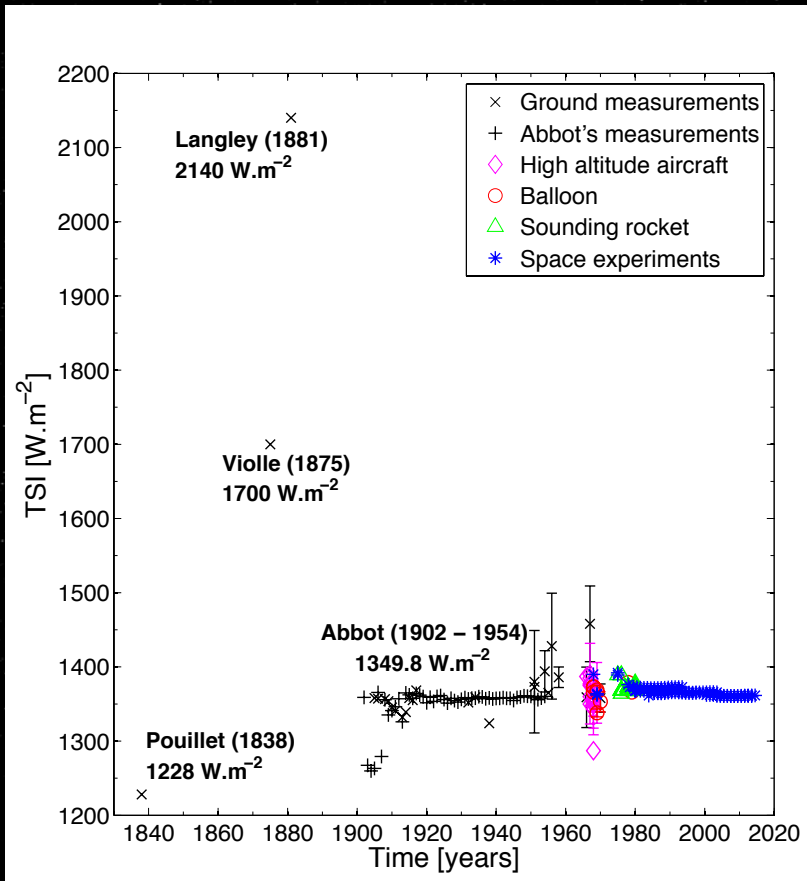

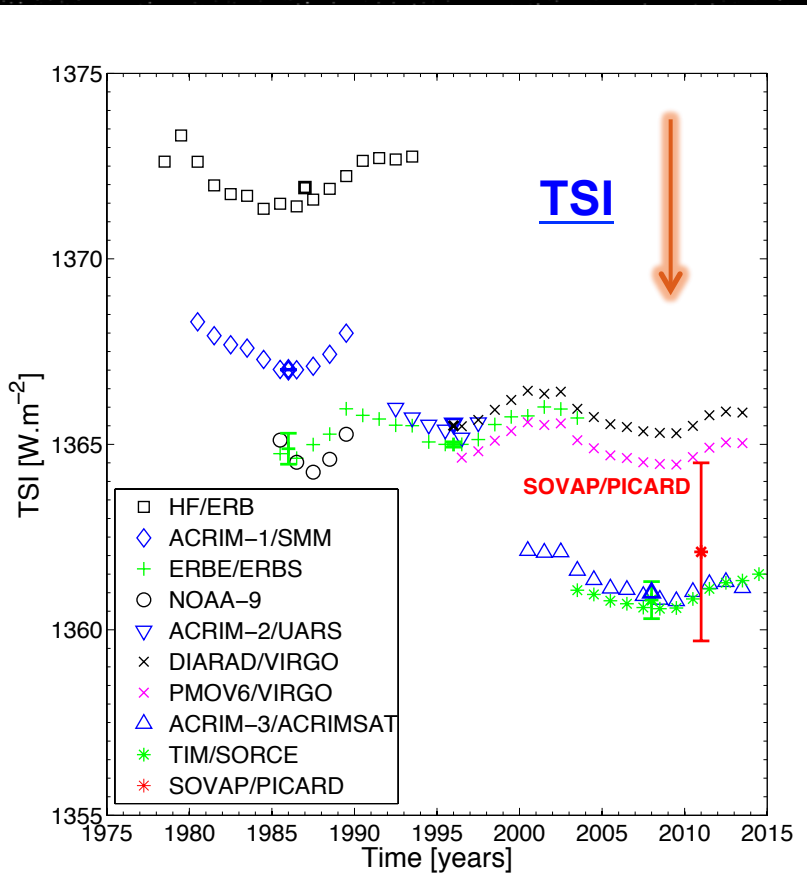

Importance of uncertainty budgets and calibration.

4 – Scientific results

Total Solar Irradiance (TSI) changes over time

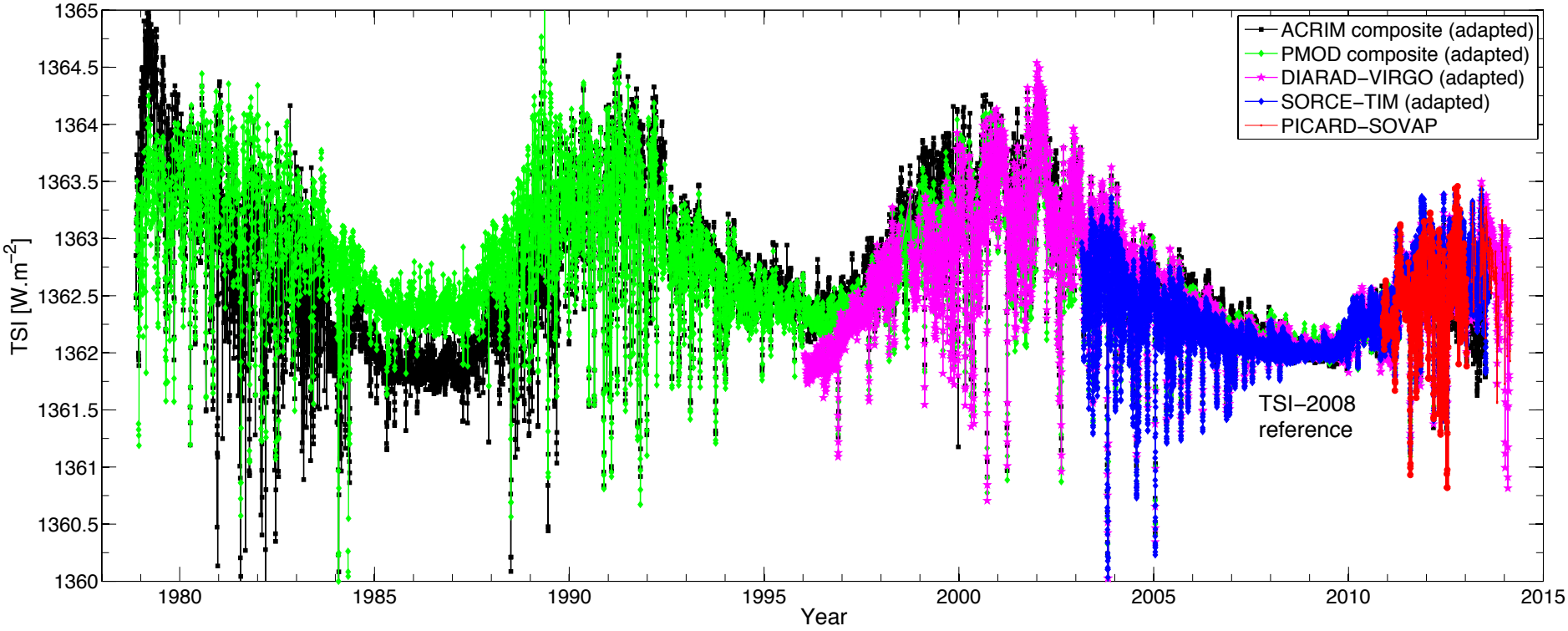

The TSI variation during a solar cycle is easier to measure than the absolute value (ground and space calibration are needed).

Conclusion

Conclusion

Achievable scientific objectives

- Measurement of the solar oblateness at different wavelength

- Measurement of the photospheric diameter during the transit of Venus

- Solar radius variability with SODISM (short time scale in space) and SODISM 2 (long time scale on ground)

- I-v diagram at 535.7 nm and 393.37 nm

…

- Solar radius: 696,156± 145 kilometers
- TSI (luminosity of the Sun): 1,362± 2.4 $W.m^{-2}$
- Solar oblateness: 5.9± 0.5 kilometers
- Solar radius variations less than 15 km

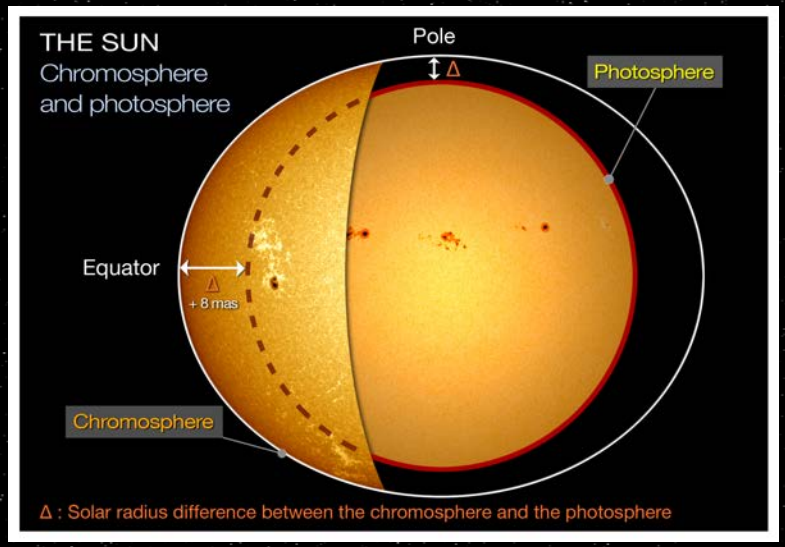

Conclusion

Metrology and science of the diameter and the limb (Sci. fld. 1)	• Measurement of the radial profile (shape) of the solar limb • Measurement of the angular profile (asphericity) of the solar disc • Measurement of the photospheric diameter
Helio-seismology (Sci. fld. 2)	• Inference of the helio-seismic diameter • Detection and characterization of solar intensity oscillations, and especially of g modes
Science of the solar irradiance (Sci. fld. 3)	• Accurate, precise and redundant measurements of the Total Solar Irradiance (TSI) • Contribution to the estimation of the spectral irradiance
Other solar physics studies (Sci. fld. 4)	• Measurement of the photospheric solar differential rotation • Assessment of the magnetic activity and delivery of SpW information • (serendipity)
Solar-terrestrial relationships & aeronomy (Sci.fld.5)	• Studies of the Earth atmosphere via e.g. solar occultations during the eclipse seasons, albedo studies with the BOS, etc. • Contribution of PICARD to the understanding of Sun-Earth connection processes and of terrestrial climate

Thank you for your attention